A dissertation

submitted in partial fulfillment of the

requirements for the degree of

University of Washington

Reading Committee:

Program Authorized to Offer Degree:

University of Washington

Abstract

Constructing Hybrid Cytokine Receptors to Amplify CAR T Cell Anti-Tumor Potency

Christopher Saxby

Chair of the Supervisory Committee:

Michael C. Jensen

Department of Bioengineering

Chimeric antigen receptors (CARs) have achieved remarkable therapeutic efficacy against cancer by linking natural circuits of T cell activation to the recognition of tumor-associated antigens, but optimal anti-tumor responses require an additional input: cytokine stimulation. Here, we explored cellular engineering approaches to deliver cytokine signals directly to CAR T cells to enhance T cell expansion and functional durability. First, we compared a set of engineered receptors providing constitutive gamma chain cytokine signaling (Ch. 1) and found that cytokine inputs promote distinct and potentially complementary behavior in CAR T cells. To investigate combinatorial cytokine signaling, we developed a hybrid IL-7 and IL-21 receptor platform (Ch. 2), which amplified CAR T cell anti-tumor potency and yielded insights into the roles of cytokine signaling outputs (Ch. 3). In some cases, cytokine-driven improvements in CAR T cell efficacy were accompanied by unrestricted T cell growth and subsequent toxicity *in vivo*. Therefore, we implemented strategies to safely deploy cytokine signaling technology, including drug-responsive molecular switches (Ch. 4) and a synthetic T cell activation-dependent promoter (Ch. 5).

Table of Contents

Chapter 1: Engineered Gamma Chain Cytokine Receptors Enhance CAR T-Cell Mediated Tumor Regression

ABSTRACT

Adoptive T cell cancer therapy requires robust activation of T cells to ensure sufficient T cell expansion and persistence within patients. Chimeric antigen receptors (CARs) recapitulate signaling through the T cell receptor (TCR) and costimulatory signals, but optimal T cell activation requires a third signal mediated by stimulatory cytokines. To provide this third signal directly to CAR T cells, we engineered a panel of chimeric cytokine receptors (CCRs) that trigger T cell-intrinsic constitutive interleukin signaling. Each of the three engineered receptors recapitulates the signaling events of a gamma chain cytokine: IL-2, IL-7, or IL-21, and each signaling pattern mediates distinct impacts on T cell survival, proliferation, and effector function. CCRIL2 and CCRIL7-expressing human $CD8^+$ CAR T cells showed increased proliferation and survival when exposed to tumor cells *in vitro*. In contrast, CCRIL21 specifically primed CAR T cells for increased effector function via the upregulation of IL-21-sensitive transcription factors. When exposed to subcutaneous neuroblastoma tumors *in vivo*, CCRIL2 and CCRIL7-expressing CAR T cells extended mouse survival compared to T cells bearing CAR alone, and this effect was associated with greater CAR T cell expansion and persistence. CCR technology offers a promising cytokine signaling platform to improve T cell immunotherapy by promoting T cell expansion, persistence, and anti-tumor potency.

INTRODUCTION

Improvements in the design of CARs are being propelled by increased understanding of the cellular signals that drive these therapeutic cells to expand and persist within patients. Current CAR designs incorporate a domain for T cell activation, CD3z, and domains for co-stimulation, derived from CD28 or 4-1BB. These receptor engineering advances have resulted in CAR T cells with improved expansion and persistence,[1] properties associated with positive patient outcomes in clinical trials.[2] Such findings suggest that additional strategies to optimize pro-proliferative and pro-survival signals may yield improved clinical outcomes. In addition to CD3 activation and co-stimulation, optimal T cell activation requires a third signal mediated by immunostimulatory cytokines.[3] CAR T cells and other tumor-resident immune cells generate immunostimulatory cytokines, but there is high variability in type and concentration, dependent on the cellular milieu of the tumor microenvironment. In particular, the solid tumor setting often features a signaling network promoting T cell deactivation and immunosuppression,[4] which can impede CAR T cell proliferation and survival, limiting CAR T cell efficacy.

Several pre-clinical studies have paired CAR T cells with cytokine stimuli and have shown enhanced anti-tumor activity compared to CAR T cells alone. For instance, engineering CD19CAR T cells to constitutively secrete gamma chain cytokines led to increased survival rates in mice inoculated with human lymphoma Raji tumors, compared to CD19CAR T cells without augmentation.[5] Similarly, engineering melanoma-specific TCR-transgenic T cells to secrete IL-12 improved clearance of murine B16 melanoma tumors.[6]

The use of soluble cytokines, whether administered exogenously or secreted by the administered T cells, may, however, stimulate non-CAR T cell populations, raising the risk of

adverse effects. Systemic administration of IL-2, approved for the treatment of metastatic melanoma and metastatic renal cell carcinoma,[7] can lead to pulmonary edema, low blood pressure and hematologic, renal, and hepatic toxicity.[8] A common effect of CAR T cell therapy is cytokine release syndrome, which is mediated by excessive cytokine activity,[9] further complicating engineering strategies that boost cytokine activity. Exogenous cytokines also require expression of the native cytokine receptors by the therapeutic T cells for their activity, and the expression levels of these receptors vary with cell differentiation state and signaling inputs.

Several approaches have been developed to address these challenges, and various immunostimulatory cytokine signals have been explored as T cell therapy supplements. IL-2 offers a particularly attractive form of signal three, as it drives T cell division[10] and differentiation of $CD8^+$ T cells into cytolytic effector cells.[11] Researchers have engineered a modified IL-2 cytokine to specifically recognize only a modified IL-2 receptor.[12] This approach that has been tested in mice bearing TCR-transgenic T cells expressing the modified IL-2 receptor, resulting in improved clearance of B16 melanoma tumors upon administration of the modified IL-2. Another member of the gamma chain cytokine family, IL-7, promotes the survival of memory T cells and preserves polyfunctionality in CD4 T cells.[13-16] To engineer these beneficial characteristics into CAR T cells, researchers have modified CAR T cells to express a constitutively active IL-7 receptor.[17] These modified CAR T cells markedly improved the clearance of human neuroblastoma and glioblastoma cells in mice, compared to CAR T cells without IL-7 augmentation. Regions of cytokine receptors have also been incorporated into the structure of the CAR to enable triggering

of JAK-STAT signaling upon CAR activation, a feature that improves CAR-T cell mediated regression of human leukemia tumors *in* mice.[18]

These studies have shown the advantages of pairing cytokine stimuli with adoptively transferred T cells, but further work is needed to explore alternative approaches to cytokine supplementation. Our group has developed a modular platform to engineer constitutively active cytokine receptors with the aim of augmenting therapeutic cell activity. For instance, we built a chimeric cytokine receptor for IL-7 signaling (CCRIL7) by fusing the IL7 cytokine to the N-terminus of the IL-7 receptor via a flexible linker, allowing the synthetic receptor to heterodimerize with the endogenous gamma chain cytokine receptor and propagate IL7 signaling events.[19] We then iterated on this design by replacing the intracellular domain of CCRIL7 with that of IL2Rb to generate a chimeric cytokine receptor for IL-2 signaling (CCRIL2). In previous work, we modified T cells with either CCRIL7 or CCRIL2 and showed that both cytokine receptors improved T cell engraftment in mice.[19]

Here, we widened our panel of synthetic receptors and generate a third chimeric cytokine receptor for constitutive IL-21 signaling (CCRIL21). IL-21 is an attractive candidate cytokine for CAR T cell supplementation, as it prevents T cell exhaustion in chronic viral infection models[20,21] and sustains T cell effector function against tumor.[10] Our panel of chimeric cytokine receptors thus included CCRIL2, CCIRL7, and CCRIL21, designed to recapitulate IL-2, IL-7 and IL-21 signaling, respectively. We introduced each CCR alongside an anti-B7H3 CAR into human T cells and examined the effects of each candidate on CAR T cell expansion, persistence, and anti-tumor activity. We found that all three CCRs improved CAR T cell persistence in response to repeated exposure to tumor *in vitro*. In addition, each CCR also imparted a set of unique characteristics to

the CAR T cells. CCRIL2 and CCRIL7 specifically imparted proliferative potential and resistance to apoptosis compared to T cells expressing only the CAR, whereas CCRIL21 primed CD8 cytotoxicity and dampened T cell expression of inhibitory receptors. We also tested CCR-equipped CAR T cells in NSG mice bearing human subcutaneous neuroblastoma tumors. CAR T cells equipped with CCRIL2 or CCRIL7 resulted in greater tumor clearance, accompanied by increased CAR T cell expansion and persistence. CCR technology provides insights into the effects of various cytokine stimuli on CAR T cell therapy and offers a promising platform for tailoring cytokine signaling profiles to fit the therapeutic niches of specific solid tumors in the future.

MATERIALS AND METHODS

CCR Construct Design. The CCR constructs consist of a single reading frame coding for two polycistronic proteins separated by a T2A ribosomal skip sequence. The sequence begins with a truncated CD19 marker protein fused to a drug-responsive suicide gene SR39TK, which is followed by one of three distinct CCR sequences (Fig. 1c). The CCR sequences all begin with the IL-7 cytokine, which is tethered via a flexible linker to the extracellular and transmembrane domains of the endogenous IL7R. Each of the three CCR sequences features a distinct intracellular domain endogenous sequence of either IL2Rb, IL7R or IL21R. The human elongation factor 1α (EF1α) promoter was added upstream of the coding sequence to drive expression, and the entire sequence was inserted into the epHIV7.2 lentiviral transfer plasmid for gene delivery. Sequence fragments were amplified via PCR and combined via Gibson assembly.

Lentivirus Production. Recombinant lentivirus was generated by transiently transfecting a 293T producer cell line with lentiviral packaging plasmids alongside a transfer plasmid containing the transgenes of interest. Transfection was performed using Lipofectamine 2000 (Life Technologies, Cat. # 11668-500). Four days after transfection, lentivirus was isolated from the 293T cell culture supernatant via ultracentrifugation and stored at -80° C until the day of transduction.

T Cell Production and Culture. Protocols to acquire human cells were approved by the institutional review board of Seattle Children's Hospital. $CD8^+$ T cells were isolated from human peripheral blood mononuclear cells (PBMCs) by magnetic activated cell sorting with a $CD8^+$ T cell isolation kit (Miltenyi Biotech, Cat. # 130-096-495). The cells were immediately subjected to a bead-based CD3/CD28 stimulation using Dynabeads (Thermo Fisher Scientific, Cat. # 11131D) at a bead to cell ratio of 1:1. Unless otherwise indicated, T cell culture media consisted of RPMI 1640 (Gibco, Cat. # 22400-089) supplemented with 10% FBS (Hyclone, Cat. # SH30071.03), 2mM L-glutamine (Gibco, 25030-081), 50 U/mL IL-2 (Chiron, Cat. # 53905-991-01) and 0.5 ng/mL IL-15 (Miltenyi, Cat. # 130-095-765) throughout the culture period. Two days post-stimulation, cells were transduced with lentivirus housing CCR and/or CAR transgenes at multiplicities of infection (MOIs) of 1 and 2, respectively. In some cases, an additional lentivirus housing GFP and a firefly luciferase (ffluc) was added at an MOI of 1 to allow for later T cell bioluminescent imaging *in vivo*. Between days 10 and 24 post-stimulation, methotrexate (MTX) was added to the culture at a concentration of 50nM to select CAR-expressing populations. Twenty-four days post-stimulation, cells were magnetically sorted for CD19 expression using 0.25 uL of biotinylated anti-CD19 antibody (BioLegend, Cat. # 302204) per million cells and anti-biotin microbeads (Miltenyi, Cat. #

130-090-485) according to manufacturer's instructions. Sorted populations were subjected to a rapid expansion protocol (REP) as previously described.[26] MTX was supplemented to a concentration of 50 nM between days 5 and 10 post-REP and 100 nM between days 10 and 14. At 14 days post-REP, flow cytometry was used to confirm the purification of T cell populations expressing CCR and/or CAR constructs. T cells were then transferred into a cryopreservation solution consisting of 80% culture media, 10% FBS and 10% DMSO (Sigma, Cat. # D2650) and frozen for later culture periods. Upon thaw, T cells put immediately into a second REP, and flow cytometry analysis, in vitro co-culture assays and in vivo studies were performed 10-14 days later.

Flow Cytometry. Flow cytometric analysis was performed to determine transduction marker expression and phenotypic surface marker expression. Cells were removed from culture and placed into 96-well round-bottom plates, washed twice with PBS (Gibco, Cat. # 10010-023), stained with pre-titered quantities of antibody, washed three more times with PBS and finally fixed with 0.5% paraformaldehyde (Electron Microscopy Sciences, Cat. # 15713) in PBS before analysis. Flow cytometric data was collected using a BD LSRFortessa flow cytometer and later analyzed using FlowJo software. Final flow plots were populated by cell populations remaining after the following gating strategy was performed. First, a "lymphocyte" gate was generated by drawing a polygon within the forward scatter vs side scatter scatterplot to isolate events with size and granularity characteristic of lymphocytes and remove debris and dead cell events. Within the lymphocyte gate, a second "single cell" gate was generated by gating on events that followed a linear relationship between forward scatter in the height and area dimensions to remove cell doublets from downstream analysis. If applicable, a "live cells" gate was generated using the live

dead stain to exclude cells with compromised membranes. Finally, during analysis of co-culture assays, T cells populations were isolated using a gate for high expression of CD3.

Apoptotic Status Assay. Cells were stained with Annexin V and 7-AAD (BioLegend, Cat. # 640908) to determine viability and apoptotic status. Cells were removed from culture and placed into 96-well round-bottom plates, washed twice with 1X BioLegend Annexin V Staining Buffer, stained with Annexin V and 7-AAD, washed two more times with Annexin V Buffer and analyzed by flow cytometry within 12 hours.

IncuCyte Cytotoxicity Assay. T cell cytotoxicity was evaluated over a period of seven days using the S3 IncuCyte Live Cell Imager (Sartorius). To begin, fifty thousand K562 tumor cells expressing mCherry (K562-mCherry) were cultured per well of a flat-bottom 96-well plate. Next, T cells were added at effector to tumor ratios of 2:1, 1:1, 0.5:1 or 0.25:1. All cell populations were cultured in cytokine-free media for these studies. Fluorescent and phase images of these co-cultures were collected every hour for 8 days. IncuCyte image analysis software was used to identify live tumor cells via mCherry expression, and the number of remaining tumor cells across the co-culture was used to quantify the cytotoxic capacity of T cell groups.

Intracellular Cytokine Staining. T cells were co-cultured with K562 cells at a 2:1 effector to tumor ratio for 6 hours. Two hours after the co-culture began, a transport inhibitor cocktail (Thermo Fisher Scientific, Cat. # 00-4980-03) was added to prevent T cell release of secretory proteins. At the end of co-culture, the cells were incubated with 10 uL of Fc block (Miltenyi Cat. # 130-059-

901) for 10 minutes at room temperature to avoid indiscriminate antibody binding by tumor cells. Cells were then stained with Live Dead Fixable Aqua viability dye (Thermo Cat # L34957) and BV421-conjugated anti-CD3 antibody (BD Cat # 562426) to allow gating of live T cells. Next, samples were fixed and permeabilized using the Fixation/Permeabilization Kit (BD, Cat. # 554714) according to the manufacturer's protocol. Next, the cells were stained with antibodies specific for secretory proteins: Granzyme B (BD, Cat. # 560213), Interferon-gamma (BD, Cat. # 563731) and Perforin (BioLegend, Cat. # 353303). Flow cytometric data was collected using a BD LSRFortessa flow cytometer and analyzed using FlowJo software.

Intracellular Flow Cytometry. Expression of BCL2 was examined by flow cytometry using the Fixation/Permeabilization Kit (BD, Cat. # 554714) according to manufacturer's protocols. Once fixed and permeabilized, cells were stained with PE anti-BCL2 antibody (BioLegend, Cat. # 658705) and analyzed by flow cytometry within 48 hours.

Transcription Factor Expression Assays. T cell expression of transcription factors was evaluated 24 hours after T cells were co-cultured with K562 cells at a 1:1 effector to tumor ratio. Co-cultures were stained with Live/Dead Aqua viability dye (Thermo Fisher Scientific, Cat. # L34957) and anti-CD3 antibody (BioLegend, Cat. # 300324) and then fixed and permeabilized with the Transcription Factor Staining Buffer Set (Thermo Fisher Scientific, Cat. # 00-5523-00) according to manufacturer's instructions. Finally, cells were stained with anti-BATF (BioLegend, Cat. # 654803) and anti-Tbet (BioLegend, Cat. # 644809) antibodies and flow cytometric analysis was performed.

Serial Tumor Challenge Assays. Fourteen days after the second REP, T cell populations were subjected to weekly tumor challenges by co-culture with irradiated LCL cells or K562 cells at a 2:1 effector to target ratio in cytokine-free T cell culture media. Total viable cell counts were determined by hemocytometer, and 200 uL of each co-culture were then transferred to 96-well round-bottom plates to be analyzed by flow cytometry. Cells were stained with Live Dead Fixable Aqua viability dye (Thermo Cat # L34957) and BV421-conjugated anti-CD3 (BD Cat # 562426) to distinguish T cells. Flow cytometric data was analyzed using FlowJo software, and co-cultures with T cells accounting for 50% or more of live cells were subjected to further tumor challenge. Subsequent challenges were administered at the same 2:1 effector to target ratio.

Subcutaneous Neuroblastoma Mouse Studies. All mouse experiments were conducted under protocols approved by the Seattle Children's Research Institute's Institutional Animal Care and Use Committee (IACUC). *In vivo* anti-tumor efficacy of CCR-expressing CAR T cells was assessed against subcutaneous neuroblastoma tumors. 10-13 week-old NSG mice were subcutaneously injected with five million human Be2 cells expressing mCherry (Be2-mCherry) on both flanks. Tumor engraftment was assessed using manual caliper measurements. Five days after tumor injection, mice were designated into groups of five with the lowest possible inter-group variation in tumor size. Then, each mouse was injected via tail vein with ten million $CD8^+$ T cells, engineered to express firefly luciferase (ffluc). Twice per week tumor volume was monitored by manual measurement, and mice imaged for mCherry fluorescent signal (a secondary measure of tumor growth) and bioluminescent signal (T cells). Mice were euthanized if the tumor on either flank grew to exceed 1500 mm^3. 150 uL of 28.57 mg/mL D-luciferin (Perkin Elmer, Cat. # 122799) was injected subcutaneously 15 minutes before bioluminescent imaging. All imaging was performed

using an IVIS Spectrum In Vivo Imaging System (Perkin Elmer) and analysis on Living Image Software.

Phospho-Flow. Phosphorylation status of signaling proteins was assessed by flow cytometry as previously described.[27] Concentrated paraformaldehyde (Electron Microscopy Sciences, Cat. # 15713) was added directly to culture plate to fix cells before staining. Cells were then permeabilized with 100% methanol and stained with anti-phosphoSTAT3 (BioLegend, Cat. # 651004) and anti-phosphoSTAT5 (BD, Cat. # 612598) antibodies.

RESULTS

Chimeric cytokine receptors recapitulate endogenous gamma chain cytokine signaling.

In a previous study, we generated a prototype chimeric cytokine receptor for IL-7 signaling (CCRIL7) by fusing the gene encoding IL7 cytokine to the start of the gene encoding the IL-7 receptor via a flexible linker sequence (**Fig. 1a**).[19] We showed that the tethered IL-7 allows the CCR to dimerize with the endogenous common gamma chain receptor and mediate a constitutive IL-7 signal. We also demonstrated the modularity of this system, generating CCRIL2 by exchanging the intracellular portion of IL7R for that of IL2Rb (Fig. 1b).

To expand our panel of synthetic receptors, we generated CCRIL21, exchanging the intracellular portion of IL7R for that of IL21R (**Fig. 1b**). Transgenes encoding CCRIL2, CCRIL7 and CCRIL21 were each inserted into lentiviral transfer plasmids (**Fig. 1c**) and introduced into human CD8+ T cells via transduction (**Fig. 1d**). We next assessed whether CCRIL2, CCRIL7 and CCRIL21 triggered signaling events in accord with endogenous cytokine counterparts. We first quantified phosphorylated STAT3 and STAT5 in the CCR-expressing T cells (**Fig. 1e**). Each CCR mimicked the

phosphorylation pattern of its endogenous cytokine counterpart, with cells expressing CCRIL2 and CCRIL7 showing increased pSTAT5 (phosphorylated STAT) and CCRIL21 showing increasing pSTAT3. Next, we assessed whether STAT1 and members of the ERK and MAPK signaling cascades were also differentially activated by CCRs (**Fig. 1e**). We found that CCRIL2 expression led to the phosphorylation of the ERK pathway mediator protein SHC, while CCRIL21 expression heightened phosphorylation of STAT1 and AKT. Each CCR therefore recapitulates, in a cell-intrinsic manner, the unique set of signaling events triggered by its counterpart endogenous gamma chain cytokine.

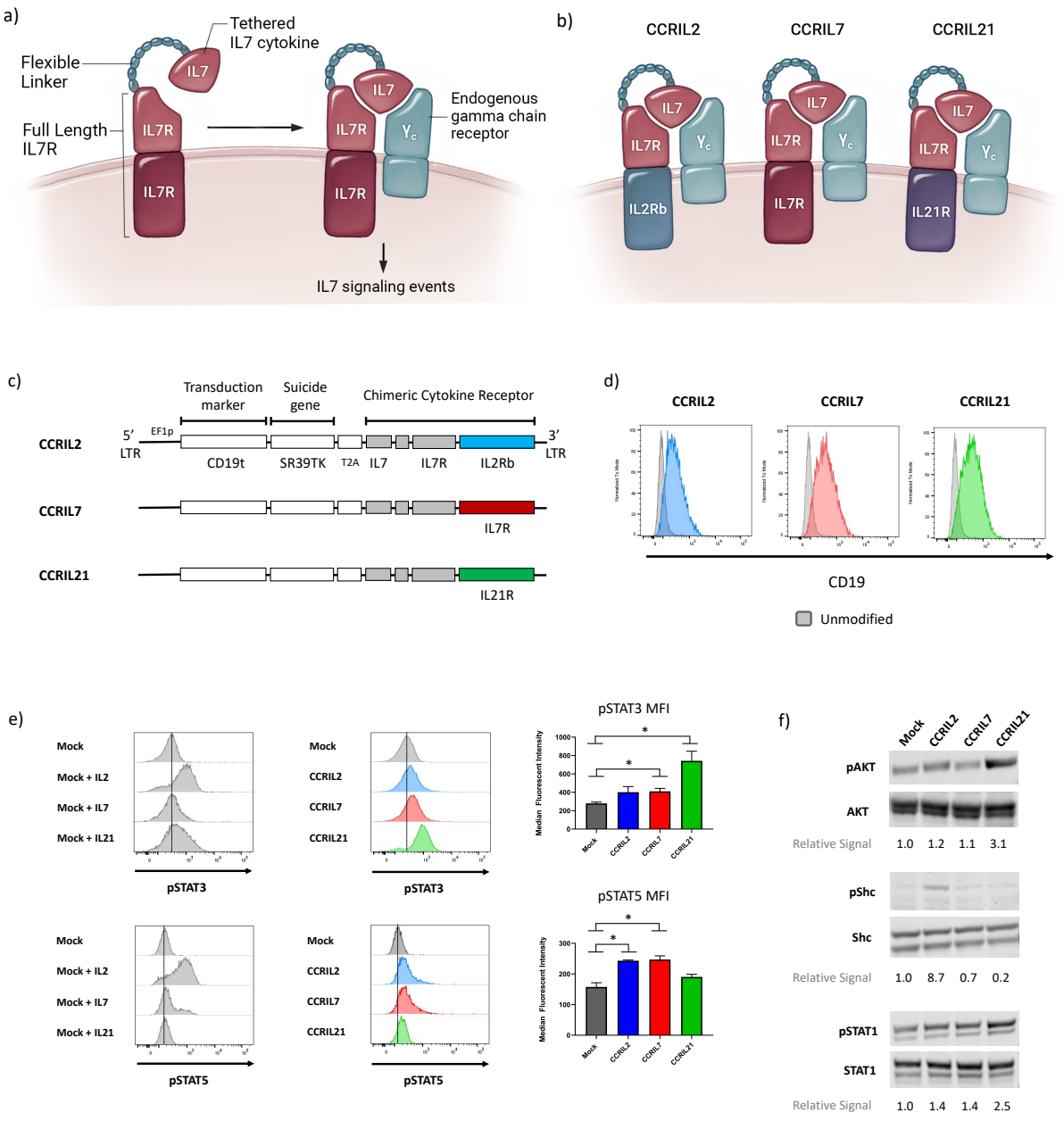

Figure 1: Chimeric cytokine receptors recapitulate endogenous interleukin signaling. **a**, Chimeric cytokine receptor design and signaling functionality. **b**, Panel of chimeric cytokine receptors (CCRs) developed by modular replacement of intracellular domains. **c**, Lentiviral constructs used to introduce CCR transgenes into T cells. **d**, Transduction marker (CD19t) expression by immunofluorescence flow cytometry in $CD8^+$ T cells transduced with CCR lentiviral vectors. **e**, Presence of phosphorylated STAT3 and STAT5 in unmodified (mock) and CCR-expressing $CD8^+$ T cells in the absence of cytokine (16 hours post cytokine removal) and in unmodified cells treated with IL2 (50 U/mL), IL7 (10 ng/mL) or IL21 (10 ng/mL) for 16 hours. Vertical lines mark the MFI of untreated mock cells. **f**, Western blot to detect phosphorylated AKT, Shc, and STAT1 across T cell populations. Cellular isolates were also assessed for total AKT, Shc and STAT1 as controls, showing similar expression levels. Asterisks indicate p-values derived from one-way ANOVA tests: *$p < 0.05$.

Chimeric Cytokine Receptors Promote Growth and Survival of CAR T Cells *In Vitro*

Given the role of gamma chain cytokines in T cell survival and expansion, we examined the CCRs as candidate proteins to supplement CAR T cell therapy. First, we generated dual-purified T cell populations expressing each CCR alongside a CAR targeting B7H3 (B7H3CAR), a receptor aberrantly expressed on many types of cancer.[22] Briefly, CD8+ T cells were dual-transduced with lentiviruses carrying the B7H3CAR construct and the CCR constructs (**Fig. 1c**). Dual-positive cells were purified using drug selection of CAR-positive cells and magnetic sorting of CCR-positive cells (**Fig. 2a**). We began our characterization of these T cell populations by examining T cell survival and expansion upon weekly exposures to irradiated human LCL lymphoblastoid cells *in vitro* in the absence of exogenous cytokine (**Fig. 2b**). CCRIL2 and CCRIL7 extended the lifespan of CAR T cells repeatedly challenged with tumor, with CCRIL2 providing the greatest proliferative boost.

In addition, CCRIL2 and CCRIL7 promoted T cell survival, as shown by flow cytometric analysis of Annexin V binding to mark pre-apoptotic cells after seven days of co-culture with human K562 leukemia cells (**Fig. 2c**). CCRIL2 and CCRIL7 expression significantly dampened the presence of pre-apoptotic cells ($p < 0.01$), while CCRIL21-expressing cells appear to apoptose at similar rates to T cells expressing B7H3CAR alone. Finally, we examined expression of the anti-apoptotic protein BCL2, as gamma chain cytokines are known to mediate T cell survival via increases in BCL2 expression (**Fig. 2d**).[23] T cells expressing CCRIL2 or CCRIL7 showed significantly higher expression of BCL2 after seven days of co-culture with K562s ($p < 0.05$). Overall, CCRIL2 and CCRIL7, unlike CCRIL21, increased CAR T cell survival and expansion upon exposure to tumor cells *in vitro*.

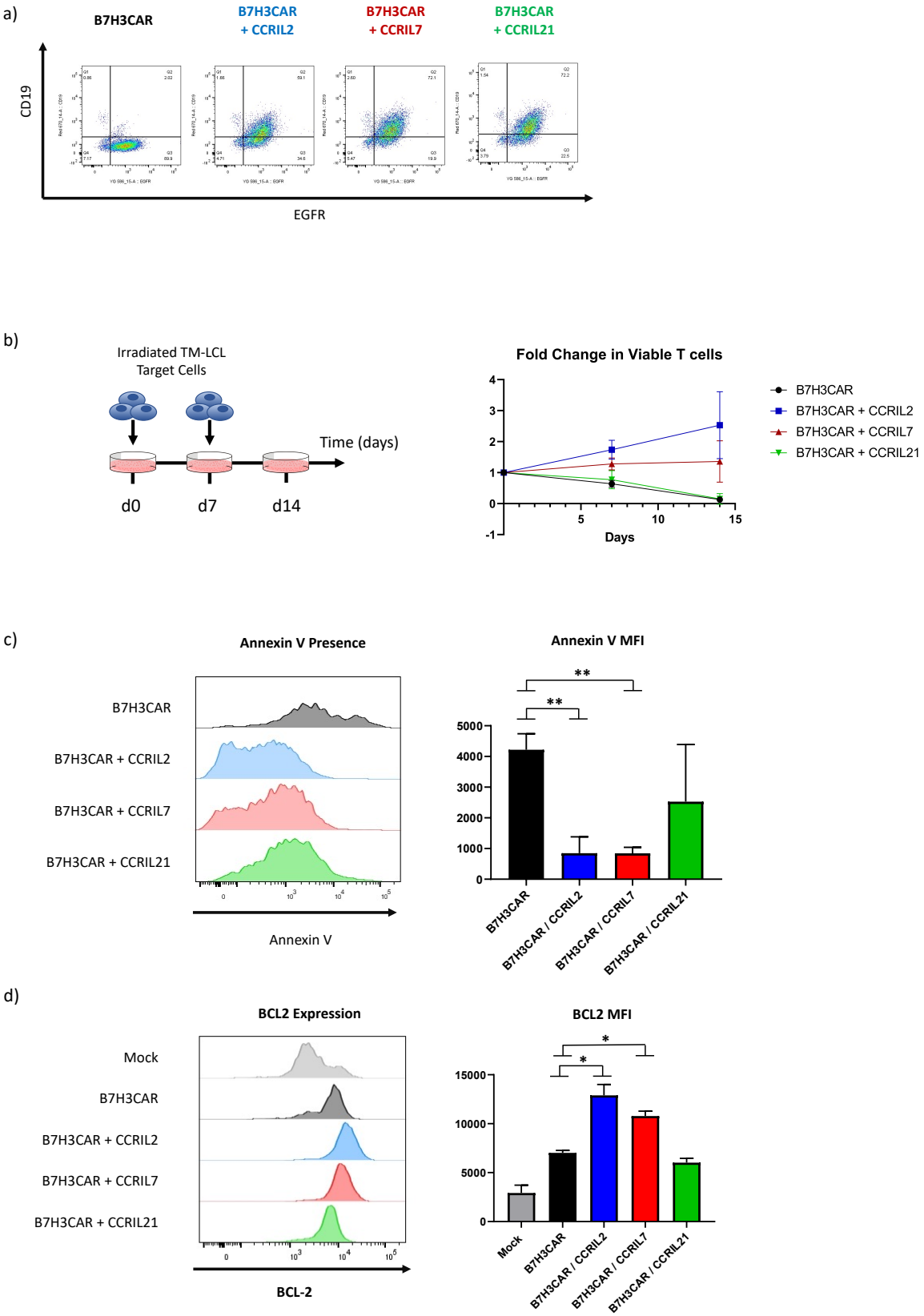
a)
B7H3CAR
B7H3CAR + CCRIL2
B7H3CAR + CCRIL7
B7H3CAR + CCRIL21
CD19
EGFR
b)
Irradiated TM-LCL Target Cells
Time (days)
d0
d7
d14
Fold Change in Viable T cells
B7H3CAR
B7H3CAR + CCRIL2
B7H3CAR + CCRIL7
B7H3CAR + CCRIL21
Days
c)
Annexin V Presence
B7H3CAR
B7H3CAR + CCRIL2
B7H3CAR + CCRIL7
B7H3CAR + CCRIL21
Annexin V
Annexin V MFI
B7H3CAR
B7H3CAR / CCRIL2
B7H3CAR / CCRIL7
B7H3CAR / CCRIL21
d)
BCL2 Expression
Mock
B7H3CAR
B7H3CAR + CCRIL2
B7H3CAR + CCRIL7
B7H3CAR + CCRIL21
BCL-2
BCL2 MFI
Mock
B7H3CAR
B7H3CAR / CCRIL2
B7H3CAR / CCRIL7
B7H3CAR / CCRIL21

Figure 2: CCRs mediate promote growth and survival of CAR T cells *in vitro*. a, Dual-purified T cell populations expressing CCRs (marked by CD19t expression) alongside B7H3CAR (marked by EGFRt expression). **b,** Survival and expansion of CAR T cells across two challenges with irradiated LCL tumor cells. Cells were co-cultured in a 2:1 T cell to tumor cell ratio every seven days without the addition of exogenous cytokine. **c,** Apoptotic status of T cells seven days after co-culture with K562 tumor cells, as determined by immunofluorescence flow cytometric detection of Annexin V. 10,000 cells were analyzed per condition. **d,** BCL2 expression by intracellular immunofluorescence flow cytometry seven days after co-culture with K562 tumor cells. Asterisks indicate p-values derived from one-way ANOVA tests: *$p < 0.05$ **$p < 0.01$.

CCRIL21 Primes CD8$^+$ CAR T Cells for Sustained Effector Function

In addition to expansion and persistence, effective CAR T cells must exhibit cytotoxic capacity until tumor clearance is achieved. We examined CAR T cell cytotoxicity against K562 target cells over a weeklong period using live cell imaging to track the presence of tumor cells (**Fig. 3a**). CCRIL2 and CCRIL7 expression did not affect B7H3CAR T cell cytotoxicity, as these T cell groups initially decreased K562 cell numbers but were eventually overrun by tumor outgrowth. In contrast, CCRIL21 expression afforded B7H3CAR T cells the capacity to suppress tumor growth throughout the co-culture period.

We went on to examine the mechanism underlying this heightened cytotoxic potency of CCRIL21-expressing CAR T cells. Previous studies have suggested that IL-21 plays a key role in the modulation and maintenance of T cell effector function under conditions of chronic antigen exposure. T cell activation in the presence of IL-21 leads to upregulation of the transcription factors Tbet and BATF, which in turn promote sustained expression of T cell effector proteins and resistance to T cell exhaustion, respectively.[24,25] Intracellular flow cytometric analysis revealed that CCRIL21-expression likewise promotes increased expression of these two key transcription factors (**Fig. 3b**).

Furthermore, CCIL21-expressing T cells featured higher levels of cytotoxic proteins Granzyme B, Interferon-Gamma, and Perforin (**Fig. 3c**) compared to T cells expressing CAR alone. We also observed lower inhibitory receptor expression in CCRIL21-expressing cells compared to T cells expressing the other CCRs (**Fig. 3d**). Specifically, CCRIL21-expressing T cells maintained lower levels of PD1, Lag3 and Tim3 after two weeks of co-culture with K562 cells. Together these findings suggest that $CD8^+$ T cells expressing CCRIL21 are primed for increased cytotoxic activity, compared to cells expressing CCR2 and CCR7, and may be less susceptible to deactivation by inhibitory ligands expressed by tumor cells.

a)

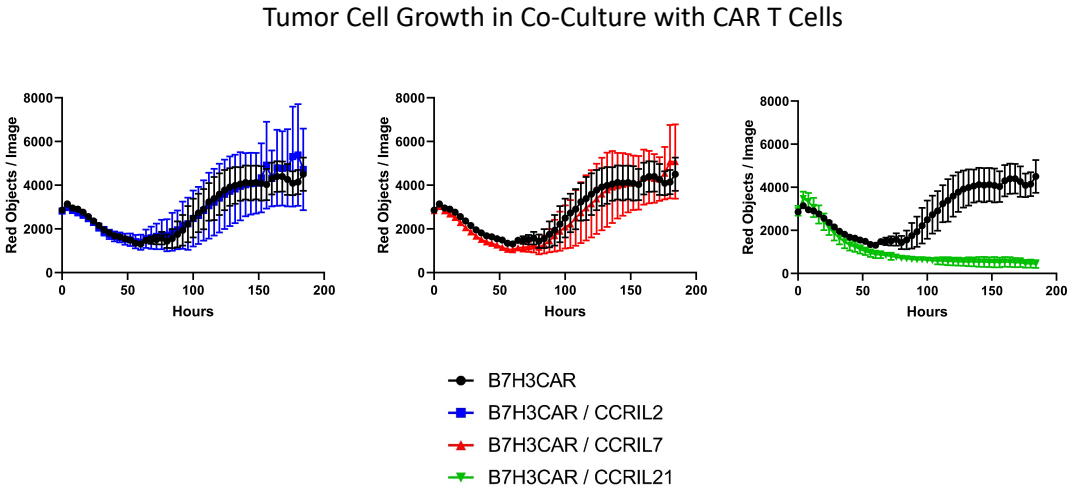
Tumor Cell Growth in Co-Culture with CAR T Cells
Red Objects / Image
Hours
B7H3CAR
B7H3CAR / CCRIL2
B7H3CAR / CCRIL7
B7H3CAR / CCRIL21

b)

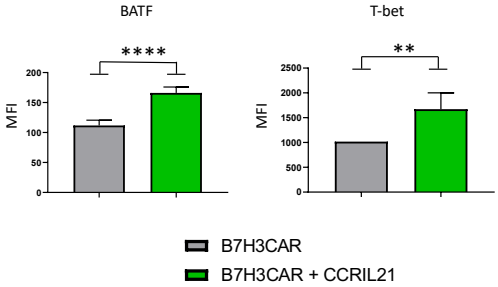
BATF
T-bet
MFI
****
**
B7H3CAR
B7H3CAR + CCRIL21

c)

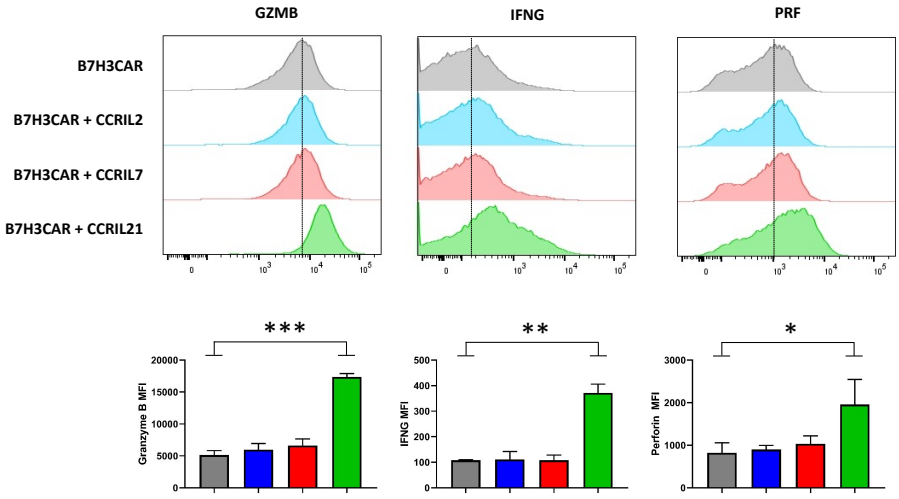
GZMB
IFNG
PRF
B7H3CAR
B7H3CAR + CCRIL2
B7H3CAR + CCRIL7
B7H3CAR + CCRIL21
***
**
*
Granzyme B MFI
IFNG MFI
Perforin MFI

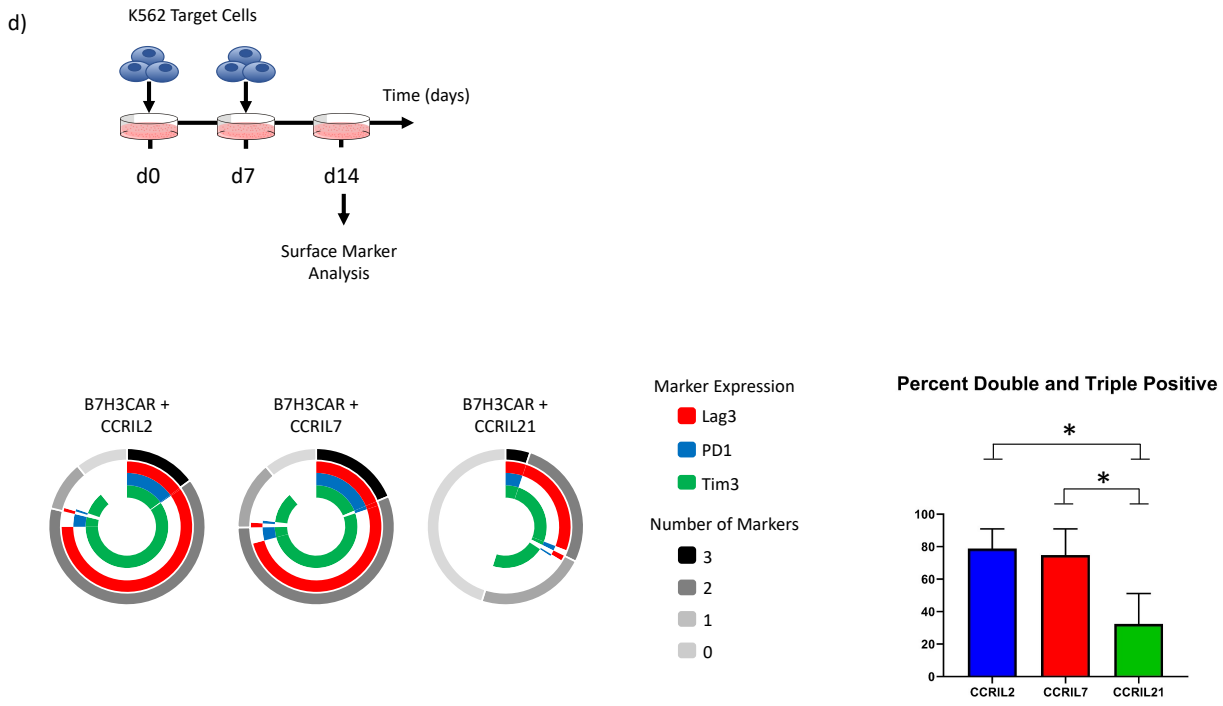

Figure 3: CCRIL21 primes CD8⁺ CAR T cells for sustained effector function. a, K562 tumor cell growth when co-cultured with CAR T cell populations for 7 days (1:2 T cell to tumor cell ratio). Tumor presence was monitored by fluorescent live cell imaging of mCherry-expressing K562 cells. **b**, CCRIL21 signaling upon T cell activation leads to the upregulation of Tbet and BATF. Cells were co-cultured with K562 cells and analyzed by intracellular flow cytometry 24 hours later. **c**, Expression of Granzyme B, IFNg, and Perforin proteins by intracellular flow cytometry after CAR T cells were co-cultured with K562 tumor cells for 6 hours. Histograms display results from one biological replicate, and bar graphs display average MFI and standard deviation using three biological replicates. **d**, Percentage of T cell population expressing Lag3, PD1 and Tim3 post serial challenges with K562 target cells. Asterisks indicate p-values derived from one-way ANOVA tests: *p < 0.05 **p < 0.01 ***p < 0.001.

CCRIL2 and CCRIL7 Enhance Subcutaneous Neuroblastoma Elimination by CD8⁺ CAR T Cells

To examine the effects of CCR expression on CAR T cell efficacy *in vivo*, we intravenously injected CD8⁺ CCR-expressing B7H3CAR T cells into NSG mice bearing subcutaneous human Be2 neuroblastoma tumors. CCRIL2 and CCRIL7-expressing CAR T cells extended tumor-free survival of mice compared to T cells expressing CAR alone (**Fig. 4a**). Bioluminescent imaging allowed *in vivo* tracking and relative quantification of T cells expressing the firefly luciferase (ffluc)

transgene. CCRIL2 and CCRIL7 expression led to greater accumulation and persistence of B7H3CAR T cells in mice (**Fig. 4b**), suggesting that the mitogenic and pro-survival tendencies promoted by these receptors allow for a robust anti-tumor response.

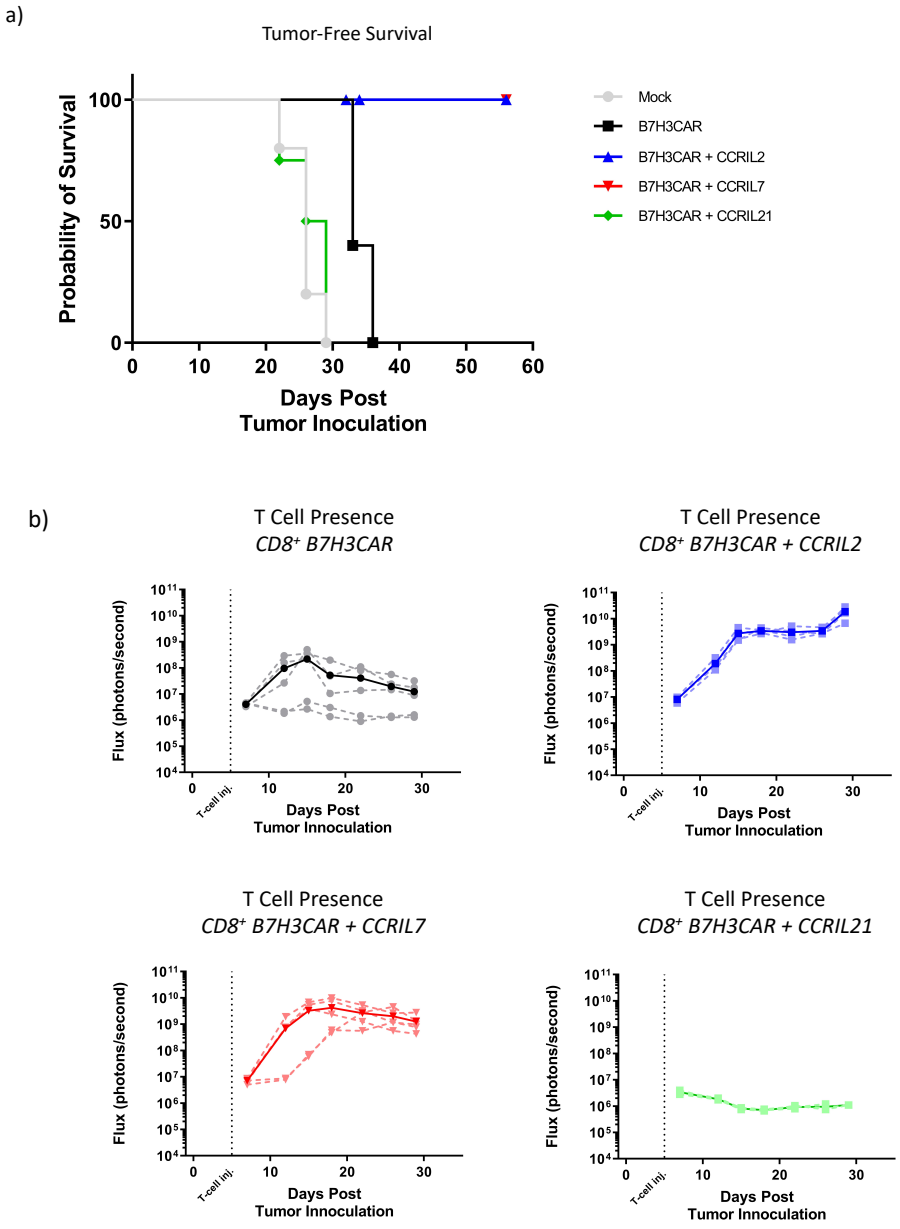

Figure 4: CCRIL2 and CCRIL7 enhance subcutaneous neuroblastoma elimination by CD8⁺ CAR T cells. a, Kaplan Meier tumor-free survival curve of neuroblastoma-bearing mice treated with experimental T cell groups. Each group contained four or five mice that were implanted with two flank tumors each. **b**, T cell presence as measured by bioluminescent imaging.

DISCUSSION

While each CCR mediates a distinct set of signaling outputs, CCRIL2 and CCRIL7 promote similar CAR T cell behaviors, including increased growth upon tumor exposure and resistance to apoptosis via upregulation of BCL2. CCRIL21, in contrast, did not promote CAR T cell expansion nor survival but rather heightened cytotoxicity and decreased expression of inhibitory receptors. The lack of CAR T cell expansion evoked by CCRIL21 may be attributed to STAT3-mediated inhibition of IL-2 production.[28] While the subcutaneous neuroblastoma tumor model employed here heightened the advantages of CAR T cells expressing CCRIL2 or CCRIL7, other contexts may favor CCRIL21-expressing cells. For example, CCRIL21 may prove more effective in supplementing CAR T cells against tumors with high levels of inhibitory ligands and low levels of CAR target-antigen. CCR technology provides insights into the effects of various cytokine stimuli on CAR T cell capacities and offers a promising platform for tailoring cytokine signaling profiles to fit the therapeutic niches of specific solid tumors in the future.

ACKNOWLEDGEMENTS

I would like to thank my colleagues Niels Rekers Ph.D. and Michael Baldwin for assistance in planning and carrying out the *in vivo* studies described in this chapter. Jason Yokoyama provided crucial T cell culture expertise, and Adam Johnson Ph.D. provided guidance on experimental design and data synthesis. My research advisor and mentor Michael Jensen M.D. provided key insights and direction to the projects detailed in all chapters of this work.

REFERENCES

1. Subklewe, M., Von Bergwelt-Baildon, M. & Humpe, A. Chimeric Antigen Receptor T Cells: A Race to Revolutionize Cancer Therapy. *Transfus. Med. Hemotherapy* **46,** 15–24 (2019).
2. Porter, D. L. *et al.* Chimeric antigen receptor T cells persist and induce sustained remissions in relapsed refractory chronic lymphocytic leukemia. *Sci. Transl. Med.* **7**, 303ra139-303ra139 (2015).
3. Gutcher, I. & Becher, B. APC derived cytokines and T cell polarization in autoimmune inflammation. *J. Clin. Invest.* **117**, 1119–27 (2007).
4. Lim, W. A. & June, C. H. The Principles of Engineering Immune Cells to Treat Cancer. *Cell* **168**, 724–740 (2017).
5. Markley, J. C. & Sadelain, M. IL-7 and IL-21 are superior to IL-2 and IL-15 in promoting human T cell-mediated rejection of systemic lymphoma in immunodeficient mice. *Blood* **115**, 3508–19 (2010).
6. Zhang, L. *et al.* Improving adoptive T cell therapy by targeting and controlling IL-12 expression to the tumor environment. *Mol. Ther.* **19**, 751–759 (2011).
7. Alva, A. *et al.* Contemporary experience with high-dose interleukin-2 therapy and impact on survival in patients with metastatic melanoma and metastatic renal cell carcinoma. *Cancer Immunol. Immunother.* **65**, 1533–1544 (2016).
8. Rosenberg SA, Yang JC, Topalian SL, Schwartzentruber DJ, Weber JS, Parkinson DR, Seipp CA, Einhorn JH, White DE. Treatment of 283 consecutive patients with metastatic melanoma or renal cell cancer using high-dose bolus interleukin 2. JAMA. 1994; 271(12):907–913.
9. Subklewe, M., Von Bergwelt-Baildon, M. & Humpe, A. Chimeric Antigen Receptor T Cells: A Race to Revolutionize Cancer Therapy. *Transfus. Med. Hemotherapy* **46,** 15–24 (2019).
10. Moroz, A. *et al.* IL-21 enhances and sustains CD8+ T cell responses to achieve durable tumor immunity: comparative evaluation of IL-2, IL-15, and IL-21. *J. Immunol.* **173,** 900–9 (2004).
11. Vandana K, Surojit S. Regulation of Effector and Memory CD8 T Cell Differentiation by IL-2—A Balancing Act. Frontiers in Immunology. 2018; 9:2987.

12. Sockolosky, J. T. *et al.* Selective targeting of engineered T cells using orthogonal IL-2 cytokine-receptor complexes. *Science (80-.).* **359**, 1037–1042 (2018).
13. Schluns, K. S., Kieper, W. C., Jameson, S. C. & Lefrançois, L. Interleukin-7 mediates the homeostasis of naïve and memory CD8 T cells in vivo. *Nat. Immunol.* **1**, 426–32 (2000).
14. Tan, J. T. *et al.* IL-7 is critical for homeostatic proliferation and survival of naive T cells. *Proc. Natl. Acad. Sci. U. S. A.* **98**, 8732–7 (2001).
15. Melchionda, F. *et al.* Adjuvant IL-7 or IL-15 overcomes immunodominance and improves survival of the CD8+ memory cell pool. *J. Clin. Invest.* **115**, 1177–87 (2005).
16. Xu, Y. *et al.* Closely related T-memory stem cells correlate with in vivo expansion of CAR.CD19-T cells and are preserved by IL-7 and IL-15. *Blood* **123**, 3750–9 (2014).
17. Shum, T. *et al.* Constitutive Signaling from an Engineered IL7 Receptor Promotes Durable Tumor Elimination by Tumor-Redirected T Cells. *Cancer Discov.* **7**, 1238–1247 (2017).
18. Kagoya, Y. *et al.* A novel chimeric antigen receptor containing a JAK–STAT signaling domain mediates superior antitumor effects. *Nat. Med.* **24**, 352–359 (2018).
19. Hunter, M. R., Prosser, M. E., Mahadev, V., Wang, X., Aguilar, B., Brown, C. E., … Jensen, M. C. (2013). Chimeric γc cytokine receptors confer cytokine independent engraftment of human T lymphocytes. *Molecular Immunology*, *56*(1–2), 1–11. https://doi.org/10.1016/j.molimm.2013.03.021
20. Yi, J. S., Du, M. & Zajac, A. J. A Vital Role for Interleukin-21 in the Control of a Chronic Viral Infection. *Science (80-.).* **324**, 1572–1576 (2009).
21. Fröhlich, A. *et al.* IL-21R on T cells is critical for sustained functionality and control of chronic viral infection. *Science* **324**, 1576–80 (2009).
22. Dong, P., Xiong, Y., Yue, J., Hanley, S. J. B. & Watari, H. B7H3 as a promoter of metastasis and promising therapeutic target. *Front. Oncol.* **8**, 1–8 (2018).
23. Akbar, A. N. *et al.* Interleukin-2 receptor common gamma-chain signaling cytokines regulate activated T cell apoptosis in response to growth factor withdrawal: selective induction of anti-apoptotic (bcl-2, bcl-xL) but not pro-apoptotic (bax, bcl-xS) gene expression. *Eur. J. Immunol.* **26,** 294–9 (1996).

24. Sutherland, A. P. R., Joller, N., Michaud, M., Liu, S. M., Kuchroo, V. K., & Grusby, M. J. (2013). IL-21 Promotes CD8+ CTL Activity via the Transcription Factor T-bet. *The Journal of Immunology*, *190*(8), 3977–3984. https://doi.org/10.4049/jimmunol.1201730
25. Xin, G., Schauder, D. M., Lainez, B., Weinstein, J. S., Dai, Z., Chen, Y., … Cui, W. (2015). A Critical Role of IL-21-Induced BATF in Sustaining CD8-T-Cell-Mediated Chronic Viral Control. *Cell Reports*, *13*(6), 1118–1124. https://doi.org/10.1016/j.celrep.2015.09.069
26. Wang, X. *et al.* Phenotypic and functional attributes of lentivirus-modified CD19-specific human CD8+ central memory T cells manufactured at clinical scale. *J. Immunother.* **35,** 689–701 (2012).
27. Krutzik, P. O. & Nolan, G. P. Intracellular phospho-protein staining techniques for flow cytometry: Monitoring single cell signaling events. *Cytometry* **55A,** 61–70 (2003).
28. Oh, H. M. *et al.* STAT3 protein promotes T-cell survival and inhibits interleukin-2 production through up-regulation of class O forkhead transcription factors. *J. Biol. Chem.* **286,** 30888–30897 (2011).

Chapter 2: Combining IL-7 and IL-21 Signaling Outputs

ABSTRACT

Our examination of the chimeric cytokine receptors (CCRs) in Chapter 1 highlighted the distinct T cell capacities conferred by different cytokine inputs. CCRIL2 and CCRIL7 promoted CAR T cell growth and survival, while CCRIL21 promoted heightened cytotoxicity and dampened expression of inhibitory receptors. Here, we hypothesize that CAR T cells exhibiting both CCRIL2/CCRIL7 and CCRIL21-promoted characteristics will outperform CAR T cells exhibiting either set of characteristics alone. Several previous studies have shown stimulating CAR T cells with multiple cytokine signals promotes beneficial characteristics,[1-3] and the modularity of the CCR signaling platform offers a promising means to investigate new hybrid cytokine signaling profiles. This chapter explores methods to combine cytokine signaling cascades with the eventual goal of investigating how combinatorial signaling impacts CAR T cell capacities.

MATERIALS AND METHODS

Hybrid Cytokine Receptor Design. The cytokine-independent receptor for IL-7 signaling (CIndR7) was designed by linking sequences encoding three protein domains: 1) the extracellular domain of a truncated version of Her2, Her2tG,[4] 2) the transmembrane domain of IL7R featuring a cysteine insertion,[5] and 3) the native intracellular domain of IL7R. Variants of the hybrid receptor CIndR7/21 were generated by appending a peptide from the IL21R to the C-terminus of CIndR7. The IL21R peptide (IL21Rpep) sequence was selected from the endogenous IL21R sequence for incorporation into hybrid cytokine receptor designs. IL21Rpep contains the "YLRQ" signaling

motif, and protein flexibility prediction software was used to set the bounds for the peptide.[6] IL21Rpep was appended to the C-terminus of other synthetic cytokine receptors via a flexible linker region. Flexible linker sequences included triple glycine (GGG), quadruple glycine serine (GGGGS), quadruple glycine serine in duplicate (GGGGSGGGGS), and quadruple glycine serine in triplicate (GGGGSGGGGSGGGGS). Sequence fragments were amplified via PCR and inserted via Gibson assembly into the epHIV7.2 lentiviral packaging plasmid.

Lentivirus Production. Recombinant lentivirus was generated by transiently transfecting a 293T producer cell line with lentiviral packaging plasmids alongside a transfer plasmid containing the transgenes of interest. Transfection was performed using Lipofectamine 2000 (Life Technologies, Cat. # 11668-500). Four days after transfection, lentivirus was isolated from the 293T cell culture supernatant via ultracentrifugation and stored at -80° C until the day of transduction. Co-packaged lentivirus was generated using a mix of two transfer plasmids combined at a 1 to 1 molar ratio.

T Cell Production and Culture. Protocols to acquire human cells were approved by the institutional review board of Seattle Children's Hospital. $CD8^+$ T cells were isolated from human peripheral blood mononuclear cells (PBMCs) by magnetic activated cell sorting with a $CD8^+$ T cell isolation kit (Miltenyi Biotech, Cat. # 130-096-495). The cells were immediately subjected to a bead-based CD3/CD28 stimulation using Dynabeads (Thermo Fisher Scientific, Cat. # 11131D) at a bead to cell ratio of 1:1. Unless otherwise indicated, T cell culture media consisted of RPMI 1640 (Gibco, Cat. # 22400-089) supplemented with 10% FBS (Hyclone, Cat. # SH30071.03), 2mM

L-glutamine (Gibco, 25030-081), 50 U/mL IL-2 (Chiron, Cat. # 53905-991-01) and 0.5 ng/mL IL-15 (Miltenyi, Cat. # 130-095-765) throughout the culture period. Two days post-stimulation, cells were transduced with lentivirus housing synthetic cytokine receptor genes.

Flow Cytometry. Flow cytometric analysis was performed to determine transduction marker expression and phenotypic surface marker expression. Cells were removed from culture and placed into 96-well round-bottom plates, washed twice with PBS (Gibco, Cat. # 10010-023), stained with pre-titered quantities of antibody, washed three more times with PBS and finally fixed with 0.5% paraformaldehyde (Electron Microscopy Sciences, Cat. # 15713) in PBS before analysis. Flow cytometric data was collected using a BD LSRFortessa flow cytometer and later analyzed using FlowJo software. Final flow plots were populated by cell populations remaining after the following gating strategy was performed. First, a "lymphocyte" gate was generated by drawing a polygon within the forward scatter vs side scatter scatterplot to isolate events with size and granularity characteristic of lymphocytes and remove debris and dead cell events. Within the lymphocyte gate, a second "single cell" gate was generated by gating on events that followed a linear relationship between forward scatter in the height and area dimensions to remove cell doublets from downstream analysis. If applicable, a "live cells" gate was generated using the live dead stain to exclude cells with compromised membranes.

Phospho-Flow. Phosphorylation status of signaling proteins was assessed by flow cytometry. Cells were pre-stained with FITC-conjugated anti-CD19 (BioLegend, Cat. # 302256) for later gating on $CD19^{+}$ cell populations. Cells were then returned to cell culture media and controls

were treated with IL-2 (50 U/mL) or IL-21 (10 ng/mL) for 20 minutes at 37 C. One volume of pre-warmed BD Cytofix solution (BD, Cat. # 554655) was added to the culture media Concentrated paraformaldehyde (Electron Microscopy Sciences, Cat. # 15713) was added directly to culture and the cells were returned to 37 C for 10 minutes. Finally, the cells were washed with PBS, permeabilized using pre-chilled BD Perm Buffer III (BD, Cat. # 558050) and stained with anti-phosphoSTAT3 (BioLegend, Cat. # 651004) and anti-phosphoSTAT5 (BD, Cat. # 612599) antibodies.

STAT3 Reporter Assays in Jurkat Cells. A STAT3 reporter lentiviral construct was constructed by inserting six copies of a STAT3 transcriptional responsive element upstream of GFP/ffluc in the epHIV7.2 lentiviral packaging plasmid. A STAT3 reporter cell line was generated by transducing Jurkats with lentivirus housing this construct. The Lonza Cell Line Nucleofector Kit V (Lonza, Cat. # VCA-1003) and a Nucleofector II device were used to introduce synthetic cytokine receptor constructs into the STAT3 reporter cell line according to the manufacturer's optimized protocol for Jurkat cells. STAT3 signaling was quantified 16-24 hours later by flow cytometric measurement of GFP fluorescent intensity within the sub-population of cells expressing synthetic cytokine receptor surface markers.

RESULTS

Challenges of Co-Expressing CCR Proteins

In our first attempt to combine cytokine signaling profiles, we co-packaged lentivirus with transfer plasmids encoding both CCRIL7 and CCRIL21 (**Fig. 1a**). This method generates a

population of lentiviruses housing one or both transgenic sequences. Each CCR-bearing sequence also included a distinct cell surface marker sequence to allow for orthogonal detection of integration of each construct. A truncated CD19 (CD19t) and a truncated Her2 (Her2tG) were used to mark CCRIL7 and CCRIL21-expressing cells, respectively. Figure 1a displays a typical flow cytometric scatterplot of CD19t and Her2tG expression in Jurkat cells transduced with co-packaged lentivirus. The bar chart demonstrates the efficiency of this approach, with an average of only 34.1% double-positive cells within the population of cells expressing either of the two surface markers.

We then extrapolated the expected outcome of this approach in primary T cells by sampling the efficiency of three single-CCR lentiviral transductions of human $CD8^+$ T cells, which yielded an average transduction efficiency of 33.6% (**Fig. 1b**). By multiplying the expected proportion of dual-positive cells from Figure 1a, we calculate an average expected dual-positive population of 11.4%. Full characterization of T cell populations relies upon bulk population analysis, such as *in vivo* studies, necessitating the purification of double-CCR-positive cells. The difficulties posed by enriching a 11.4% dual-positive population in primary T cells would create a bottleneck in the T cell production process, extending the cell culture period and ultimately decreasing the relevancy of any subsequent findings to clinical application.

Given the challenges of co-packing CCR sequences on separate lentiviral constructs, we next designed an all-in-one CCRIL7 and CCRIL21-encoding sequence (**Fig. 1c**). The sequences for CCRIL7 and CCRIL21 were codon-diverged to decrease the tendency of homology-driven recombination. However, when this construct was packaged into lentivirus and introduced into Jurkat cells, it showed significantly lower lentiviral titers than single-CCR constructs. Low titer

viruses tend to cause more cell death than high titer viruses during transduction because the cells must be exposed to a proportionally larger volume of virus to achieve the same transduction efficiency. The all-in-one CCR construct yielded lentiviruses with titers too low to use in primary T cells, as the volume of virus needed to transduce would cause T cell death from over-exposure to lentivirus. Generally, constructs of this size are not impeded by the lentiviral genome size packaging limit but rather suffer from expression issues. While we did not investigate this possibility, it is likely that the low titers from this lentiviral construct reflect low expression rather than low integration efficiency. As a result, both strategies we explored to introduce full-length CCRIL7 and CCRIL21 proved too inefficient for use with primary human T cells.

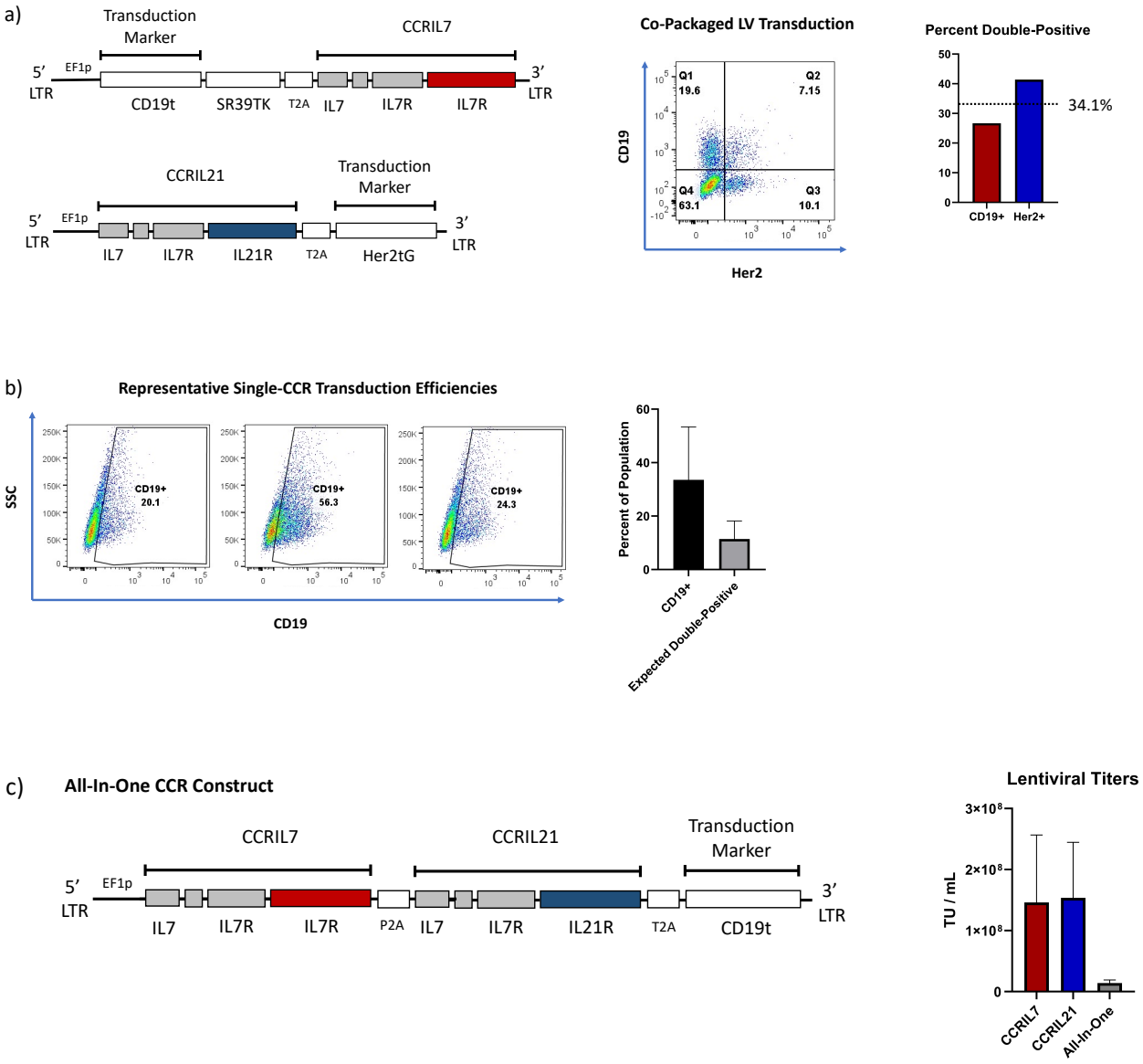

Figure 1: Challenges of Co-Expressing CCR proteins. a, Lentiviral constructs used to introduce CCRIL7 and CCRIL21 via viral co-packaging, flow cytometric analysis of marker expression in Jurkat cells transduced with co-packaged virus, and proportions of $CD19^{+}$ and $Her2^{+}$ cells found to be double-positive. **b**, Estimated percent dual-positive populations generated in primary human T cells based on three representative transduction efficiencies using single CCR-encoding lentiviruses. **c**, Design of an all-in-one CCRIL7/CCRIL21-encoding lentiviral construct and lentiviral titers of the all-in-one construct compared to single-CCR encoding lentiviruses.

Strategies to Build a Hybrid Receptor for IL-7 and IL-21 Signaling

Given the difficulties of introducing two full-length CCR transgenes into primary human T cells, we explored the possibility of generating a single synthetic cytokine receptor capable of driving the signaling outputs of IL-7 and IL-21. As discussed in Chapter 1, we ascribe the increased cytotoxicity and sustained effector function of CCRIL21-expressing cells to the activation of transcription factors T-bet and BATF, respectively. These transcription factors become activated by IL-21 via STAT1 and STAT3, suggesting that imbuing CCRIL7 with STAT1 and STAT3 signaling capacity serve to blend the signaling profiles of IL-7 and IL-21.

STAT activation in gamma chain cytokine receptors occurs through a series of molecular events common to all members of the receptor family:[7] 1) Cytokine binding causes the association of the specific cytokine receptor with the common gamma chain receptor (γ_c); 2) Janus Kinase (JAK) proteins associated with Box 1 and Box 2 motifs in the cytoplasmic region of the cytokine receptors are subsequently brought into proximity and phosphorylate each other; 3) Phosphorylated JAKs then phosphorylate key tyrosine residues on the cytoplasmic tail of the cytokine receptors, creating docking sites for STAT proteins; 4) STATs bind to phosphorylated tyrosine motifs and are subsequently activated by phosphorylation; and 5) Activated STAT proteins dimerize and translocate into the nucleus as transcription factors to alter gene expression.

A tyrosine-containing motif ("YLRQ") in the cytoplasmic domain of the IL21R has been shown to be necessary for the activation of STAT1 and STAT3 by IL-21 (**Fig. 2a**).[8] We developed four strategies to introduce this signaling motif into the CCRIL7 sequence (**Fig. 2b**): 1) Create an insertion into an existing "YQ" sequence; 2) Substitute the middle two amino acids from an

existing “YQNQ” sequence; 3) Replace the distal cytoplasmic peptide with a 38-amino acid peptide from IL21R (IL21Rpep) containing the STAT1/STAT3 signaling motif; or 4) Append the IL21Rpep to the C-terminus of CCRIL7 via a triple-glycine linker. We selected these approaches to cover a range of alterations from minimal to drastic changes in protein structure. Strategies involving IL21Rpep were included to account for the possibility that the IL21R microstructure surrounding the STAT1/STAT3 signaling motif may play an important role in signaling activity. Replacement of the distal IL7R peptide with IL21Rpep was specifically included with the goal of introducing the STAT1/STAT3 signaling motif in closer proximity to the Box 1 and Box 2 motifs, potentially increasing susceptibility of bound STAT proteins to activation by JAKs. All strategies avoided disruption of the key STAT5 signaling motif in the IL7R cytoplasmic region at Y449 to preserve the native signaling of CCRIL7.

We generated a STAT3-responsive Jurkat reporter cell line to examine the signaling capacity of our modified CCRIL7 proteins. We used lentivirus to introduce a cassette encoding GFP with an upstream promoter consisting of a series of STAT3-responsive elements. Next, we introduced our panel of CCRIL7/21 candidate transgenes into the Jurkat reporter line via electroporation. Cells expressing CCRIL7/21 candidates were selectively examined by flow cytometry and the GFP median fluorescence intensity (MFI) was collected to quantify STAT3 signaling activity. Only CCRIL7/21 candidates including IL21Rpep achieved elevated levels of STAT3 signaling compared to un-altered CCRIL7 (**Fig. 2c**). To minimize the structural changes to the CCRIL7 sequence, we selected the CCRIL7 with IL21Rpep appended via a triple glycine linker (CCRIL7-G3-IL21Rpep) as the candidate for further study (**Fig. 2d**).

We then examined the ability of CCRIL7-G3-IL21Rpep to activate IL-7 and IL-21 signaling events in primary T cells. Lentivirus was used to introduce the synthetic receptor into primary human $CD8^+$ T cells, and flow cytometric analysis was used to quantify the presence of phosphorylated STAT3 (pSTAT3) and phosphorylated STAT5 (pSTAT5). Un-altered CCRIL7 predominantly increases pSTAT5, while CCRIL21 predominantly increases pSTAT3. Unexpectedly, the introduction of the IL21Rpep to CCRIL7 did not lead to higher levels of pSTAT3 and slightly decreased levels of pSTAT5 (**Fig. 2e**). Despite the STAT3 signaling activity detected in Jurkat cells, CCRIL7-G3-IL21Rpep failed to show STAT3 activation in primary T cells, demonstrating the need for an alternative approach to combining IL-7 and IL-21 signaling profiles.

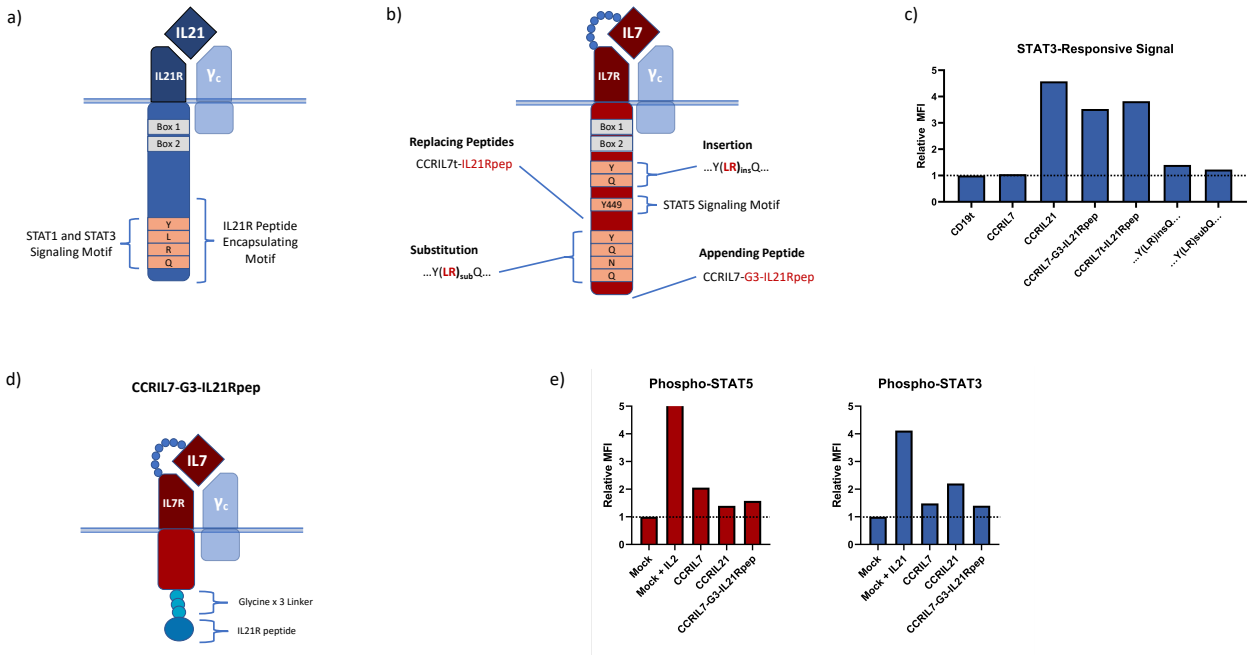

Figure 2: Strategies to build a hybrid receptor for IL-7 and IL-21 signaling. a, Endogenous IL21R activation of STAT1 and STAT3 is mediated by a "YLRQ" motif in the cytoplasmic tail. **b**, Strategies to introduce the STAT1/STAT3 signaling motif into the cytoplasmic domain of CCRIL7. **c**, Flow cytometric assessment of STAT3 signaling by CCRIL7-IL21R hybrid receptors using a Jurkat reporter cell line with GFP under regulation by STAT3 responsive elements. **d**, The preeminent CCRIL7-IL21R hybrid receptor candidate. **e**, Flow cytometric quantification of phospho-STAT3 and phospho-STAT5 in primary human $CD8^+$ T cells expressing CCRIL7, CCRIL21, or CCRIL7-G3-IL21Rpep, or treated with IL-2 (50 U/mL) or IL-21 (10ng/mL) for 20 minutes.

An Alternative Hybrid Cytokine Signaling Platform

As the CCR signaling platform was unable to achieve hybrid IL-7 and IL-21 signaling in primary human T cells, we searched for an alternative signaling platform. Leukemias often feature mutations to the IL7Ra gene which lead to the introduction of a cysteine residue into the transmembrane or extracellular juxtamembrane region.[9] These mutations lead to disulfide bonds between IL7Ra proteins, causing homodimer formation and subsequent IL7 signaling in the absence of IL7 cytokine (**Fig. 3a**). This class of IL7Ra mutations has been studied in the context of CAR T cell therapy, and CAR T cells equipped with an IL7Ra mutant led to greater clearance of human neuroblastoma and glioblastoma cells in mice, compared to CAR T cells without IL-7 signaling augmentation.[5] Because the IL7Ra mutant and CCRIL7 exhibit similar signaling profiles and effects on CAR T cells, we selected the IL7Ra mutant as a candidate for an alternative hybrid cytokine signaling platform.

To prepare the IL7R mutant for further investigation, we designed a sequence featuring the mutant IL7Ra transmembrane (with cysteine insertion) and cytoplasmic domains. We replaced the extracellular domain of IL7R with the extracellular domain of Her2tG for ease of surface staining, and the resultant transgene was dubbed the cytokine-independent receptor for IL-7 signaling (CIndR7) (**Fig. 3b**). We appended CIndR7 with a CD19t surface marker via a T2A ribosomal skip sequence and introduced the construct into Jurkat cells. Surface staining revealed that CIndR7 could be directly detected by flow cytometric quantification using anti-Her2 antibodies and that the expression level correlated with CD19t expression, as expected.

Building upon our initial successes in achieving STAT3 signaling in Jurkat cells using IL21pep-appended CCRIL7, we built the cytokine-independent receptor for IL-7 and IL-21

signaling (CIndR7/21) by appending the IL21R pep to CIndR7 via a triple glycine linker (**Fig. 3c**). Flow cytometric analysis of pSTAT3 and pSTAT5 in primary human $CD8^+$ T cells revealed that CIndR7/21, unlike CCRIL7-G3-IL21Rpep, achieved higher activation of STAT3 than its original synthetic receptor counterpart (**Fig. 3d**). The STAT5 signaling capacity of CIndR7 is also more robust than that of CCRIL7, suggesting that activation of STAT3 may only occur in hybrid receptors with a higher degree of signaling activity.

Hypothesizing that the length of the linker between IL7R C-terminus and IL21Rpep may impact STAT3 signaling activity, we created a panel of linker variants including a triple glycine, a quadruple glycine serine (GGGGS), GGGGS in duplicate, and GGGGS in triplicate. Flow cytometric analysis revealed that the GGGGS duplicate linker demonstrated the highest STAT3 and STAT5 signaling activity, so this linker will be used as the default linker for subsequence CIndR7/21 constructs. In conclusion, we have developed a novel hybrid cytokine receptor combining the signaling outputs of IL-7 and IL-21. Future studies will examine whether CIndR7/21 can achieve the downstream effects on T cells achieved separately by IL-7 and IL-21 signaling.

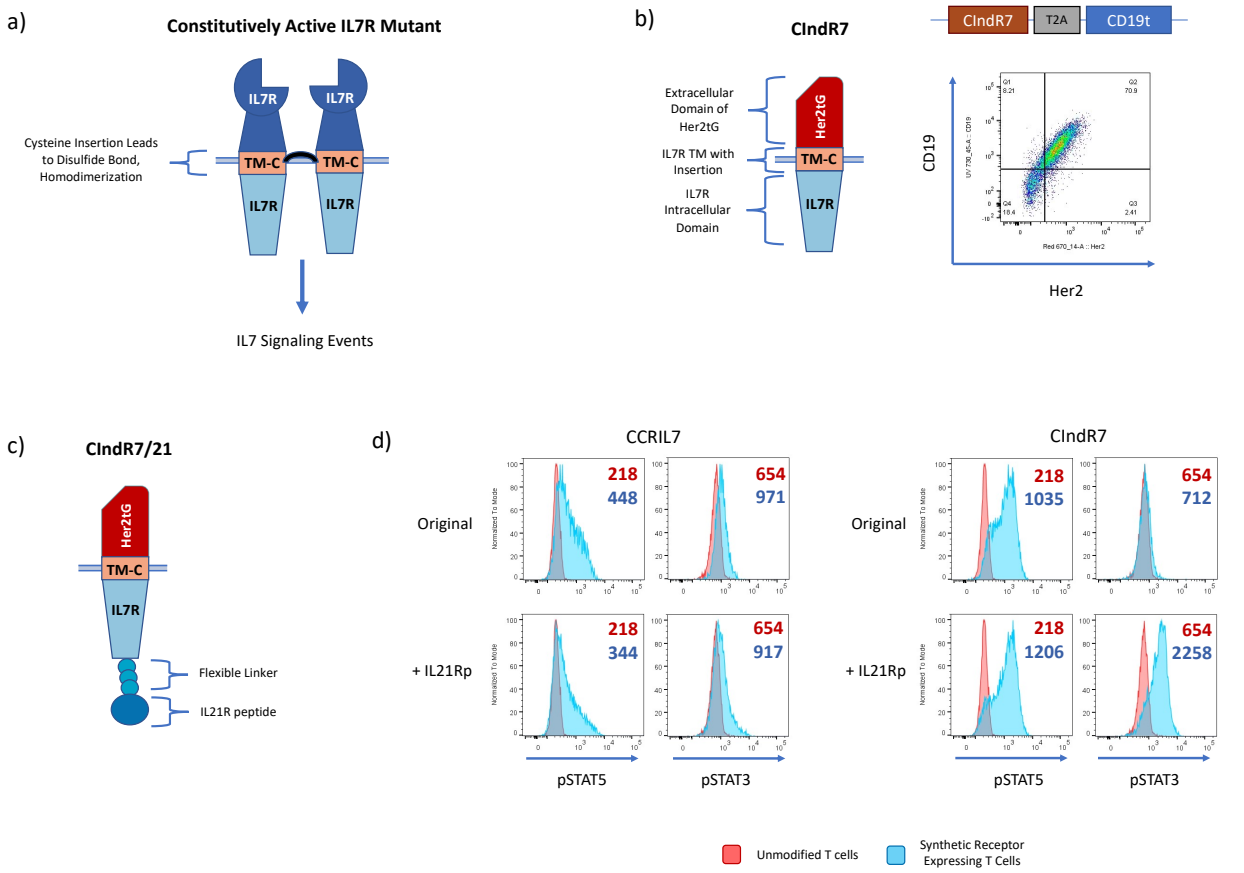

Figure 3: An Alternative Hybrid Cytokine Signaling Platform. **a**, Naturally occurridng IL7R mutants mediate constitutive IL-7 signaling in the absence of cytokine. **b**, Schematic of the cytokine-independent receptor for IL-7 signaling (CIndR7), and surface staining of Jurkat cells transduced with a lentiviral construct encoding CIndR7 with an appended CD19t marker protein. **c**, Schematic of cytokine-independent receptor for IL-7 and IL-21 signaling (CIndR7/21). **d**, Flow cytometric quantification of phospho-STAT3 and phospho-STAT5 in CCRIL7 and CIndR7, each with and without appended IL21Rpep, in primary human $CD8^+$ T cells. **e**, Effects of linker structure on STAT activation by CIndR7/21, quantified by flow cytometry as in part d.

DISCUSSION

The invention of a hybrid IL-7 and IL-21 receptor prompts future studies to examine the effects of this receptor on CAR T cell activity. We will modify primary human T cells to express CIndR7/21 alongside a CAR and investigate whether these cells exhibit the proliferative and pro-survival behavior ascribed to IL-7 and the heightened cytotoxicity and sustained effector function ascribed to IL-21. The addition of STAT3 activation by appending an IL21R peptide to IL7R highlights the modularity of cytokine receptor signaling domains. Further work may reveal that the CIndR platform is amenable to modification with other cytokine signaling domains with accompanying effects on CAR T cell activity.

ACKNOWLEDGEMENTS

My research advisor and mentor Michael Jensen M.D. provided key insights and direction to the projects detailed in all chapters of this work.

REFERENCES

1. Zhou, J. *et al.* Chimeric antigen receptor T (CAR-T) cells expanded with IL-7/IL-15 mediate superior antitumor effects. *Protein Cell* **10**, 764–769 (2019).
2. Luo, H. *et al.* Coexpression of IL7 and CCL21 Increases Efficacy of CAR-T Cells in Solid Tumors without Requiring Preconditioned Lymphodepletion. *Clin. Cancer Res.* **26**, 5494–5505 (2020).
3. Kagoya, Y. *et al.* A novel chimeric antigen receptor containing a JAK–STAT signaling domain mediates superior antitumor effects. *Nat. Med.* **24**, 352–359 (2018).
4. Johnson, A. J. *et al.* Rationally Designed Transgene-Encoded Cell-Surface Polypeptide Tag for Multiplexed Programming of CAR T-cell Synthetic Outputs. *Cancer Immunol. Res.* **9,** 1047–1060 (2021).

5. Shum, T. *et al.* Constitutive Signaling from an Engineered IL7 Receptor Promotes Durable Tumor Elimination by Tumor-Redirected T Cells. *Cancer Discov.* **7,** 1238–1247 (2017).
6. Bornot, A., Etchebest, C. & De Brevern, A. G. Predicting protein flexibility through the prediction of local structures. *Proteins Struct. Funct. Bioinforma.* **79,** 839–852 (2011).
7. Waickman, A. T., Park, J.-Y. & Park, J.-H. The common γ-chain cytokine receptor: tricks-and-treats for T cells. *Cell. Mol. Life Sci.* **73,** 253–69 (2016).
8. Zeng, R. *et al.* The molecular basis of IL-21–mediated proliferation. *Blood* **109,** 4135–4142 (2007).
9. Zenatti, P. P. *et al.* Oncogenic IL7R gain-of-function mutations in childhood T-cell acute lymphoblastic leukemia. *Nat. Genet.* **43,** 932–941 (2011).

Chapter 3: Hybrid Cytokine Receptors Amplify CAR T Cell Anti-Tumor Potency

ABSTRACT

CAR T cell therapy requires robust activation of T cells to ensure sufficient expansion and persistence within patients. Chimeric antigen receptors (CARs) recapitulate signaling through the T cell receptor (TCR) and costimulatory signals, but optimal T cell activation requires a third signal: cytokine stimulation. In Chapter 1, we examined the impact of three cytokine signals on CAR T cells and discovered that cytokines confer distinct and potentially complementary effects. Based on our studies of gamma chain cytokines, we hypothesized that CAR T cells receiving IL-7 and IL-21 signaling would exhibit enhanced growth and functional durability. To this end, we combined IL7R and IL21R signaling modules into a hybrid cytokine receptor in Chapter 2. Here, we iterate on the hybrid cytokine receptor platform to generate three variants with specific combinations of IL-7 and IL-21 signaling outputs. Anti-CD19 CAR T cells equipped with hybrid cytokine receptors demonstrate enhanced ability to proliferate, resist apoptosis, and lyse tumor cells *in vitro*. Specifically, hybrid receptors providing STAT3 activation demonstrate the most notable functional enhancements, and STAT5 signaling proved dispensable for these effects. In addition, STAT3-signaling receptors delay T cell differentiation, heighten expression of quiescence-associated genes, and dampen expression of exhaustion-associated genes. Administration of CAR T cells to leukemia bearing mice demonstrated superior anti-tumor potency from CAR T cells supplemented with STAT3-signaling hybrid cytokine receptors. The combination of STAT5 and STAT3 activation led to the greatest CAR T cell engraftment but also triggered unrestricted T cell

growth and toxicity. Our findings highlight the potential of combinatorial cytokine signaling to amplify CAR T cell anti-tumor potency.

MATERIALS AND METHODS

Construct Design. The hybrid cytokine receptor sequences included four variants: Marker-Only control, CIndR7, CIndR7/21, and CIndR21. The Marker-Only control sequence consisted of a truncated version of Her2, Her2tG.[1] As detailed in Chapter 2, the CIndR7 sequence consisted of the Her2tG extracellular domain, a mutant IL7R transmembrane domain with a cysteine-containing insertion, and the native IL7R intracellular domain. CIndR7/21 was created by appending a peptide sequence from the IL21R to the end of the CIndR7 intracellular domain sequence. Finally, CIndR21 was created by mutating the CIndR7/21 sequence to replace the tyrosine sequence at position 449 in the native IL7R sequence with a sequence encoding phenylalanine. All hybrid cytokine receptor sequences were introduced into a construct featuring a piggyBac transposon for integration into the genome.[2] The piggyBac construct harbored two divergent coding sequences: 1) A polycistronic sequence driven by the human elongation factor 1 alpha (EF1α) promoter encoding the human G01S anti-CD19CAR,[3] followed by a P2A ribosomal skip sequence,[4] a double mutant of the dihydrofolate reductase (DHFRdm) for drug selection,[5] a T2A ribosomal skip sequence, and finally a truncated epidermal growth factor receptor (EGFRt) to serve as cell surface marker;[6] and 2) an upstream sequence encoding each CIndR variant and driven by the MND promoter.[7]

T Cell Production and Culture. Protocols to acquire human cells were approved by the institutional review board of Seattle Children's Hospital. $CD4^+$ and $CD8^+$ T cells were isolated from whole blood using a STEMCELL RoboSep-S automated cell separation instrument according to manufacturer's protocols. Flow-through from the T cell sorting was subjected to a LymphoPrep (STEMCELL, Cat. # 07811) overlay centrifuge-based protocol for the isolation of residual peripheral blood mononucleated cells (PBMCs). PiggyBac transposon constructs and RNA encoding transposase were introduced into T cells by electroporation using a Lonza 4D-Nucleovector instrument and the P3 Primary Cell Kit (Lonza, Cat. # V4XP-3032). Electroporated T cells were immediately seeded into 24-well G-Rex plates (Wilson Wolf, Cat. # 80240M) along with donor-matched PBMC feeder cells. Culture media consisted of X-Vivo 15 (Lonza, Cat. # BP04-744Q) supplemented with 2% KnockOut Serum Replacement (ThermoFisher, Cat. # 10828-028) by volume, 4.6ng/mL IL-2 (STEMCELL, Cat. # 78220.3), 20ng/mL IL-4 (Miltenyi, Cat. # 130-093-924), 10ng/mL IL-7 (Miltenyi, Cat. # 130-095-363) and 20ng/mL IL-21 (Miltenyi, Cat. # 130-095-784). Unmodified T cell control conditions were cultured in the absence PBMCs and treated with a TransAct (Miltenyi, Cat. # 130-111-116) CD3/CD28 stimulation. Three days later, drug selection of modified T cells was begun by adding 50nM methotrexate (Accord, Cat. # NDC 16729-277-30) to the culture medium. 21 days after culture initiation, T cells were collected and cryopreserved in CryoStor CS5 (STEMCELL, Cat. # 07933) for subsequent studies. All post-production assays were conducted in complete RPMI media (cRPMI), which consisted of RPMI 1640 (Gibco, Cat. # 22400-089) supplemented with 10% FBS (Hyclone, Cat. # SH30071.03) and 2mM L-glutamine (Gibco, 25030-081). Unless otherwise noted, all subsequent studies were conducted after mixing $CD4^+$ and $CD8^+$ T cell groups to achieve a 1:1 starting ratio.

Flow Cytometry. Flow cytometric analysis was performed to determine transduction marker expression and phenotypic surface marker expression using the following generalized protocol. Cells were removed from culture and placed into 96-well round-bottom plates, washed twice with PBS (Gibco, Cat. # 10010-023), stained with antibodies specific for cell surface markers, washed two more times with PBS and finally fixed with 0.5% paraformaldehyde (Electron Microscopy Sciences, Cat. # 15713) in PBS before analysis. Flow cytometric data was collected using a BD LSRFortessa flow cytometer and later analyzed using FlowJo software. Final flow plots were populated by cell populations remaining after the following gating strategy was performed. First, a "lymphocyte" gate was generated by drawing a polygon within the forward scatter vs side scatter scatterplot to isolate events with size and granularity characteristic of lymphocytes and remove debris and dead cell events. Within the lymphocyte gate, a second "single cell" gate was generated by gating on events that followed a linear relationship between forward scatter in the height and area dimensions to remove cell doublets from downstream analysis. If applicable, a "live cells" gate was generated using the live dead stain to exclude cells with compromised membranes. Specific cell staining reagents are listed below, organized by context of the assay.

- Transgenic surface marker panel during T cell production: Erbitux APC (BD, Cat. # 624367), Herceptin PE (BD Cat. # 624255), Anti-CD3 BUV395 (BD, Cat. # 563546), Anti-CD4 BV785 (BioLegend, Cat. # 317442), Anti-CD8 Pacific Blue (BioLegend, Cat. # 344718) Live Dead Fixable Aqua viability dye (Thermo, Cat # L34957).

- Weekly tumor challenge panel for T cell tracking: Anti-CD4 APC-Cy7 (BioLegend, Cat. # 317418), Anti-CD8 Pacific Blue (BioLegend, Cat. # 344718), Fixable Viability Stain 520 (BD, 564407).
- T cell phenotypic characterization panel during tumor challenge assays: Anti-CD4 BV785 (BioLegend, Cat. # 317442), Anti-CD8 Pacific Blue (BioLegend, Cat. # 344718) Live Dead Fixable Aqua viability dye (Thermo, Cat # L34957), Anti-CCR7 FITC (BioLegend, Cat. # 353215), Anti-CD45RA BV786 (BD, Cat. # 741010), Anti-CD45RO APC (BioLegend, Cat. # 304210), Anti-CD62L PE (BioLegend, Cat. # 304806).
- T cell activation and exhaustion marker panel during tumor challenge assays: Anti-CD4 BV785 (BioLegend, Cat. # 317442), Anti-CD8 Pacific Blue (BioLegend, Cat. # 344718) Live Dead Fixable Aqua viability dye (Thermo, Cat # L34957), Anti-TIGIT APC (BioLegend, Cat. # 372705).

Intracellular Cytokine Staining. T cells were co-cultured with mCherry-expressing Raji tumor cells at a 2:1 effector to tumor ratio for 6 hours. Immediately after cells were plated, a CD107a-specific flow cytometry antibody (BioLegend, Cat. # 328640) was added to the culture to detect degranulation. Two hours after the co-culture began, a transport inhibitor cocktail (ThermoFisher, Cat. # 00-4980-03) was added to prevent T cell release of secretory proteins. At the end of co-culture, the cells were incubated with 10 uL of Fc block (Miltenyi, Cat. # 130-059-901) for 10 minutes at room temperature to avoid indiscriminate antibody binding by tumor cells. Cells were then stained with Live Dead Fixable Near IR viability dye (ThermoFisher, Cat # L10119), anti-CD4 BUV737 (BD, Cat # 612748) and anti-CD8 Pacific Blue (BioLegend, Cat. # 344718) to allow

gating of live T cells. Next, samples were fixed and permeabilized using the Fixation/Permeabilization Kit (BD, Cat. # 554714) according to the manufacturer's protocol. After permeabilization, the cells were stained with antibodies specific for secretory proteins: Granzyme B (BD, Cat. # 396407), Interferon-gamma (BD, Cat. # 563731), TNF-alpha (BD, Cat. # 563996), IL-2 (BioLegend, Cat. # 500326), and Perforin (BioLegend, Cat. # 353303). Flow cytometric data was collected using a BD LSRFortessa flow cytometer and analyzed using FlowJo software.

Phospho-Flow Cytometry. $CD4^+$ T cells were harvested from culture fourteen days after electroporation and seeding with PBMC feeder cells. The cells were washed to remove residual cytokine from the culture medium and replated in cytokine-free media for 48 hours. After cytokine-free rest, the cells were moved into FACS tubes and stained with Live Dead Fixable Aqua Viability Dye (Invitrogen, Cat. # L34966). Cells were then resuspended in pre-warmed cRPMI media, and control groups received media with to 5ng/mL IL-7 (Miltenyi, Cat. # 130-095-363) or 5ng/mL IL-21 (Miltenyi, Cat. # 130-095-784) added. After a 20-minute incubation at 37° C, the cells were fixed using pre-warmed CytoFix (BD, Cat. # 554655), permeabilized using pre-chilled Perm Buffer III (BD, Cat. # 558050) and stained with anti-phosphoSTAT3 Alexa Fluor 647 (BD, Cat. # 557815) or anti-phosphoSTAT5 Alexa Fluor 647 (BD, Cat. # 612599). Samples were analyzed within 16 hours of staining to avoid signal loss.

Repeated CAR T Cell Stimulation Assays. The following protocol describes how T cells were subjected to recursive tumor stimulations, either on a weekly or a three-day basis. Twenty-one

days after initial electroporation, $CD4^+$ and $CD8^+$ CAR T cells were mixed at a 1:1 ratio and seeded for repeated tumor challenge assays. On day 0, mCherry-expressing Raji tumor cells were added to T cell cultures at a 2:1 effector to target ratio. Exogenous cytokine control cultures were supplemented with 5ng/mL IL-7 (Miltenyi, Cat. # 130-095-363), 5ng/mL IL-21 (Miltenyi, Cat. # 130-095-784), or both. At either day 3 or day 7, samples of each co-culture were harvested, and live cell counts were taken using a Cellaca MX cell counting instrument (Nexcelom Biosciences). Flow cytometry was performed, as described in the "flow cytometry" section above, to assess the composition of the culture between $CD4^+$ T cells, $CD8^+$ T cells, and $mCherry^+$ Raji tumor cells. Live T cell counts were back-calculated using the percent live cells in the culture accounted for by T cells multiplied by the total live cells according to cell counts. T cells were then reseeded in fresh media and tumor cells were again added at a 2:1 effector to target ratio. The counting and flow analysis process was repeated one additional time at the end of the assay. T cell growth curves were assembled by calculating fold expansion of each T cell group across both tumor stimulations.

Incucyte Cytotoxicity Assays. CAR T cell cytotoxicity was evaluated over a variable period of days using the S3 IncuCyte Live Cell Imager (Sartorius). To begin, ten thousand mCherry-expressing Raji tumor cells were cultured per well of a flat-bottom 96-well plate. Next, T cells were added at effector to tumor ratios of 2:1, 1:1, 0.5:1 or 0.25:1. Unless otherwise specified, all groups were cultured in cytokine-free media for these studies. Exogenous cytokine control cultures were supplemented with 5ng/mL IL-7 (Miltenyi, Cat. # 130-095-363), 5ng/mL IL-21 (Miltenyi, Cat. # 130-095-784), or both. Fluorescent and phase images of these co-cultures were collected every

four hours. IncuCyte image analysis software was used to quantify tumor presence over time by mCherry signal. Simultaneously, Incucyte "Cell by Cell" analysis software was used to discriminate "low-red" objects for tracking of T cell presence over the course of the assay. Two experimental schemas were employed: 1) T cell groups received one tumor challenge at day 0 and imaging proceeded for six days, and 2) T cell groups received five tumor challenges every three days and imaging proceeded for fifteen days. In the multi-challenge schema, ten thousand tumor cells were added per well during each challenge.

Cytokine-Free Growth and Apoptotic Status Assay. To assess cytokine-free T cell growth in the absence of antigen stimulation, T cell groups were subjected to a single tumor exposure and monitored for growth thereafter. CAR T cells were co-cultured with irradiated mCherry-expressing Raji cells at a 1:1 effector to target ratio. Seven days later, cultures were washed to remove secreted cytokines, flow cytometry confirmed the absence of residual $mCherry^{+}$ tumor cells, and T cells were returned to culture. Ten days after initial tumor exposure, T cells were harvested to assess cell health and apoptotic status using the PE Annexin V Apoptosis Detection Kit I (BD, Cat. # 559763) according to manufacturer's instructions. Live T cell concentrations were monitored intermittently thereafter until day 23 using a Cellaca MX cell counting instrument (Nexcelom Biosciences).

RNA-seq. CIndR-expressing CD19CAR T cells were co-cultured with mCherry-expressing Raji tumor cells at a 2:1 effector to target ratio in cRPMI media. One week later, the cells were removed from culture and labeled with anti-CD4 APC-Cy7 (BioLegend, Cat. # 317418) and anti-

CD8 Pacific Blue (BioLegend, Cat. # 344718) antibodies and a viability dye (BD, Cat. # 564407). Labeled cell populations were sorted for live $CD4^+$ and $CD8^+$ T cells using a Sony MA900 cell sorter, excluding $mCherry^+$ Raji tumor cells. Sorted cell populations were snap-frozen in liquid nitrogen and stored at -80° C.

RNA was isolated from cell pellets using Directzol RNA Miniprep (Zymo) including the optional DNase treatment. RNA quality was assessed using a 4150 TapeStation (Agilent) with an RNA 6,000 Nano Kit (Agilent). RNA sequencing libraries were made using the TruSeq Stranded mRNA kit (Illumina) according to manufacturer instructions. The resulting RNA-seq libraries' quality and concentration were assessed using the D1000 DNA Kit (Agilent) on the TapeStation and a Qubit Fluorometer with the Qubit dsDNA HS Assay Kit (Life Technologies). RNA-seq libraries were pooled and sequenced via paired end 150 bp reads using Genewiz's sequencing only service (HiSeq or Novaseq 6000) at a target depth of 25M reads per library (Illumina). RNA-seq was attempted on all cytokine samples, with libraries for 37 samples passing minimum quality metrics for inclusion in the analysis. RNA-seq data was analyzed using the nf-core RNA-seq pipeline version 3.4.[8] Briefly, reads were mapped to the human genome (GRCh38) using STAR aligner (v2.6.1d). Gene expression counts were generated using salmon (v1.5.2).

Differential gene expression. Differential gene expression analysis between two phenotypes (Cindr vs cytokine) was performed using edgeR version 3.32.1.[9] First, genes whose expression was very low in most samples were discarded from further analyses. Next, *estimateCommonDisp* and *estimateTagwiseDisp* were run to properly handle over-dispersion at the global and single gene level. Across samples, normalization was then performed

using TMM, via the function *calcNormFactors*. Differentially expressed genes were determined using the *exactTest* function, as those showing the multiple testing corrected FDR <0.05, a two-sided raw p value <0.01 and $|\log_2(\text{fold change})| >= 1$. The total number of expressed genes includes all genes present in at least two samples with normalized CPM (counts per million) of at least 1. PCA was performed using the log2-transformed, TMM-normalized expression values as input. PCA results were robust to the choice of the most variable genes used as input (range tested: 1,000 to 10,000).

Leukemia Xenograft Mouse Studies. T cells were cryopreserved for *in vivo* studies after being mixed to achieve a ~3:2 ratio of $CD4^+$ to $CD8^+$ T cells (Supp. Fig 4c). 11-13 week old NOD scid gamma (NSG) immunodeficient mice were injected via the tail vein with one million human leukemia Nalm-6 tumor cells, modified to express a fusion protein of mCherry and firefly luciferase. Six days after tumor injection, tumor engraftment in each mouse was quantified via bioluminescent imaging using an IVIS Spectrum In Vivo Imaging System (Perkin Elmer) and Living Image Software. Mice were then distributed into treatment groups to normalize average engraftment across groups as much as possible. Seven days after tumor injection, mice were injected via the tail vain with four million T cells. Thereafter, mice were monitored for tumor growth by bioluminescent imaging. Health metrics and weight changes were also recorded to capture effects of different T cell treatment groups. Mice were euthanized when they showed moderate to severe hind-limb paralysis, a result of unchecked tumor progression, or otherwise as recommended by veterinary staff. Beginning on day 17 and at weekly intervals thereafter, retro-orbital bleeds were performed to examine T cell engraftment in the peripheral blood.

T Cell Quantification in Retro-Orbital Bleed Samples. Peripheral blood samples were taken by retro-orbital bleeds of mice on a weekly basis, and the following flow cytometry protocol was performed to quantify T cells in the blood. 40uL of blood was moved into a 96 well plate. Remaining blood was pooled across samples and mixed with T cells from culture to serve as an FMO control staining mix. Other controls included T cell only samples and Nalm-6 only samples to allow for discrimination of these populations in the blood during analysis. Red blood cells were lysed using Pharm Lyse Buffer (BD, Cat. # 555899), and samples were treated with Fc blocking reagent (Miltenyi, Cat. # 130-059-901) to prevent indiscriminate antibody binding. Next, cells were stained with the following panel of reagents: anti-CD3 BUV737 (BD, Cat. # 612751), anti-human CD45 APC-Cy7 (BD, Cat. # 557833), anti-mouse CD45 PerCP/Cy5.5 (BioLegend, Cat. # 103132), and fixable viability stain 520 (BD, Cat. # 564407). Finally, samples were fixed in 0.5% paraformaldehyde (Electron Microscopy Sciences, Cat. # 15713) in PBS before analysis. CountBright absolute counting beads (Invitrogen, Cat. # 2207530) were added to each sample to allow for back-calculation of T cell counts per uL of blood analyzed. Flow cytometric data was collected using a BD LSRFortessa flow cytometer and analyzed using FlowJo software.

RESULTS

Modularly Designed Cytokine Receptors Provide Constitutive IL-7 and IL-21 Signaling in CAR T Cells

We developed a hybrid cytokine-independent receptor (CIndR) to provide constitutive IL-7 and IL-21 signaling in T cells. The CIndR protein is composed of four key domains, each imparting

a distinct functionality **(Fig. 1a)**. The extracellular portion of CIndR features a Her2 domain recognized by the Herceptin antibody, allowing for direct detection of CIndR on the cell surface by flow cytometry.[1] The CIndR transmembrane domain is a IL7R transmembrane a variant harboring a cysteine insertion, which facilitates auto-homodimerization via a disulfide bridge and subsequent constitutive signaling.[10] The IL7R intracellular domain and a tethered peptide from the IL21R were included to provide STAT5 and STAT3 signaling, respectively.

STAT5 and STAT3 activation both promote T cell survival,[11-13] but activation of STAT5 specifically supports T cell proliferation,[14] while activation of STAT3 specifically confers durable effector function.[15] We therefore hypothesized that supplementing CAR T cells with CIndR expression would bolster CAR T cell therapeutic potency by: 1) supporting robust CAR T cell expansion, 2) enhancing CAR T cell survival and persistence, and 3) promoting durable anti-tumor activity (**Fig. 1b**). The modular design of the CIndR protein allowed us to develop a panel of hybrid cytokine receptors featuring a variety of signaling capacities (**Fig. 1c**). We included a "Marker Only" receptor featuring no intracellular signaling domains as a placeholder control. Three signaling variants of CIndR were developed: 1) CIndR7 featured only the IL7R intracellular domain, activating predominantly STAT5, 2) CIndR7/21 featured the IL7R intracellular domain and the tethered IL21R peptide, activating STAT5 and STAT3, respectively, and 3) CIndR21 was an iteration of CIndR7/21 with an ablated STAT5 activation motif, conferring predominantly STAT3 activation.

These four transgenes were inserted into a divergent dual-promoter construct for simultaneous expression with an anti-CD19 CAR. Dual-promoter construct architecture was employed because initial attempts to express anti-CD19CAR and CIndRs from a single polycistron

failed to yield robust CIndR expression (**Supp. Fig 1a**). Constitutive promoters were vetted to achieve high expression from the CIndR cistron (**Supp. Fig 1b**). Introduction of these constructs into $CD4^+$ and $CD8^+$ T cells resulted in dual-positive populations expressing CIndRs, as marked by Her2tG, and the anti-CD19CAR-encoding polycistron, as marked by EGFRt (**Fig. 1d, Supp Fig 2a-c**). Next, we examined the ability CIndR-expressing cells to activate STAT3 and STAT5 via flow cytometry (**Fig. 1e**). As expected, compared to Marker-Only, CIndR7 and CIndR21 predominantly activated STAT5 and STAT3, respectively, matching activation patterns in controls treated with exogenous IL-7 and IL-21. CIndR7/21-expressing cells showed activation of both STAT3 and STAT5, achieving an IL-7 and IL-21 hybrid signaling pattern. Having built a hybrid cytokine receptor panel with three distinct signaling outputs, we went on to investigate how each receptor impacted CAR T cell functionality.

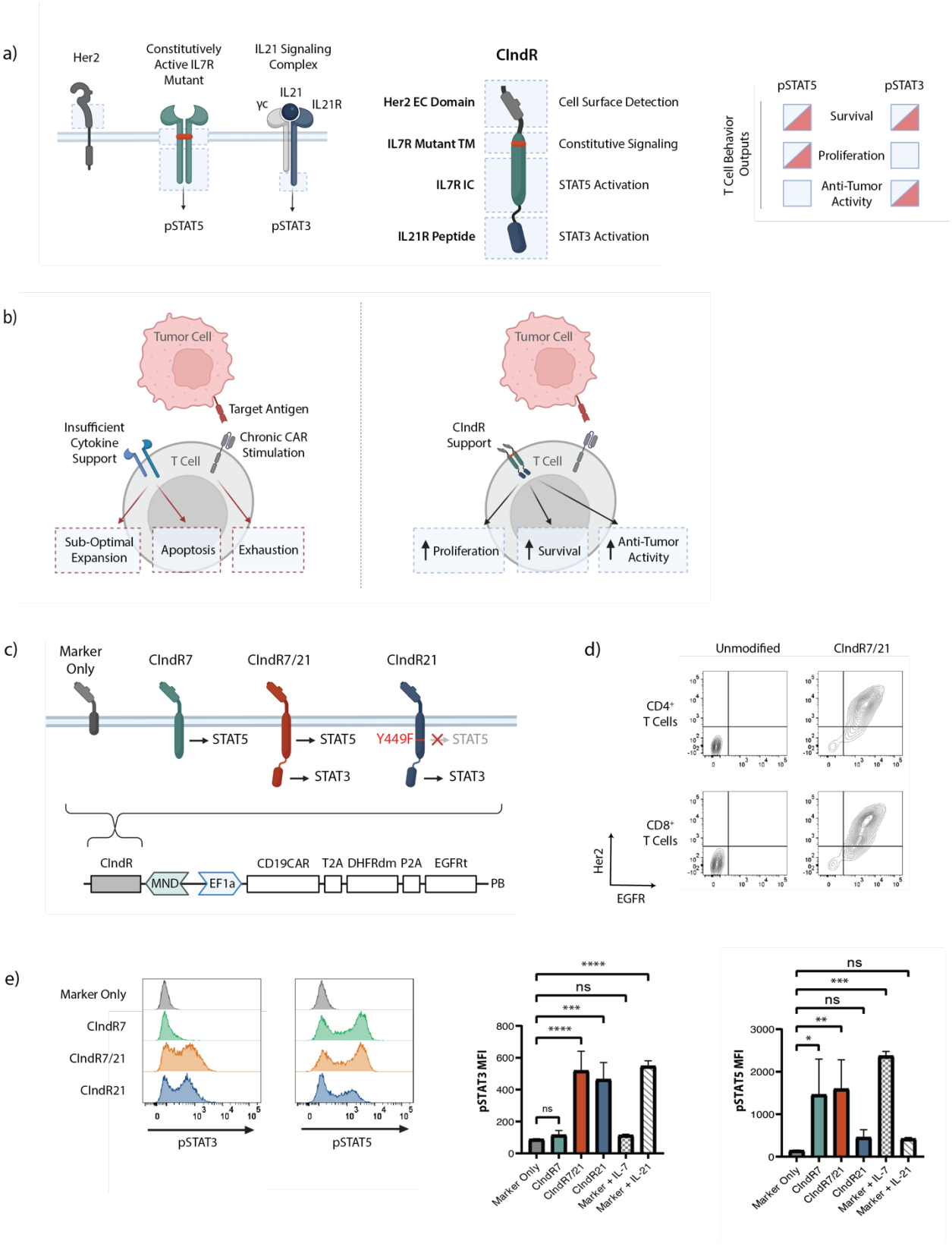
a)
Her2
Constitutively Active IL7R Mutant
IL21 Signaling Complex
IL21
γc
IL21R
pSTAT5
pSTAT3
ClndR
Her2 EC Domain
Cell Surface Detection
IL7R Mutant TM
Constitutive Signaling
IL7R IC
STAT5 Activation
IL21R Peptide
STAT3 Activation
pSTAT5
pSTAT3
T Cell Behavior Outputs
Survival
Proliferation
Anti-Tumor Activity
b)
Tumor Cell
Target Antigen
Insufficient Cytokine Support
Chronic CAR Stimulation
T Cell
Sub-Optimal Expansion
Apoptosis
Exhaustion
Tumor Cell
ClndR Support
T Cell
Proliferation
Survival
Anti-Tumor Activity
c)
Marker Only
ClndR7
ClndR7/21
ClndR21
STAT5
STAT3
Y449F
ClndR
MND
EF1a
CD19CAR
T2A
DHFRdm
P2A
EGFRt
PB
d)
Unmodified
ClndR7/21
CD4+ T Cells
CD8+ T Cells
Her2
EGFR
e)
Marker Only
ClndR7
ClndR7/21
ClndR21
pSTAT3
pSTAT5
pSTAT3 MFI
pSTAT5 MFI
ns
Marker Only
ClndR7
ClndR7/21
ClndR21
Marker + IL-7
Marker + IL-21

Figure 1: Modularly designed cytokine receptors provide constitutive IL-7 and IL-21 signaling in CAR T cells. a, Construction of the cytokine-independent receptor (CIndR) scaffold from elements of Her2, IL7R and IL21R for constitutive activation of STAT3 and STAT5. **b**, Hypothetical effects of CIndR technology on CAR T cell expansion, longevity, and anti-tumor function. **c**, Panel of CIndR variants designed for specific STAT signaling outputs, and introduction of these variants into a divergent dual-promoter construct for co-expression with the anti-CD19CAR in T cells. **d**, Flow cytometry analysis of surface expression of CIndR, marked by Her2tG, and the anti-CD19CAR polycistron, marked by EGFRt. **e**, Flow cytometry analysis of phosphorylated STAT3 and STAT5 in CIndR-expressing CAR T cells. Histograms on left display cell distributions from a representative donor, and bar charts on right display median fluorescent intensity (MFI) averages across three donors. *Statistics: Plots show mean +/- standard deviation. One-way ANOVA was performed with multiple comparisons to Marker-Only group. p < 0.05* 0.01** 0.001*** 0.0001****.*

Hybrid Cytokine Receptors Increase CAR T Cell Proliferation and Suppress Apoptosis Without Triggering Cytokine-Independent Growth *In Vitro*

Proliferative capacity and longevity are key features of potent CAR T cell products, as an effective anti-tumor response requires that CAR T cells expand *in situ* upon encountering tumor cells and persist until tumor can be eradicated. We examined the effects of CIndR expression on CAR T cell proliferation and survival *in vitro* after co-culture with antigen-bearing tumor cells. When subjected to weekly exposures to human $CD19^+$ lymphoma Raji cells, CIndR7/21 and CIndR21-expressing CAR T cells displayed significantly enhanced growth (**Fig. 2a, b**). In keeping with this finding, Marker-Only cells cultured with IL-7 and IL-21 or IL-21 alone likewise showed a proliferative benefit. Surprisingly, CindR21-expressing CAR T cells demonstrated greater proliferation than all other groups, including Marker Only cells cultured with exogenous IL-7 and/or IL-21. Augmented proliferation in CIndR7/21 and CIndR21-expressing CAR T cells did not result in skewing toward $CD4^+$ of $CD8^+$ populations, as these groups roughly maintained the starting 1:1 ratio of $CD4^+$ to $CD8^+$ T cells after two weeks in culture (**Fig. 2c**). As such, CIndRs with STAT3 signaling activity provide enhanced $CD4^+$ and $CD8^+$ T cell proliferation *in vitro*, roughly

mimicking the effects of treatment with exogenous cytokines. However, while Marker Only T cells required both IL-7 and IL-21 supplementation to achieve maximal expansion, unexpectedly, the greatest proliferative boost was conferred by CIndR21, suggesting that STAT5 signaling from CIndRs may be dispensable for augmented antigen-dependent proliferation. Furthermore, the pro-proliferative effects documented here appear to stem from T cell intrinsic signaling, as endogenous cytokine secretion is not significantly affected by CIndR expression (**Supp. Fig 3a, b**).

To examine T cell behavior in the absence of cytokine *and* antigen, we subjected T cell groups to a single stimulation with irradiated Raji cells, followed by a wash-out of secreted cytokines seven days later, at which point all Raji tumor cells had been eliminated (**Fig. 2d**). Assessing cell viability status three days later revealed that CIndR7/21 and CIndR21-expressing T cells had significantly decreased proportions of apoptosed and pre-apoptotic cells, identified as 7-AAD^{+} and 7-AAD^{-}/Annexin-V^{+} populations, respectively (**Fig. 2e**). This pro-survival effect did not correlated with BCL2 expression, as revealed by RNA-seq in CD8^{+} T cells (**Fig. 2f**). However, CIndR7/21 and CIndR21-expressing cells showed significantly lower expression of the pro-apoptotic gene BCL2L11, suggesting a mechanism of maintaining live T cells. After cytokines were washed out at day 7, T cells from all groups fully diminished over the course of several weeks, with CIndR7/21-expressing T cells showing the greatest longevity (**Fig. 2g**). STAT3 signaling distinguishes CIndRs that show a significant pro-survival effect *in vitro* in the absence of cytokine and CAR antigen. However, the superiority of CIndR7/21 in extending T cell persistence suggests that pairing STAT3 and STAT5 activation may yield the greatest resistance to apoptosis.

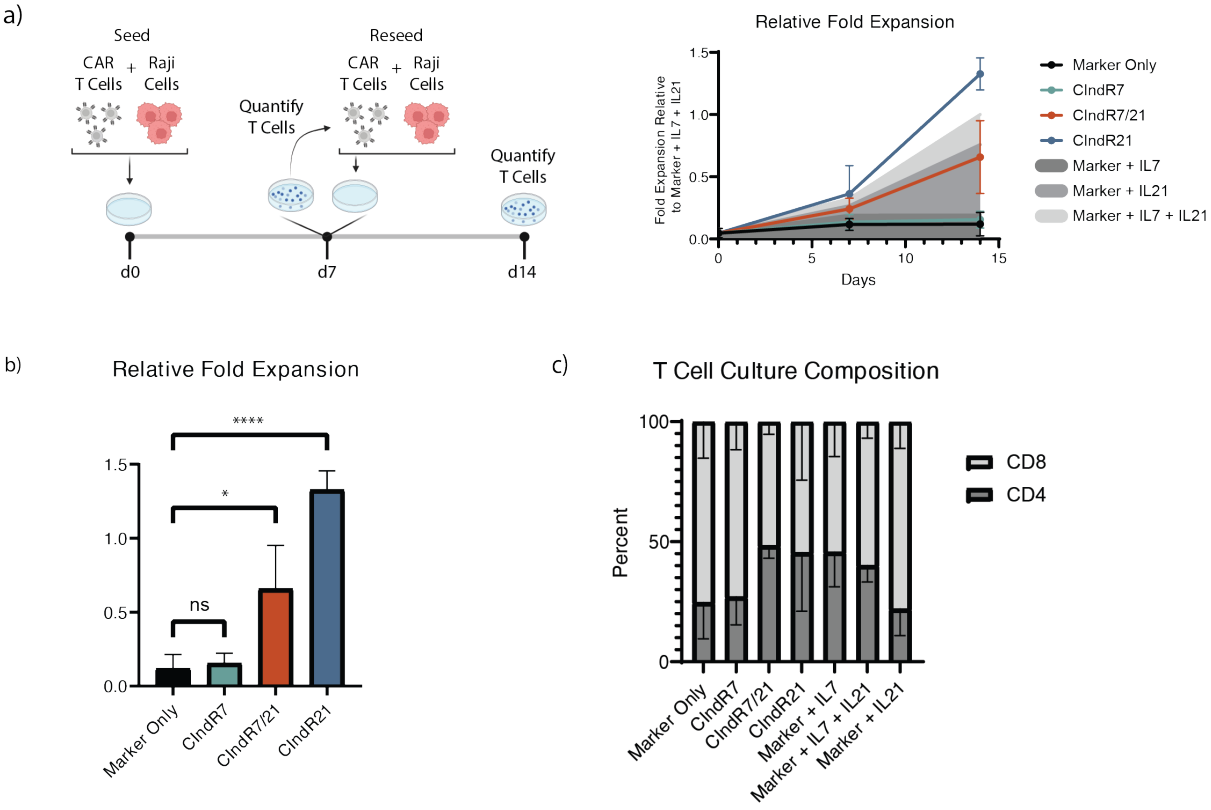
a)
Seed
CAR T Cells + Raji Cells
Reseed
CAR T Cells + Raji Cells
Quantify T Cells
Quantify T Cells
d0
d7
d14
Relative Fold Expansion
Fold Expansion Relative to Marker + IL7 + IL21
Days
Marker Only
ClndR7
ClndR7/21
ClndR21
Marker + IL7
Marker + IL21
Marker + IL7 + IL21
b)
Relative Fold Expansion
****
*
ns
Marker Only
ClndR7
ClndR7/21
ClndR21
c)
T Cell Culture Composition
Percent
CD8
CD4
Marker Only
ClndR7
ClndR7/21
ClndR21
Marker + IL7
Marker + IL7 + IL21
Marker + IL21
d)
Seed
CAR T Cells + Irradiated Raji Cells
Wash Out Cytokines
Cytokine-Free Culture
d0
d7
d10
d14
Annexin V Analysis
e)
Cell Viability Status, Day 10
*
**
ns
Percent of Cells
7AAD- AnnexinV-
7-AAD- AnnexinV+
7-AAD+
Marker Only
ClndR7
ClndR7/21
ClndR21
f)
BCL2 Expression
BCL2L11 Expression
ns
ns
ns
**
**
ns
Normalized Counts
Normalized Counts
Marker Only
ClndR7
ClndR7/21
ClndR21
g)
T Cell Fold Expansion
Fold Change in Live T Cells
Days
Cytokines Washed Out
Marker Only
ClndR7
ClndR21
ClndR7/21

Figure 2: Hybrid cytokine receptors increase CAR T cell proliferation and suppress apoptosis without triggering cytokine-independent growth *in vitro*. a, T cell proliferation upon two exposures to Raji tumor cells one week apart. Schema on left details experimental process. Line graph on right displays the average relative fold expansion. All fold expansion values were normalized on a donor-by-donor basis to the Marker Only + IL-7 + IL-21 condition to account for differences in baseline proliferative capacity across donors. The shaded areas indicate the average relative expansion of Marker Only cells treated with cytokines. **b**, Average relative fold expansion at day 14. **c**, Average percent $CD4^+$ and $CD8^+$ populations in T cell culture at day 14. **d**, Experimental schema to assess T cell growth and survival in absence of cytokines and CAR antigen. **e**, Cell viability status ten days after stimulation with irradiated Raji tumors, assessed by flow cytometry to detect cell incorporation of 7-AAD and Annexin V. **f**, Normalized transcript counts of BCL2 and BCL2L11 genes by RNA-seq. **g**, T cell fold expansion after stimulation with irradiated Raji cells. *Statistics: Plots show mean +/- standard deviation from three biological replicates. One-way ANOVA was performed with multiple comparisons to Marker-Only group. p < 0.05* 0.01** 0.001*** 0.0001****.*

STAT3-Signaling Receptors Improve CAR T Cell Anti-Tumor Activity Under Prolonged Tumor Exposure

In addition to proliferation and survival, we were interested in the ability of CIndRs to augment CAR T cell anti-tumor activity. Live cell fluorescent imaging allowed us to track mCherry-marked Raji tumor cells in co-culture with CIndR-bearing CAR T cells at a range of effector to target cell ratios. In an assay of short-term cytotoxicity, we co-cultured T cells and $mCherry^+$ Raji cells and monitored fluorescence for six days thereafter (**Fig 3a, left**). Comparing the tumor signal in each CAR T cell group to that of unmodified T cells allowed us to calculate the percent tumor suppression over the six-day period (**Fig. 3a, middle**). While CindR7/21 and CIndR21 generally outperformed other groups, the only statistically significant finding appeared at the 0.5:1 effector to target ratio with CIndR21 showing greater tumor suppression (**Fig. 3a, right**). Expression of cytotoxic proteins GZMB and PRF as well as degranulation marker CD107A in $CD8^+$ T cells did not vary significantly across CIndR groups (**Supp. Fig. 3c**), suggesting an alternative mechanism for enhanced anti-tumor function. Treatment of Marker-Only CAR T cells with cytokines yielded

similar changes in tumor suppression to CIndR supplementation. However, in contrast to the dominance of CIndR21 amongst the CIndR T cell groups, treatment of Marker-Only cells with IL-21 alone did not confer greater tumor suppression than treatment with IL-7 and IL-21. As with proliferative capacity, the superiority of CIndR21 suggests STAT5 signaling may be dispensable for optimal short-term anti-tumor activity afforded by CIndRs.

Looking to investigate effects of CIndR expression on T cell cytotoxicity on a longer timescale, we exposed T cell groups to series of five "tumor challenges" every three days (**Fig. 3b**). Longitudinal tracking of tumor signal revealed that STAT3-signaling CIndRs conferred a significant enhancement of tumor suppression by CAR T cells, and that these trends were mimicked by treatment of Marker Only control cells with exogenous cytokines (**Fig. 3c**). Furthermore, simultaneous tracking of T cell populations showed a correlated increase in T cell growth by STAT3-signaling CIndRs over the fifteen-day period (**Fig. 3d**). Taken together, these findings suggest that STAT3 activation, either by CIndR expression or treatment with exogenous IL-21, leads to durable anti-tumor activity *in vitro*.

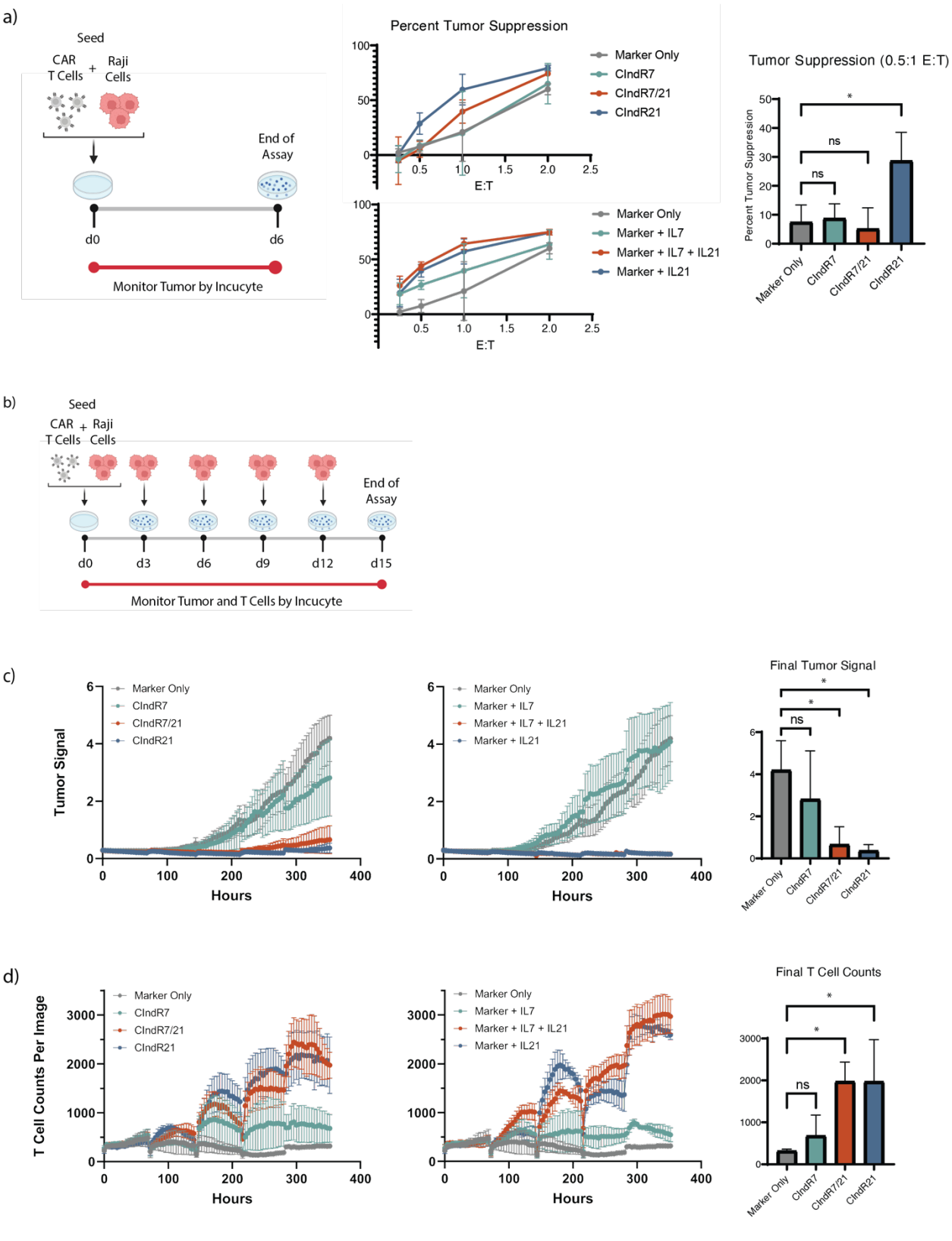
a)
Seed
CAR T Cells + Raji Cells
End of Assay
d0
d6
Monitor Tumor by Incucyte
Percent Tumor Suppression
Marker Only
CIndR7
CIndR7/21
CIndR21
E:T
Marker Only
Marker + IL7
Marker + IL7 + IL21
Marker + IL21
E:T
Tumor Suppression (0.5:1 E:T)
Percent Tumor Suppression
ns
ns
*
Marker Only
CIndR7
CIndR7/21
CIndR21
b)
Seed
CAR T Cells + Raji Cells
End of Assay
d0
d3
d6
d9
d12
d15
Monitor Tumor and T Cells by Incucyte
c)
Tumor Signal
Marker Only
CIndR7
CIndR7/21
CIndR21
Hours
Marker Only
Marker + IL7
Marker + IL7 + IL21
Marker + IL21
Hours
Final Tumor Signal
*
*
ns
Marker Only
CIndR7
CIndR7/21
CIndR21
d)
T Cell Counts Per Image
Marker Only
CIndR7
CIndR7/21
CIndR21
Hours
Marker Only
Marker + IL7
Marker + IL7 + IL21
Marker + IL21
Hours
Final T Cell Counts
*
*
ns
Marker Only
CIndR7
CIndR7/21
CIndR21

Figure 3: STAT3-signaling receptors improve CAR T cell anti-tumor activity under prolonged tumor exposure. a, Schema of a short-term cytotoxicity assay using live cell fluorescent imaging (left). Percent tumor suppression at day six by CIndR-expressing CAR T cell groups (middle, top) and Marker-Only groups (middle, bottom) across various effector to target (E:T) ratios. Percent tumor suppression by CIndR-expressing groups at 0:5:1 E:T. **b**, Schema of a long-term cytotoxicity assay with five recursive tumor challenges with Raji cells every three days. **c**, Longitudinal tumor signal in CIndR groups (left) and Marker-Only groups (middle). Average final tumor signal across CIndR groups (right). **d**, Longitudinal T cell counts in CIndR groups (left) and Marker-Only groups (middle). Average final T cell counts across CIndR groups (right). *Statistics: Plots show mean +/- standard deviation from three biological replicates. One-way ANOVA was performed with multiple comparisons to Marker-Only group. $p < 0.05$*.*

STAT3-Signaling Receptors Sustain a Subset of Stem Cell Memory CAR T Cells

Our studies thus far have highlighted differences in CAR T cell behavior conferred by expression of CIndRs, with the STAT3-activating CIndRs standing apart as mediators of enhanced CAR T cell proliferation, survival, and long-term anti-tumor activity. T cell proliferative capacity specifically depends on differentiation state, with more naïve T cell populations displaying greater ability to proliferate.[16] We therefore examined the effects of CIndR expression on CAR T cell differentiation by repetitively stimulating T cell groups with Raji tumor cells every three days and tracking expression of differentiation markers CD45RA, CD62L and CCR7 by flow cytometry (**Fig. 4a**). We found that STAT3-signaling CIndRs, and most predominantly CIndR21, showed higher percentages of $CD8^+$ T cells expressing markers of stem cell memory T cells (**Fig. 4b**). The differences in marker expression between STAT3-signaling CIndRs and other T cell groups widened between the first and second tumor exposures, suggesting that the effects of CIndR7/21 and CIndR21 on differentiation become more apparent as CAR T cells are exposed to more antigen. In addition, treatment of Marker-Only cells with IL-21 had a similar effect of preserving a population of T cells with stem cell memory phenotype.

To examine potential effects of CIndRs on T cell exhaustion, we concurrently examined TIGIT expression as CAR T cells were repeatedly exposed to antigen. TIGIT is an inhibitory receptor marking exhausted T cells[17] and associated with CAR T cell dysfunction in treatment of non-Hodgkin's lymphoma.[18] While no statistically significant differences emerged, we observed a trend that STAT3-signaling CIndRs as well as treatment with IL-21 led to decreased TIGIT expression (**Fig. 4c**), suggesting that equipping CAR T cells with CIndR7/21 or CIndR21 may decrease susceptibility to T cell exhaustion and deactivation via TIGIT ligation.

Next, we investigated the effects CIndRs on gene expression by performing RNA sequencing on $CD8^+$ CAR T cells. We prepared T cells for sequencing by stimulating with Raji tumor cells and then sorting $CD8^+$ T cell populations a week later (**Fig. 4d**). A list of differentially expressed genes (DEGs) was assembled by comparing normalized transcript levels between each CIndR group and the Marker-Only control. As expected, given its hybrid STAT3 and STAT5 signaling profile, CIndR7/21-expressing T cells showed the greatest number of DEGs in common with the other two groups. However, CIndR21-expressing CAR T cells showed the greatest number of DEGs total, suggesting that STAT3 activation without supplemental STAT5 activation maximizes changes in gene expression. Furthermore, genes downregulated in CIndR21-expressing T cells compared to the Marker-Only group included exhaustion-associated genes TOX2, NR4A2 and NR4A3[19] (**Fig. 4e**). CIndR21 expression was also marked by increased expression of KLF2 and KLF3, transcription factors promoting T cell quiescence.[20,21] Taken together, our findings demonstrate that expression of CIndR21 and, to a lesser degree, CIndR7/21 maintains a quiescent, stem cell memory phenotype and decreases genes involved in T cell exhaustion.

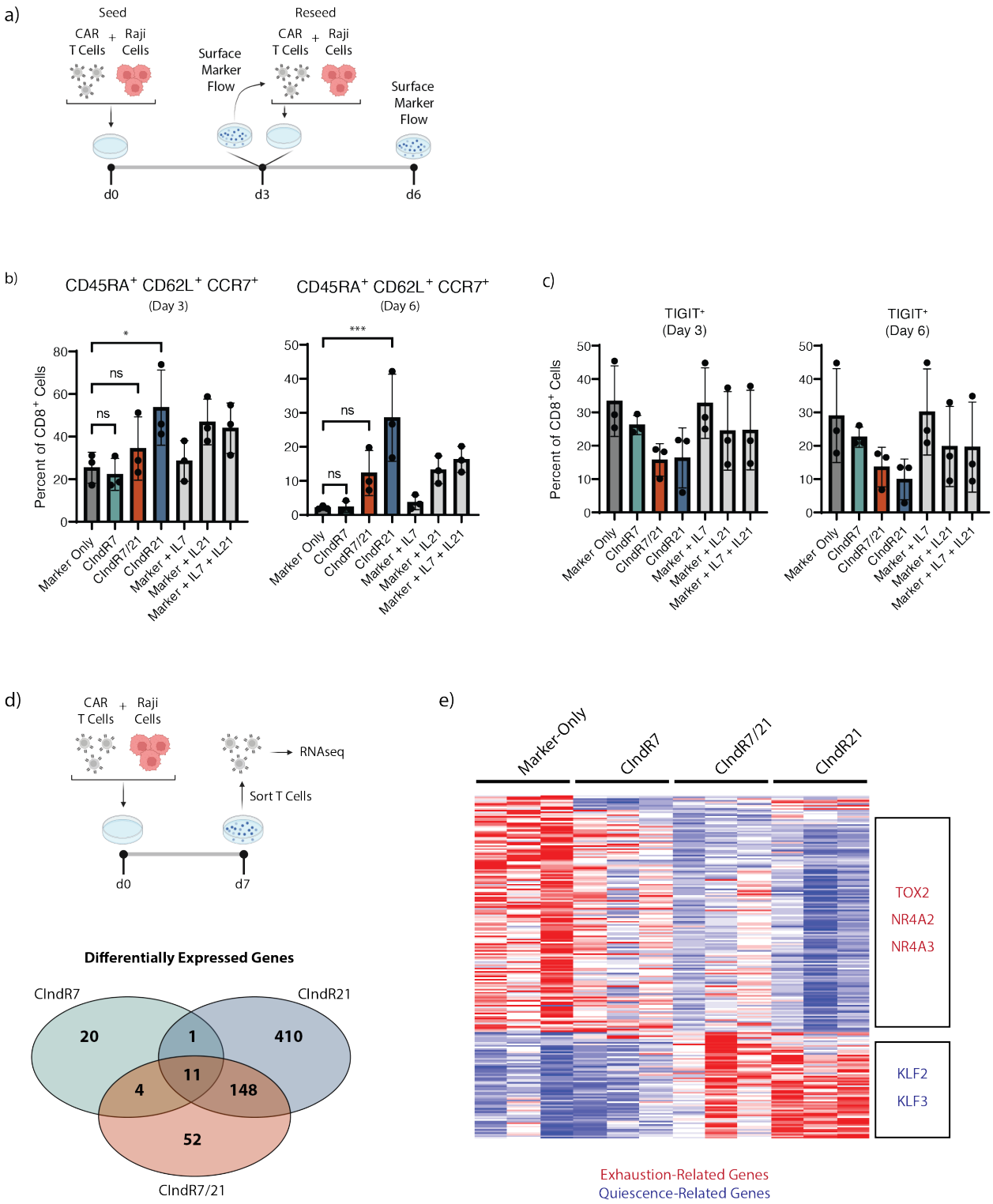

Figure 4: STAT3-signaling receptors sustain a subset of stem cell memory CAR T Cells. a, Experimental approach of to track T cell phenotypic markers upon two stimulations with Raji tumors every three days. **b**, Percent of CD8+ T cell populations expressing CD45RA, CD62L and CCR7 at day 3 and day 6. **c**, Percent of CD8+ T cell populations expressing TIGIT at day 3 and day 6. **d**, Schema to prepare CAR T cells for RNA-

seq (top), and differentially expressed genes (DEGs) in $CD8^+$ T cells across CIndR groups compared to Marker-Only control. DEG list includes all genes with a multiple-testing corrected FDR < 0.05, a two-sided raw p-value < 0.01 and $\log_2$(fold change)| >=1. **e**, Heatmap displaying DEGs arrayed by expression pattern across T cell groups with designated positions of genes of interest. *Statistics: Plots show mean +/- standard deviation from three biological replicates. One-way ANOVA was performed with multiple comparisons to Marker-Only group. p < 0.05* 0.01** 0.001***.*

Hybrid Cytokine Receptors Support CAR T Cell Mediated Elimination of Leukemia Tumors *In Vivo*, but CIndR7/21 Triggers Unrestricted T Cell Growth

In vitro studies have highlighted the impacts of CIndR expression on CAR T cell proliferation, survival, anti-tumor capacity, and differentiation. We went on to examine whether these dynamics affect the ability of CAR T cells to eliminate tumors *in vivo*. To this end, we employed a human leukemia xenograft model in NSG mice using $CD19^+$ Nalm-6 tumor cells modified to express firefly luciferase for bioluminescent tracking (**Fig. 5a**). T cells were administered one week after tumor injection, and T cell engraftment and persistence were monitored by *ex vivo* flow cytometry on peripheral blood. As expected, mice treated with any anti-CD19CAR T cell product showed a delay in tumor progression compared to mice treated with Unmodified T cells (**Fig 5b**). However, all mice treated with CIndR7/21 or CIndR21-expressing CAR T cells showed a complete elimination of tumor signal and return baseline flux values. CIndR7 CAR T cells achieved greater reductions in tumor burden than Marker Only CAR T cells, but never achieved full tumor eradication.

These differences in tumor control led to significant differences in mouse survival (**Fig. 5c**), with CIndR7/21 and CIndR21 extending survival beyond other treatment groups. However, unexpectedly, several mice treated with CIndR7/21 CAR T cells developed abdominal swelling

and became moribund despite absence of tumor signal, necessitating euthanasia. Necropsy of moribund mice revealed abdominal swelling to originate from enlarged liver and spleen (detailed in Chapter 5), suggesting a pathological role of circulating cells. CIndR7/21 CAR T cells appeared at the highest concentrations in peripheral blood early in the study and remained elevated throughout (**Fig. 5d**), especially in mice suffering from idiopathic liver and spleen enlargement. Given that CIndR7/21 CAR T cells continued to expand and persist in mice after tumor had been eliminated, we hypothesize that moribundity arose in this group due to unrestricted T cell growth and engraftment in the liver and spleen, eventually leading to organ failure. This phenomenon was only observed in the CIndR7/21 treatment group and penetrance was 60%.

In contrast, CIndR21 CAR T cells appeared at elevated concentrations compared to Marker-Only CAR T cells at early timepoints, but these concentrations fell below the limit of detection by day 38 post-tumor injection. We conclude that the combination of constitutive STAT3 and STAT5 signaling in CIndR7/21 triggers unrestricted CAR T cell growth after tumor has been eliminated. In-built STAT5 activation appears to be dispensable for CIndR enhancement of anti-tumor responses, however, as CIndR21 CAR T cells achieved the same level of tumor control as CIndR7/21 without licensing unchecked T cell growth.

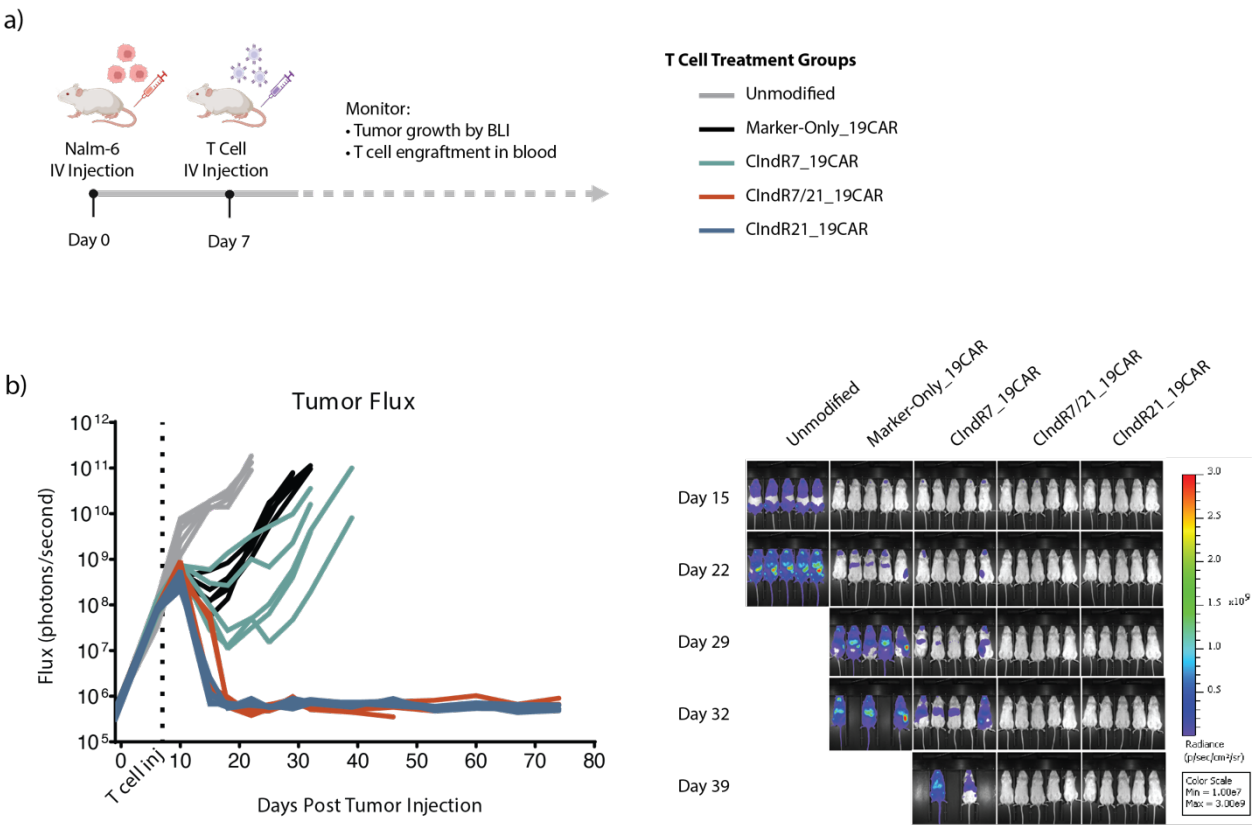
a)
Nalm-6
IV Injection
T Cell
IV Injection
Day 0
Day 7
Monitor:
• Tumor growth by BLI
• T cell engraftment in blood
T Cell Treatment Groups
Unmodified
Marker-Only_19CAR
CIndR7_19CAR
CIndR7/21_19CAR
CIndR21_19CAR
b)
Tumor Flux
Flux (photons/second)
T cell inj
Days Post Tumor Injection
Unmodified
Marker-Only_19CAR
CIndR7_19CAR
CIndR7/21_19CAR
CIndR21_19CAR
Day 15
Day 22
Day 29
Day 32
Day 39
Radiance
Color Scale
c)
Survival Proportions
Percent survival
Days Post Tumor Injection
Unmodified
Marker-Only_19CAR
CIndR7_19CAR
CIndR7/21_19CAR
CIndR21_19CAR
n.s.
d)
T Cell Engraftment in Blood
T Cells per uL Blood
Limit of
Detection
Days Post Tumor Injection

Figure 5: Hybrid cytokine receptors support CAR T cell mediated elimination of leukemia tumors *in vivo*, but CIndR7/21 triggers unrestricted T cell growth. **a**, Experimental schema of human Nalm-6 leukemia xenograft *in vivo* model (n = 5 mice per group). **b**, Tumor tracking by bioluminescent imaging of mice. Each line represents an individual mouse. **c**, Kaplan Meier survival curve with accompanying statistics to determine significance (Mantel-Cox test, Bonferroni-corrected threshold: $p < 0.0083$*). **d**, Tracking of T cell concentration in peripheral blood. Each line represents an individual mouse.

DISCUSSION

The modular design of our hybrid cytokine receptor allowed us to generate CIndR variants with constitutive signaling outputs of STAT5, STAT3, or STAT5 and STAT3. *In vitro* studies revealed that CIndRs providing STAT3 activation led to the most pronounced improvements in T cell proliferation, survival, and anti-tumor activity. Surprisingly, CIndR7/21 did not outperform CIndR21 on these metrics, suggesting that in-built STAT5 activation is dispensable to mediate *in vitro* functional enhancements to CAR T cells. In fact, in some cases STAT5 activation appeared to counteract effects of STAT3 activation, as CIndR21 showed greater impacts on T cell differentiation markers and gene expression than CIndR7/21.

In vivo, however, STAT5 activation by CIndRs yielded more notable effects on CAR T cell behavior. Though CIndR7 supplementation did not yield significant functional enhancements *in vitro*, CIndR7-expressing CAR T cells increased tumor suppression and survival *in vivo*. In addition, CIndR7/21-equipped CAR T cells displayed the highest T cell concentrations in the peripheral blood. Perhaps the unremarkable effects of STAT5 activation *in vitro* can be attributed to an abundance of endogenous cytokines secreted by CAR T cells, such as IL-2 and IL-15. The presence of these endogenous cytokines may have created an elevated background level of STAT5 activation, effectively washing out the effect of CIndR-born STAT5 activity.

Only CIndRs providing STAT3 activation resulted in complete elimination of leukemia tumors *in vivo*, and this effect can likely be attributed to the heightened T cell engraftment achieved by CIndR7/21 and CIndR21. Other effects observed *in vitro*, such as delayed T cell differentiation and downregulation of exhaustion-related genes, may have also played a role. However, it is unlikely that differences in T cell differentiation status occurred during the T cell production culture period, as all T cell groups showed similar differentiation markers at the end of culture (**Supp. Fig. 4c**).

The combination of STAT3 and STAT5 activation provided by CIndR7/21 resulted in unrestricted T cell growth after tumors were eliminated, a pattern not observed in mice treated with CIndR21-equipped CAR T cells. STAT3 activation appears to license T cells for robust expansion upon encounter with tumor *in vivo*, but STAT5 activation is required for sustaining T cell populations after antigen-bearing tumor diminishes. This finding is keeping with cytokine literature, as IL-7 has been shown to promote homeostatic proliferation of T cells,[22] an effect that can be recapitulated by the introduction of a constitutively active variant of STAT5.[23]

CIndR21 mediated durable anti-tumor responses without triggering unchecked T cell growth, making it the most attractive candidate to supplement CAR T cell products. Future work will examine other signaling cascades triggered by CIndR21 beyond STAT3 activation, specifically focusing on the AKT and ERK pathways. Perhaps investigation of other signaling outputs will elucidate the networks responsible for the T cell behavior promoted by CIndR21.

ACKNOWLEDGEMENTS

I would like to thank my colleagues Cailyn Spurrell Ph.D. and Justin Giles for providing aid and expertise in transcriptional profiling of CIndR-expressing T cells. James Rosser Ph.D. optimized the T cell production method used here to introduce dual-promoter constructs into human T cells. As my research advisor and mentor, Michael Jensen M.D. provided key insights and direction to the projects detailed in all chapters of this work. I would also like to thank my colleagues Michael Baldwin, LaTrice King, and Niels Rekers Ph.D. for assistance in planning and carrying out the *in vivo* studies described in this chapter.

REFERENCES

1. Johnson, A. J. *et al.* Rationally Designed Transgene-Encoded Cell-Surface Polypeptide Tag for Multiplexed Programming of CAR T-cell Synthetic Outputs. *Cancer Immunol. Res.* **9,** 1047–1060 (2021).
2. Li, X. *et al.* piggyBac transposase tools for genome engineering. *Proc. Natl. Acad. Sci.* **110,** (2013).
3. Sommermeyer, D. *et al.* Fully human CD19-specific chimeric antigen receptors for T-cell therapy. *Leukemia* **31,** 2191–2199 (2017).
4. Liu, Z. *et al.* Systematic comparison of 2A peptides for cloning multi-genes in a polycistronic vector. *Sci. Rep.* **7,** 2193 (2017).
5. Jonnalagadda, M. *et al.* Efficient selection of genetically modified human T cells using methotrexate-resistant human dihydrofolate reductase. *Gene Ther.* **20,** 853–60 (2013).

6. Wang, X. *et al.* A transgene-encoded cell surface polypeptide for selection, in vivo tracking, and ablation of engineered cells. *Blood* **118,** 1255–1263 (2011).

7. Robbins, P. B. *et al.* Increased probability of expression from modified retroviral vectors in embryonal stem cells and embryonal carcinoma cells. *J. Virol.* **71,** 9466–74 (1997).

8. Ewels, P. A. *et al.* The nf-core framework for community-curated bioinformatics pipelines. *Nat. Biotechnol.* **38,** 276–278 (2020).

9. Robinson, M. D., McCarthy, D. J. & Smyth, G. K. edgeR: a Bioconductor package for differential expression analysis of digital gene expression data. *Bioinformatics* **26,** 139–40 (2010).

10. Shum, T. *et al.* Constitutive Signaling from an Engineered IL7 Receptor Promotes Durable Tumor Elimination by Tumor-Redirected T Cells. *Cancer Discov.* **7,** 1238–1247 (2017).

11. Oh, H. M. *et al.* STAT3 protein promotes T-cell survival and inhibits interleukin-2 production through up-regulation of class O forkhead transcription factors. *J. Biol. Chem.* **286,** 30888–30897 (2011).

12. Chetoui, N., Boisvert, M., Gendron, S. & Aoudjit, F. Interleukin-7 promotes the survival of human CD4+effector/memory T cells by up-regulating Bcl-2 proteins and activating the JAK/STAT signalling pathway. *Immunology* **130,** 418–426 (2010).

13. Tripathi, P. *et al.* STAT5 Is Critical To Maintain Effector CD8+ T Cell Responses. *J. Immunol.* **185,** 2116–2124 (2010).

14. Burchill, M. A. *et al.* Distinct Effects of STAT5 Activation on CD4+ and CD8+ T Cell Homeostasis: Development of CD4+CD25+ Regulatory T Cells versus CD8+ Memory T Cells. *J. Immunol.* **171,** 5853–5864 (2003).

15. Xin, G. *et al.* A Critical Role of IL-21-Induced BATF in Sustaining CD8-T-Cell-Mediated Chronic Viral Control. *Cell Rep.* **13,** 1118–1124 (2015).

16. Gattinoni, L., Speiser, D. E., Lichterfeld, M. & Bonini, C. T memory stem cells in health and disease. *Nat. Med.* **23,** 18–27 (2017).

17. Chew, G. M. *et al.* TIGIT Marks Exhausted T Cells, Correlates with Disease Progression, and Serves as a Target for Immune Restoration in HIV and SIV Infection. *PLoS Pathog.* **12,** e1005349 (2016).

18. Jackson, Z. *et al.* Sequential Single-Cell Transcriptional and Protein Marker Profiling Reveals TIGIT as a Marker of CD19 CAR-T Cell Dysfunction in Patients with Non-Hodgkin Lymphoma. *Cancer Discov.* **12,** 1886–1903 (2022).

19. Seo, H. *et al.* TOX and TOX2 transcription factors cooperate with NR4A transcription factors to impose CD8+ T cell exhaustion. *Proc. Natl. Acad. Sci. U. S. A.* **116,** 12410–12415 (2019).

20. Preston, G. C., Feijoo-Carnero, C., Schurch, N., Cowling, V. H. & Cantrell, D. A. The Impact of KLF2 Modulation on the Transcriptional Program and Function of CD8 T Cells. *PLoS One* **8,** 1–16 (2013).

21. Fang, F. *et al.* Human Transcription Factor KLF3 Maintains T Lymphocyte Quiescent Phenotype Via Inhibiting SHP-1 Expression. *Blood* **126,** 3426–3426 (2015).

22. Schluns, K. S., Kieper, W. C., Jameson, S. C. & Lefrançois, L. Interleukin-7 mediates the homeostasis of naïve and memory CD8 T cells in vivo. *Nat. Immunol.* **1,** 426–32 (2000).

23. Burchill, M. A. *et al.* Distinct Effects of STAT5 Activation on CD4+ and CD8+ T Cell Homeostasis: Development of CD4+CD25+ Regulatory T Cells versus CD8+ Memory T Cells. *J. Immunol.* **171,** 5853–5864 (2003).

24. Figures created with BioRender.com

SUPPLEMENTAL FIGURES

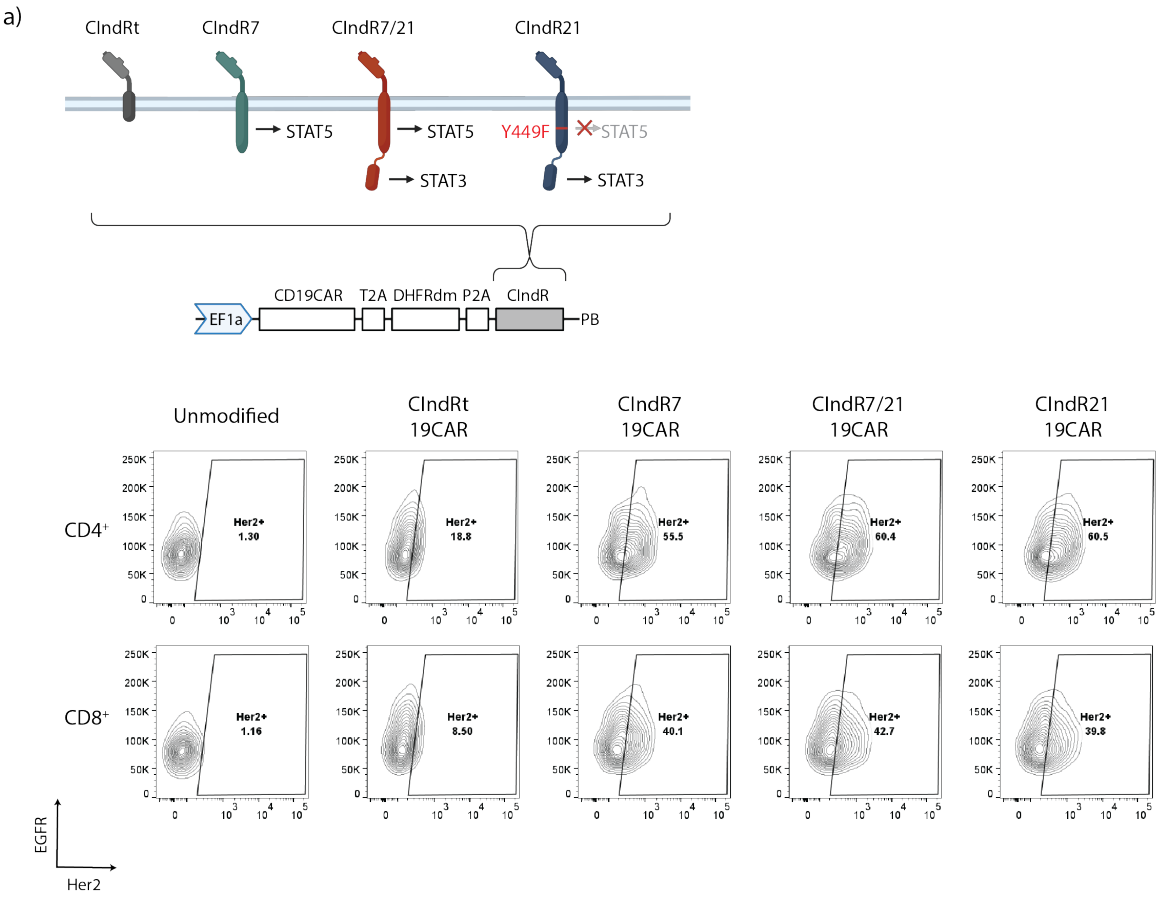

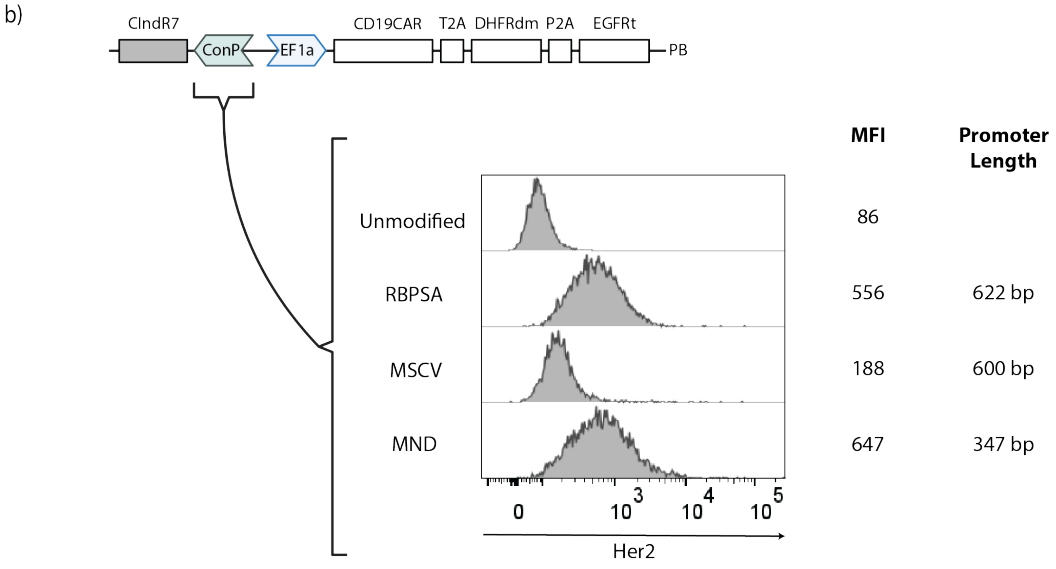

Supplemental Figure 1: Optimization of constructs for constitutive expression of hybrid cytokine receptors. a, Schematic of single-promoter construct architecture attempting to express CIndR and anti-CD19CAR from a single polycistron (top). Flow cytometric analysis of CIndR expression, marked by Her2tG, in T cells modified with single-promoter constructs (bottom). **b**, Divergent dual-promoter construct architecture with a panel of constitutive promoters ("ConP") (top). Flow cytometric analysis of CIndR expression, marked by Her2tG, when driven by three constitutive promoters in the dual-promoter format.

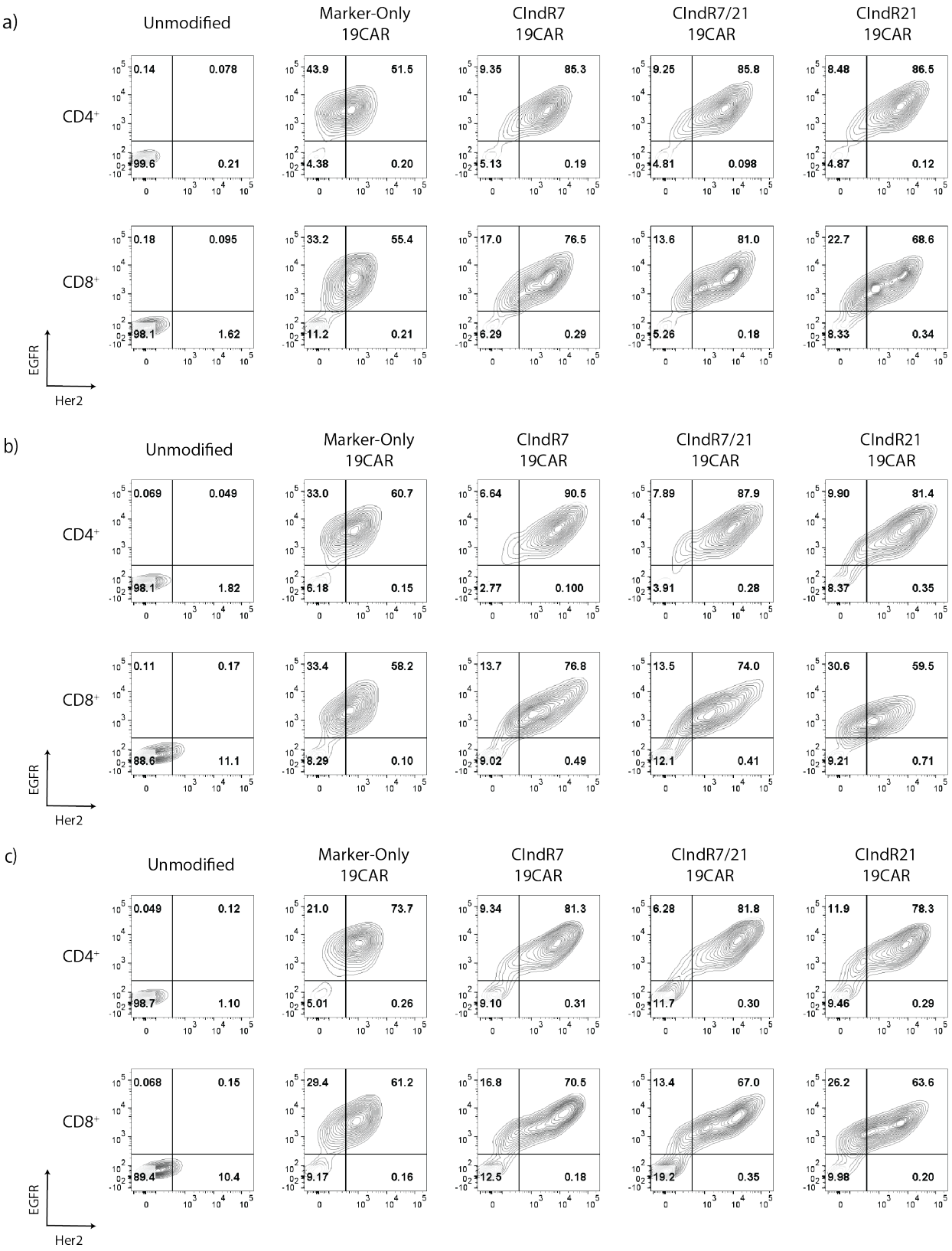
a)
Unmodified
Marker-Only 19CAR
CIndR7 19CAR
CIndR7/21 19CAR
CIndR21 19CAR
CD4+
CD8+
0.14
0.078
99.6
0.21
43.9
51.5
4.38
0.20
9.35
85.3
5.13
0.19
9.25
85.8
4.81
0.098
8.48
86.5
4.87
0.12
0.18
0.095
98.1
1.62
33.2
55.4
11.2
0.21
17.0
76.5
6.29
0.29
13.6
81.0
5.26
0.18
22.7
68.6
8.33
0.34
EGFR
Her2
b)
Unmodified
Marker-Only 19CAR
CIndR7 19CAR
CIndR7/21 19CAR
CIndR21 19CAR
CD4+
CD8+
0.069
0.049
98.1
1.82
33.0
60.7
6.18
0.15
6.64
90.5
2.77
0.100
7.89
87.9
3.91
0.28
9.90
81.4
8.37
0.35
0.11
0.17
88.6
11.1
33.4
58.2
8.29
0.10
13.7
76.8
9.02
0.49
13.5
74.0
12.1
0.41
30.6
59.5
9.21
0.71
EGFR
Her2
c)
Unmodified
Marker-Only 19CAR
CIndR7 19CAR
CIndR7/21 19CAR
CIndR21 19CAR
CD4+
CD8+
0.049
0.12
98.7
1.10
21.0
73.7
5.01
0.26
9.34
81.3
9.10
0.31
6.28
81.8
11.7
0.30
11.9
78.3
9.46
0.29
0.068
0.15
89.4
10.4
29.4
61.2
9.17
0.16
16.8
70.5
12.5
0.18
13.4
67.0
19.2
0.35
26.2
63.6
9.98
0.20
EGFR
Her2

Supplemental Figure 2: Transgenic cell surface marker expression in T cells generated from three donors for *in vitro* studies. Flow cytometry contour plots showing cell surface expression of transgenic markers in $CD4^+$ and $CD8^+$ cells modified with divergent dual-promoter constructs. EGFR marks expression of the anti-CD19CAR-containing polycistron, and Her2 marks expression of CIndR variants. Plots display marker expression in three donors (donor 1 in **a**, donor 2 in **b**, and donor 3 in **c**) used as biological replicates for *in vitro* assays.

a)

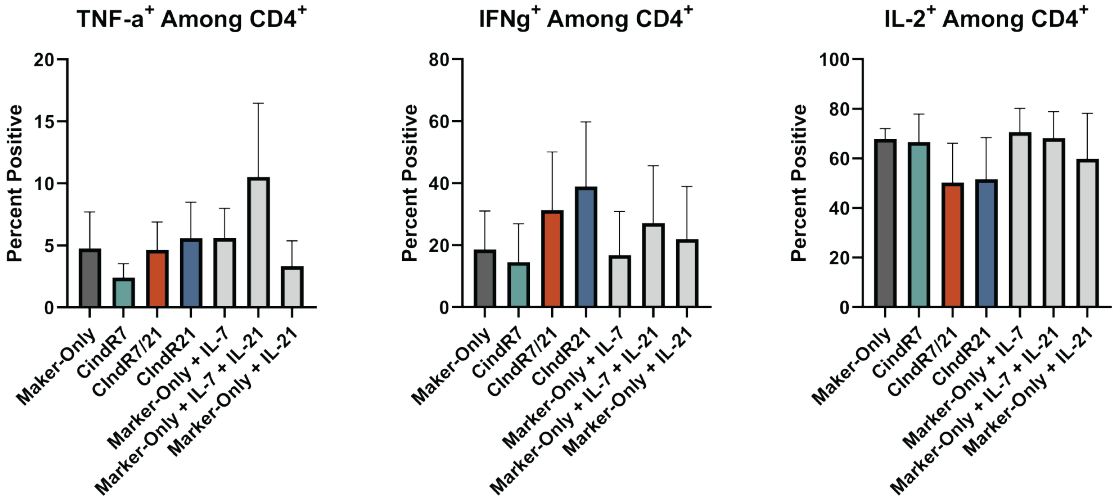
TNF-a+ Among CD4+
IFNg+ Among CD4+
IL-2+ Among CD4+
Percent Positive
Maker-Only
CindR7
CIndR7/21
CIndR21
Marker-Only + IL-7
Marker-Only + IL-7 + IL-21
Marker-Only + IL-21

b)

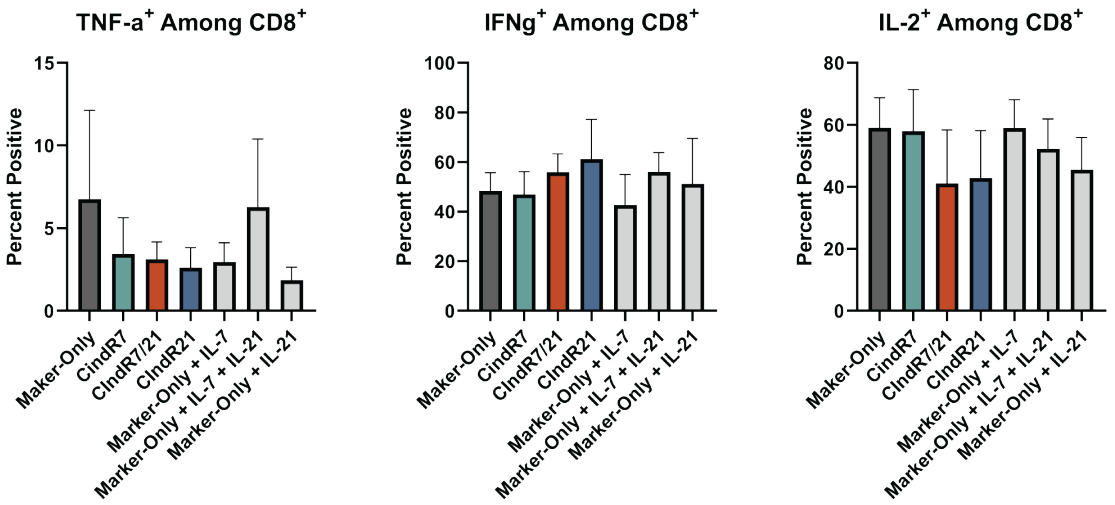
TNF-a+ Among CD8+
IFNg+ Among CD8+
IL-2+ Among CD8+
Percent Positive
Maker-Only
CindR7
CIndR7/21
CIndR21
Marker-Only + IL-7
Marker-Only + IL-7 + IL-21
Marker-Only + IL-21

c)

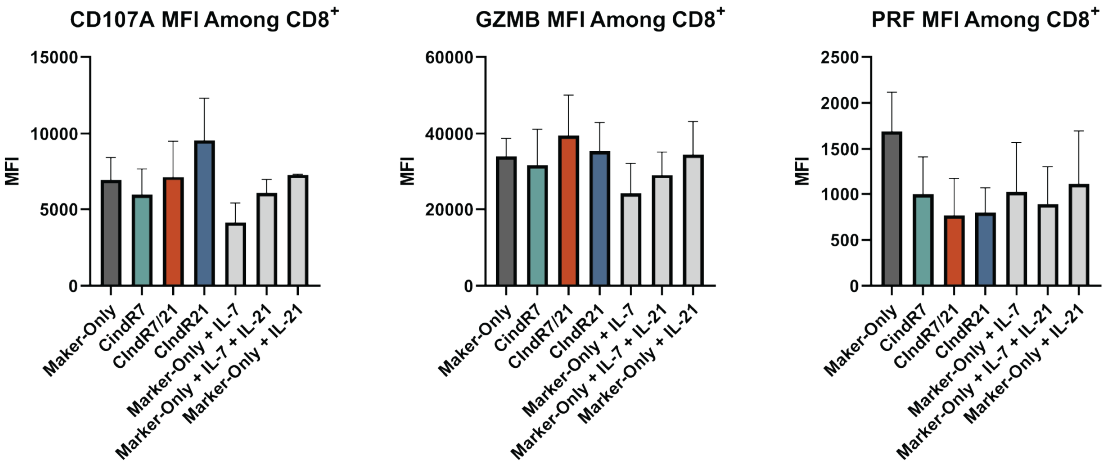
CD107A MFI Among CD8+
GZMB MFI Among CD8+
PRF MFI Among CD8+
MFI
Maker-Only
CindR7
CIndR7/21
CIndR21
Marker-Only + IL-7
Marker-Only + IL-7 + IL-21
Marker-Only + IL-21

Supplemental Figure 3: CIndR expression does not significantly impact cytokine or cytotoxic protein expression in $CD4^+$ and $CD8^+$ CAR T cells. a, Percent of $CD4^+$ CAR T cells expressing TNF-a, IFNg, and IL-2 when co-cultured with Raji tumor cells, as determined by flow cytometry with intracellular cytokine staining. **b**, Percent of $CD8^+$ CAR T cells expressing TNF-a, IFNg, and IL-2 when co-cultured with Raji tumor cells, as determined by flow cytometry with intracellular cytokine staining. **c**, Median fluorescence intensity (MFI) of cytotoxic proteins GZMB and PRF as well as degranulation marker CD107A in $CD8^+$ CAR T cells as determined by flow cytometry with intracellular and cell surface staining. *Statistics: Plots show mean +/- standard deviation from three biological replicates. One-way ANOVA was performed with multiple comparisons to Marker-Only group, and no statistically significant differences were found.*

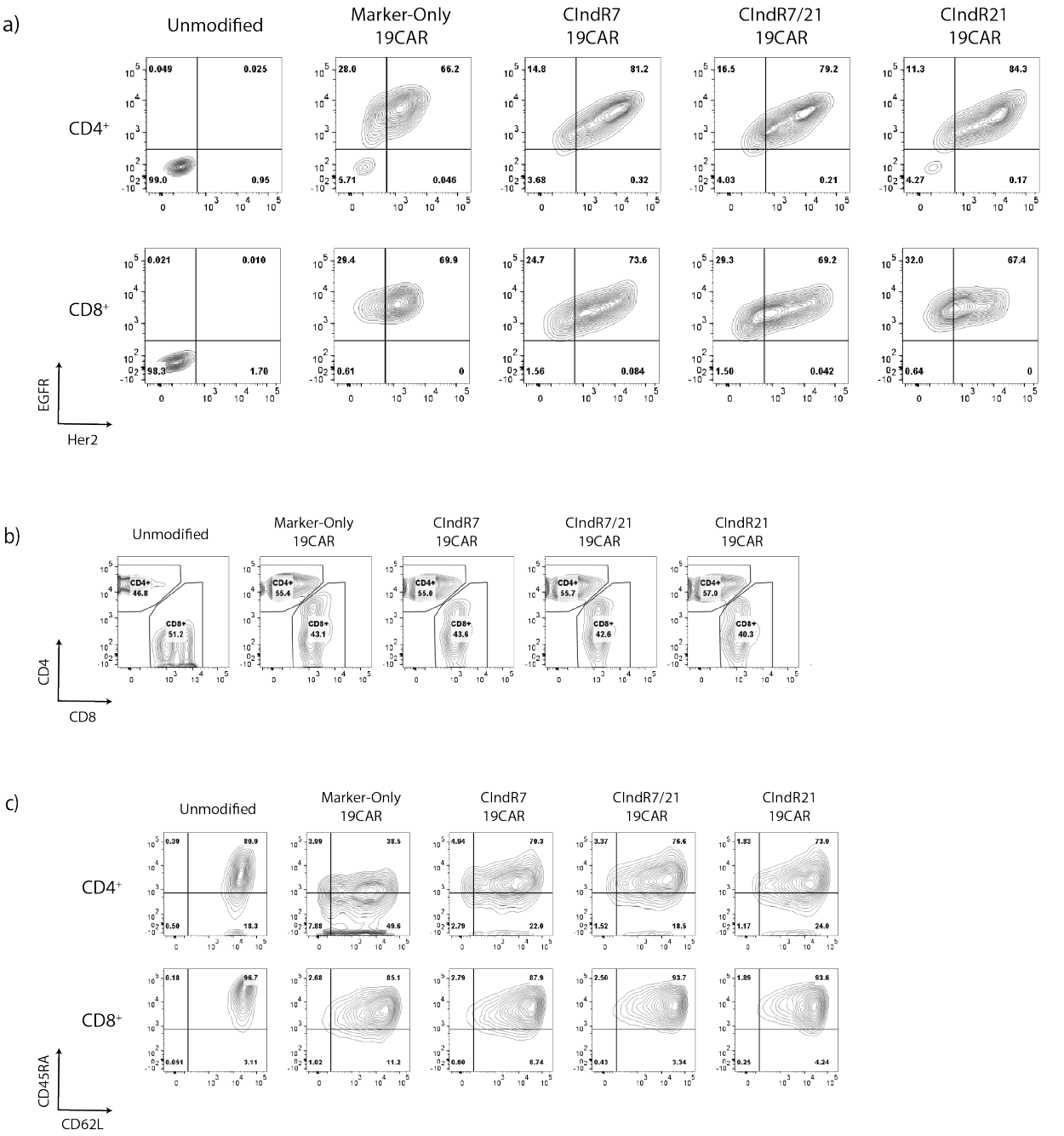

Supplemental Figure 4: Transgenic cell surface marker and phenotypic marker expression by T cells generated for *in vivo* studies. a, Flow cytometry contour plots showing cell surface expression of transgenic markers in CD4$^+$ and CD8$^+$ cells modified with divergent dual-promoter constructs for *in vivo* studies. EGFR marks expression of the anti-CD19CAR-containing polycistron, and Her2 marks expression of CIndR variants. **b**, CD4$^+$ and CD8$^+$ T cell cultures were mixed to normalize the CD4:CD8 ratio across groups before cryopreservation in preparation for *in vivo* studies. Contour plots show CD4 and CD8 expression in each T cell group after thaw for *in vivo* studies. **c**, Expression of differentiation markers CD45RA and CD62L in CD4$^+$ and CD8$^+$ T cells produced for *in vivo* studies.

Chapter 4: Drug-Responsive Molecular Switches for the Control of Cytokine-Augmented CAR T Cells

ABSTRACT

Engineering CAR T Cells with in-built cytokine signaling introduces a risk of triggering cytokine- and antigen-independent T cell growth. This chapter examines two potential regulation mechanisms to control CAR T cell cytokine signaling and curtail unrestricted CAR T cell growth. First, we implement a drug-responsive suicide switch to abrogate growth of CCR-expressing T cells post-tumor elimination. Second, we optimize a drug-responsive transcriptional regulation system for control of CIndR expression.

MATERIALS AND METHODS

Subcutaneous Neuroblastoma Mouse Studies. All mouse experiments were conducted under protocols approved by the Seattle Children's Research Institute's Institutional Animal Care and Use Committee (IACUC). *In vivo* activity of CCRIL2-expressing CAR T cells was assessed using subcutaneous neuroblastoma tumors. 10-13 week-old NSG mice were subcutaneously injected with five million human Be2 cells expressing mCherry (Be2-mCherry) on both flanks. Tumor engraftment was assessed using manual caliper measurements. Five days after tumor injection, mice were injected via tail vein with ten million $CD8^+$ B7H3CAR + CCRIL2 T cells, additionally engineered to express firefly luciferase (ffluc) (see methods in Chapter 1 for T cell production details). Twice per week tumor volume was monitored by manual measurement, and mice imaged for mCherry fluorescent signal (a secondary measure of tumor growth) and

bioluminescent signal (T cells). Mice were euthanized if the tumor on either flank grew to exceed 1500 mm^3. 150 uL of 28.57 mg/mL D-luciferin (Perkin Elmer, Cat. # 122799) was injected subcutaneously 15 minutes before bioluminescent imaging. All imaging was performed using an IVIS Spectrum In Vivo Imaging System (Perkin Elmer) and analysis on Living Image Software.

In Vivo GCV Treatment. Eighteen days after tumor injection, mice were arranged into two groups of five to normalize bioluminescent signal between vehicle and GCV treatment groups. Beginning on day eighteen, mice were injected intraperitoneally each day with 10mg/kg GCV or equivalent volume of water (vehicle control) for seventeen consecutive days. T cell presence was monitored throughout by bioluminescent imaging.

In Vitro GCV Cell Survival Assays. $CD8^+$ T cells originating from three separate donors were removed from cell culture vessels at day 11 of REP[1] and plated at 1 x 10^6 cells per mL in a 48-well plate. All T cell groups were cultured in 10 μM GCV or vehicle control, and live cell counts were collected by hemocytometer seven and fifteen days after the start of treatment. "Relative Viable Cell Concentration" was determined for each T cell group by dividing the live cell concentration in the GCV-treatment group by that in the vehicle control group.

TamR Construct Design. Sequence fragments were amplified via PCR and inserted via Gibson assembly into the epHIV7.2 or epHIV7.3 lentiviral packaging plasmids, as noted in the text.

Lentivirus Production. Recombinant lentivirus was generated by transiently transfecting a 293T producer cell line with lentiviral packaging plasmids alongside a transfer plasmid containing the

transgenes of interest. Transfection was performed using Lipofectamine 2000 (Life Technologies, Cat. # 11668-500). Four days after transfection, lentivirus was isolated from the 293T cell culture supernatant via ultracentrifugation and stored at -80° C until the day of transduction. Co-packaged lentivirus was generated using a mix of two transfer plasmids. Plasmids encoding the TamR chimeric transcription factor were mixed with plasmids encoding the TamR-responsive cassette at a 1 to 2 molar ratio.

T Cell Production and Culture. Protocols to acquire human cells were approved by the institutional review board of Seattle Children's Hospital. $CD8^+$ T cells were isolated from human peripheral blood mononuclear cells (PBMCs) by magnetic activated cell sorting with a $CD8^+$ T cell isolation kit (Miltenyi Biotech, Cat. # 130-096-495). The cells were immediately subjected to a bead-based CD3/CD28 stimulation using Dynabeads (Thermo Fisher Scientific, Cat. # 11131D) at a bead to cell ratio of 1:1. Unless otherwise indicated, T cell culture media consisted of RPMI 1640 (Gibco, Cat. # 22400-089) supplemented with 10% FBS (Hyclone, Cat. # SH30071.03), 2mM L-glutamine (Gibco, 25030-081), 50 U/mL IL-2 (Chiron, Cat. # 53905-991-01) and 0.5 ng/mL IL-15 (Miltenyi, Cat. # 130-095-765) throughout the culture period. Two days post-stimulation, cells were transduced with lentivirus housing TamR components and/or CAR and drug resistance transgenes. Between days 10 and 21 post-stimulation, methotrexate (MTX) was added to the culture at a concentration of 50nM to select CAR-expressing populations. Twenty-one days post-stimulation, cells were magnetically sorted for EGFR expression using of biotinylated Erbitux antibody and anti-biotin microbeads (Miltenyi, Cat. # 130-090-485) according to manufacturer's instructions. Sorted populations were subjected to a rapid expansion protocol (REP) as previously

described.[1] MTX was supplemented to a concentration of 50 nM between days 5 and 10 post-REP and 100 nM between days 10 and 14. At 14 days post-REP, flow cytometry was used to confirm the purification of T cell populations expressing CCR and/or TamR constructs. T cells were then transferred into a cryopreservation solution consisting of 80% culture media, 10% FBS and 10% DMSO (Sigma, Cat. # D2650) and frozen for later culture periods. Upon thaw, T cells were advanced immediately into a second REP, and flow cytometric induction assays were performed 10-14 days later.

Flow Cytometry. Flow cytometric analysis was performed to determine transduction marker expression and phenotypic surface marker expression. Cells were removed from culture and placed into 96-well round-bottom plates, washed twice with PBS (Gibco, Cat. # 10010-023), stained with pre-titered quantities of antibody, washed three more times with PBS and finally fixed with 0.5% paraformaldehyde (Electron Microscopy Sciences, Cat. # 15713) in PBS before analysis. Flow cytometric data was collected using a BD LSRFortessa flow cytometer and later analyzed using FlowJo software. Final flow plots were populated by cell populations remaining after the following gating strategy was performed. First, a “lymphocyte” gate was generated by drawing a polygon within the forward scatter vs side scatter scatterplot to isolate events with size and granularity characteristic of lymphocytes and remove debris and dead cell events. Within the lymphocyte gate, a second “single cell” gate was generated by gating on events that followed a linear relationship between forward scatter in the height and area dimensions to remove cell doublets from downstream analysis. If applicable, a “live cells” gate was generated using the live dead stain to exclude cells with compromised membranes.

TamR Induction. Jurkats or primary T cells were cultured overnight with 50 nM 4-hydroxytamoxifen (4-OHT) to induce expression of TamR-regulated transgenes. Primary T cells were additionally treated with anti-CD3/CD28 Dynabeads (Thermo Fisher Scientific, Cat. # 11131D) at a 1:1 bead to cell ratio to provide the T cell activation signals necessary for TamR induction.

Intracellular Cytokine Staining. IL-2 production by the IL-2-encoding TamR construct was quantified using intracellular cytokine staining. The day before staining, T cells were induced with 4-OHT as discussed above. Four hours prior to staining, a transport inhibitor cocktail (Thermo Fisher Scientific, Cat. # 00-4980-03) was added to prevent T cell release of secretory proteins. Cells were then stained with Live Dead Fixable Aqua viability dye (Thermo Cat # L34957) and relevant surface markers to allow gating of live, modified T cells. Next, samples were fixed and permeabilized using the Fixation/Permeabilization Kit (BD, Cat. # 554714) according to the manufacturer's protocol. The cells were then stained with PE-Cy7-conjugated anti-human IL-2 (BioLegend, Cat. # 500326). Flow cytometric data was collected using a BD LSRFortessa flow cytometer and analyzed using FlowJo software.

RESULTS

Ablation of CCR-Expressing T Cells Using a Drug-Sensitive Suicide Switch

During our investigation of the *in vivo* performance of CCR-equipped B7H3CAR T cells, we found that CCRIL2 and CCRIL7-expressing T cells exhibited unchecked growth after tumors had

been cleared. This overzealous CAR T cell expansion eventually led to mouse death, as shown by the Kaplan Meier survival curves in Figure 1a. The tumor-free survival only reflects avoidance of death related to tumor progression, while the absolute survival reflects avoidance of any cause of death. Treatment with both CCRIL2 and CCRIL7-expressing CAR T cells prevented any deaths due to tumor progression, but 0% and 20% of the mice treated with CCRIL2 and CCRIL7-expressing T cells, respectively, survived 100 days after tumor injection. Bioluminescent imaging of mouse organs post-euthanasia revealed an accumulation of adoptively transferred T cells in the spleens, lungs, and livers of sick mice (data not shown). This suggests that the mitogenic and pro-survival effects mediated by CCRIL2 and CCRIL7, as discussed in Chapter 1, drive CAR T cells to continue expanding in mice beyond the point of tumor clearance. A system to regulate CCR expression or activity will be key to ensuring safety when applying this technology.

We investigated a potential fail-safe system in the form of a drug-responsive cellular suicide switch. The antiviral drug ganciclovir (GCV) can be used to treat herpesviruses through inhibition of DNA polymerase.[2] Virally encoded thymidine kinase phosphorylates GCV, which is then converted into GCV-triphosphate, a nucleotide analogue. The analogue competes with naturally occurring nucleotides during the process of DNA replication, eventually resulting in slowing or termination of replication. Researchers later discovered the applicability of this system as a suicide switch, showing that ganciclovir triggers apoptosis in human cells expressing the herpes simplex virus thymidine kinase (HSV-TK) and is not recognized by endogenously expressed thymidine kinase.[3] Subsequent work increased the sensitivity of HSV-TK to ganciclovir through semi-random mutagenesis of the TK active site.[4]

We hypothesized that a suicide switch mechanistically dependent upon DNA replication would successfully curtail overgrowth of CCR-expressing T cells, as these cells must undergo DNA replication to continue expanding. To this end, we included a thymidine kinase mutant with high sensitivity (SR39TK) in the sequence of our CCR-encoding lentiviral constructs, appended to the cytoplasmic domain of CD19t (**Fig. 1b**). *In vitro* studies revealed that ganciclovir exposure led to T cell apoptosis across T cell donors and across all three CCR constructs, with no effect on the growth of SR39TK-negative control T cells.

We next examined the efficacy of this approach *in vivo*. Mice bearing subcutaneous human neuroblastoma (Be2) tumors were treated with $CD8^+$ T cells expressing B7H3CAR, CCRIL2/SR39TK and ffluc. Beginning 18 days after tumor injection, mice were treated with 10mg/kg ganciclovir per day for 17 days. Bioluminescent imaging revealed that ganciclovir-treated mice had a significantly decreased presence of T cells during and after drug treatment compared to vehicle controls (**Fig. 1c**). Furthermore, by day 65 post tumor injection, all vehicle treated mice had succumbed to death from T cell outgrowth, while all GCV-treated mice remained healthy. SR39TK-mediated cell suicide offers a promising means to curtail the outgrowth of CCR-expressing CAR T cells using an FDA approved drug. Furthermore, the kinetics of T cell ablation appear to be relatively slow, suggesting that this system may be used to titrate the level of T cell growth to ensure safety without compromising therapeutic goals.

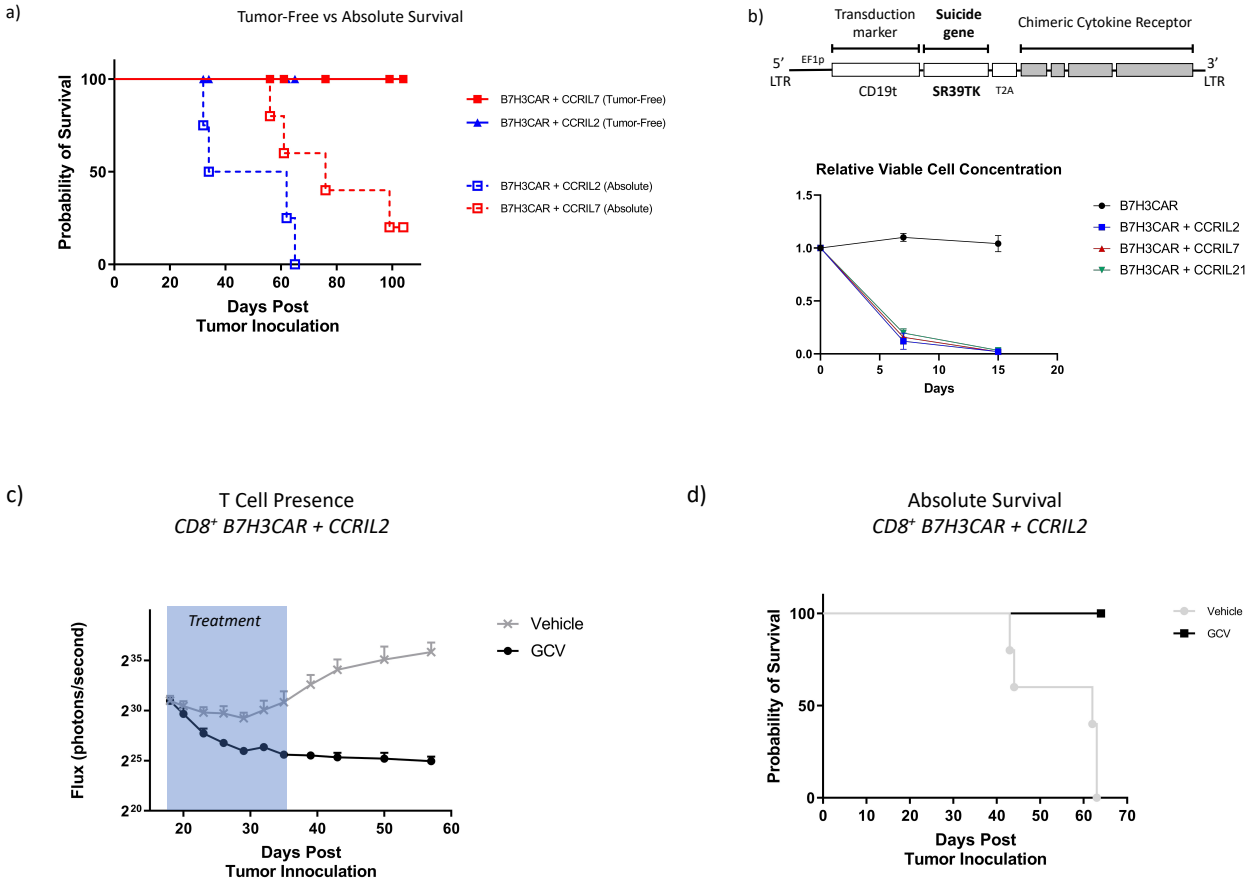

Figure 1: Ablation of CCR-Expressing T Cells Using a Drug-Sensitive Suicide Switch. a, Kaplan Meier tumor-free vs absolute survival curves of mice treated with CCRIL2 and CCRIL7-expressing CAR T cells. **b**, CCR-encoding lentiviral construct with suicide gene SR39TK highlighted, and primary human CD8+ T cell survival curve when cultured in 10 μM GCV. Relative viable T cell concentration reflects concentrations of live T cells under GCV treatment relative to vehicle-treated controls. **c**, T cell presence in mice treated with CD8+ B7H3CAR + CCRIL2/SR39TK T cells upon exposure to GCV (10mg/kg/day) or vehicle. **d**, Kaplan Meier absolute survival curves of mice treated with GCV or vehicle.

An Orthogonal Drug-Responsive Transcriptional Regulation System for Control of Cytokine Signaling

While the SR39TK suicide gene technology effectively curtails CCR-mediated T cell overgrowth in mice, an ON switch could perhaps avoid the occurrence of T cell overgrowth by creating a default OFF state. Furthermore, a regulation system derived from human genes would

pose less risk of immunogenicity and greater viability as a clinically translational product. To temporally control the expression of transgenes such as the CCRs, our lab has developed a tamoxifen-dependent transcriptional regulation system (TamR). In this system, tamoxifen allows translocation of a chimeric transcription factor into the nucleus, where it binds to a responsive promoter and activates transcription of the regulated transgene (**Fig. 2a**). The chimeric transcription factor (HEA) is composed of: 1) **H**epatocyte nuclear factor 1α DNA biding domain; 2) **E**strogen receptor ligand-binding domain, which is released from heat shock protein 90 (HSP90) by tamoxifen, allowing translocation to the nucleus; and 3) Rel**A** transcriptional activation domain. Mutations were introduced into the estrogen receptor ligand-binding domain that abrogate binding to endogenously expressed estradiol. This adjustment along with use of the hepatocyte-specific DNA binding domain ensure the orthogonality of the TamR system.

Given the necessity of regulating CCR activity to avoid unchecked T cell growth, we examined the ability of the TamR system to regulate expression of CCRs. Unfortunately, CCR expression could not be activated by the TamR system in Jurkat cells (data not shown). However, because this regulation system could allow for tight control of transgene expression, we expanded our cytokine supplementation candidate genes to include secreted cytokines. IL-2 was selected as a candidate of interest, as it promotes T cell growth and survival, and its mandatory receptor (IL2Rb) is widely expressed across T cell subsets. We generated an IL-2 encoding regulated cassette by inserting the IL-2 gene downstream of the responsive promoter (7XHBD) and appending a T2A ribosomal skip sequence followed by a GFP/ffluc transgene for fluorescent and bioluminescent detection. Flow cytometric analysis and intracellular cytokine staining

revealed that treatment with the tamoxifen metabolite 4-hydroxytamoxifen (4-OHT) induced expression of GFP and IL-2 in Jurkats modified with the TamR system components (**Fig. 2b**).

However, introduction of the TamR system into primary human T cells proved less efficient. Figure 2c shows the induction of GFP in primary T cells (left panel), with only a 4% GFP^+ population in cells bearing the IL-2 encoding construct under treatment with 4-OHT. The cells were subsequently flow sorted for GFP^+ cells and re-expanded to enrich inducible cells, but this only increased the GFP^+ population to 15% (**Fig. 2c, right panel**), still too minor a sub-population for bulk analysis studies. Subsequent work has focused on re-organizing the molecular components of the TamR system to increase the successful introduction of all components to primary T cells. To generate the TamR induction data discussed thus far, the chimeric transcription factor (HEA) and the inducible payload (7XHBD_[Transgene]) were introduced via separate constructs using lentiviral co-packaging (**Fig. 2d**). The inefficiency introduced by co-packaged lentivirus, as discussed in Chapter 2, stems from the low probability of integrating both constructs into a high proportion of cells.

To consolidate the TamR components onto a single lentiviral construct, we constructed a dual-promoter TamR construct (**Fig. 2d**), which includes an inducible cassette followed by a constitutive cassette encoding the transcription factor. Insulator DNA elements were introduced between the two cassettes to decrease crosstalk. The dual-promoter construct achieved slightly higher GFP induction in Jurkat cells (58%) compared to co-packed constructs (47%). Enrichment of primary T cells modified with the dual-promoter construct will likely proceed more quickly, as titers for single-packaged lentiviruses tend to outstrip titers of co-packaged lentivirus, and future work will investigate this possibility.

However, the complete list of components necessary to introduce into primary human T cells for TamR implementation also includes a CAR. A typical CAR-bearing lentiviral construct used by our lab features a CAR, a double mutant form of the drug resistance gene dihydrofolate reductase (DHFRdm),[5] and a cell surface marker (**Fig. 2e**). To develop an all-in-one TamR construct, we combined the necessary components of the CAR construct with the dual-promoter construct. The use of a CAR with a human-derived single-chain variable fragment, such as the B7H3CAR, allows direct surface detection of CAR using anti-human antigen-binding fragment (anti-hu Fab), negating the need for a separate cell surface tag. Thus, the B7H3CAR and DHFRdm were introduced into the constitutive polycistron of the dual-promoter construct downstream of HEA9, and the inducible transgene GFP/ffluc (2.4 kb) was replaced with Her2tG (429 bp) to prevent the construct size from exceeding the lentiviral packaging limit. We introduced this all-in-one construct into Jurkat cells via transduction and found a robust induction of Her2tG expression under treatment with 4-OHT.

Finally, we explored CIndR7 (see Chapter 2) as a candidate for regulation by the TamR system. CIndR7's detectability by cell surface flow cytometry negates the need for additional fluorescent or surface tags, and its small DNA footprint (1.09 kb) allow its incorporation into the all-in-one TamR construct without exceeding the maximum coding sequence for lentiviral packaging (**Fig. 2f**). Induction of the CIndR7-bearing all-in-one TamR construct in Jurkat cells only resulted in a 3% $Her2^+$ cell population by surface staining. We hypothesized that the observed variability in inducibility across regulated transgenes in the all-in-one construct could be ascribed to differences in mRNA stability, as the upstream inducible cassette does not possess a terminator or polyA sequence. To increase the mRNA stability of the regulated transgene, we

introduced the rabbit β-globulin polyA (RBGpA) sequence downstream of the CIndR7 gene.[6] This addition necessitated the re-orientation of the inducible cistron onto the reverse complement strand, as polyA sequences on the lentiviral coding strand can cause premature termination during viral production.[6] The RBGpA-appended all-in-one construct achieved 24% induction by 4-OHT, suggesting that mRNA stabilization plays a key role in transgene expression in this construct. As a result, we have built an inducible lentiviral construct housing all TamR components, a drug selection gene, and a CAR; and future work will investigate avenues for further optimization and performance in primary human T cells.

a) Tamoxifen Regulation (TamR) System

- Transcription Factor

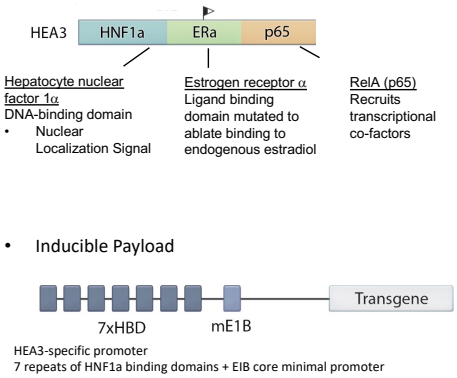

- Inducible Payload

HEA3-specific promoter
7 repeats of HNF1a binding domains + EIB core minimal promoter

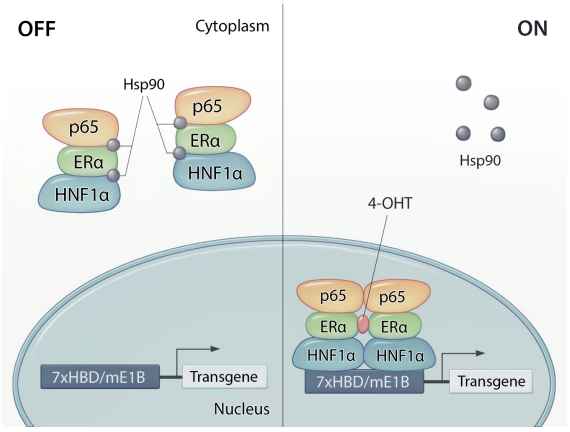

b)

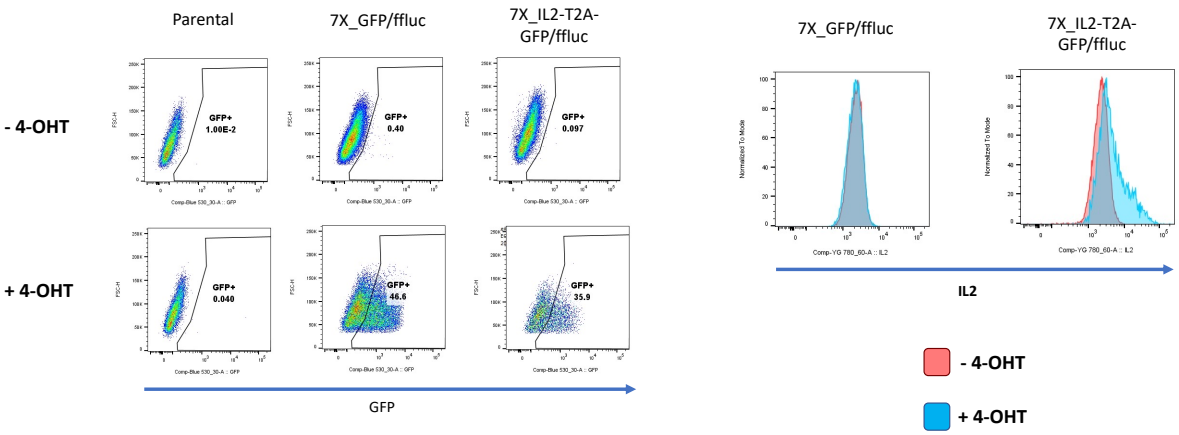

c)

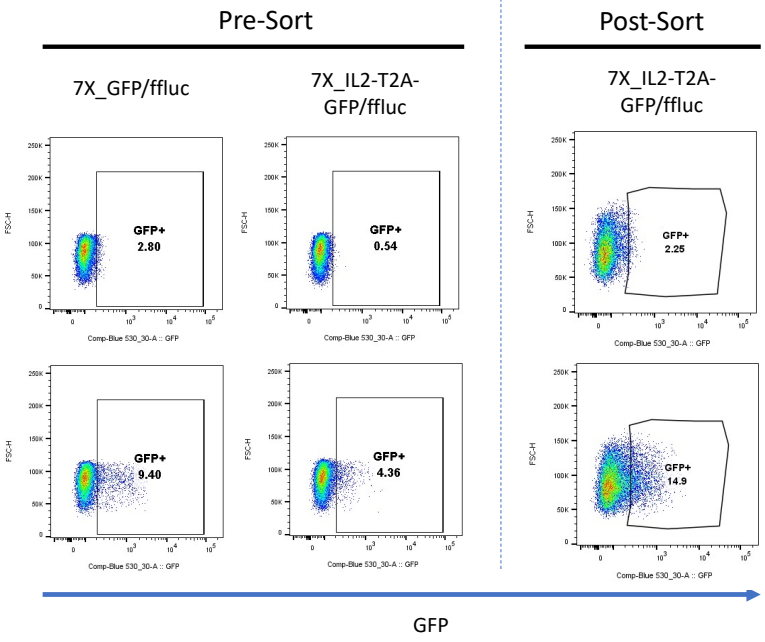

d) TamR Constructs for Co-Packaged Virus Transduction

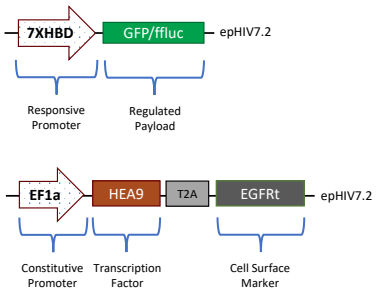

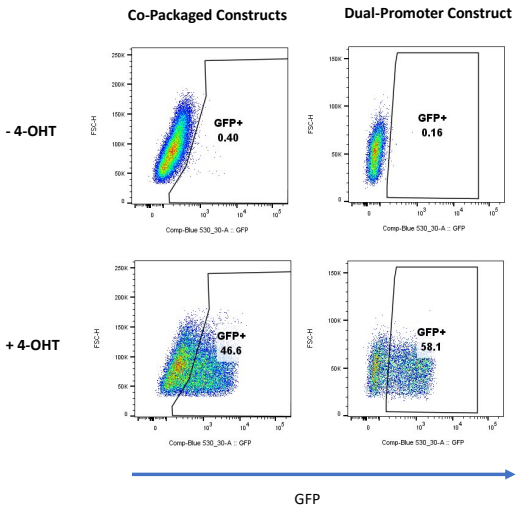

Dual-Promoter TamR Construct

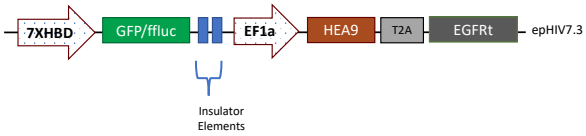

e) CAR-Bearing Lentiviral Construct

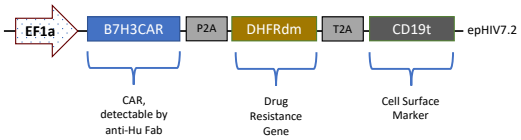

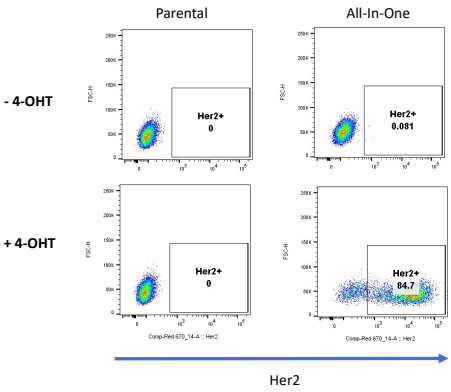

All-in-One TamR Lentiviral Construct

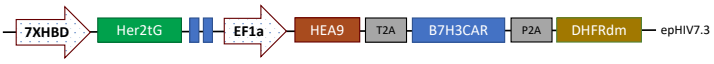

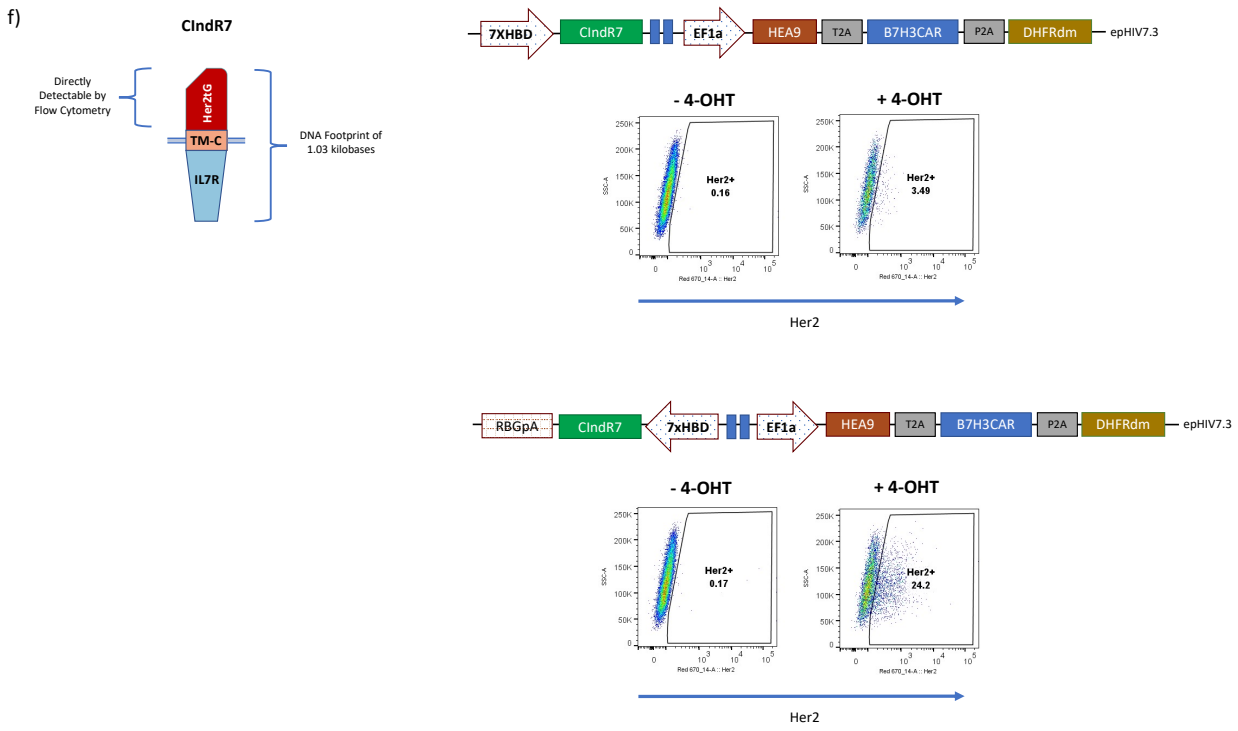

Figure 2: An Orthogonal Drug-Responsive Transcriptional Regulation System for Control of Cytokine Signaling. a, Schematic detailing the design and functionality of the TamR system. **b**, Flow cytometric quantification of induction of GFP and IL-2 expression in Jurkat cells by 4-OHT treatment. Flow plots have been pre-gated for live cells expressing the TamR chimeric transcription factor. **c**, GFP induction efficiency in primary human $CD8^+$ T cells before (left panel) and after (right panel) a flow-based sort for inducible cells. These cell groups have been enriched for expression of the TamR chimeric transcription factor, and flow plots have been pre-gated for live cells. **d**, Development of the dual-promoter TamR construct from co-packaged constructs, and induction analysis in Jurkat cells by flow cytometry. Flow plots have been pre-gated for live cells expressing the surface marker of the dual-promoter construct (EGFRt). **e**, Development of the all-in-one TamR dual-promoter construct incorporating necessary components of the CAR-bearing construct, and induction analysis in Jurkat cells by flow cytometry. Flow plots have been pre-gated for live cells expressing the surface marker of the all-in-one construct (human Fab). **f**, Schematic highlighting the advantages of CIndR7 as a regulated transgene candidate, and a modification to the all-in-one TamR dual-promoter construct to allow for CIndR7 induction. Flow plots have been pre-gated for live cells expressing the surface marker of the all-in-one construct (human Fab).

DISCUSSION

Equipping CAR T cells with receptors for constitutive cytokine signaling can lead to unchecked T cell growth, and here we have demonstrated that this overgrowth can be curtailed with a drug-responsive suicide gene. More elegant approaches may prevent the onset of

overgrowth by employing a default OFF state. One such system, TamR offers a means regulate transgene expression in a drug-inducible manner, and here we have consolidated the key components into a single lentiviral construct. As it stands, this platform fails to induce CIndR expression to levels comparable to constitutive promoters, but further optimization of the molecular architecture may allow for robust and sustained expression. If the system can achieve reliable expression levels, it will allow researchers to tune cytokine signaling in CAR T cells through the administration of drug. This offers the ability to avoid unrestricted T cell growth from cytokine supplementation and explore temporal effects of transgene expression.

ACKNOWLEDGEMENTS

The work presented in this chapter builds upon regulation systems developed by my talented colleagues. The TamR system described in Figure 2 was developed in large part by Tracy Ooi Ph.D. As my research advisor and mentor, Michael Jensen M.D. provided key insights and direction to the projects detailed in all chapters of this work. I would also like to thank my colleagues Niels Rekers Ph.D. and Michael Baldwin for assistance in planning and carrying out the *in vivo* studies described in this chapter.

REFERENCES

1. Wang, X. *et al.* Phenotypic and functional attributes of lentivirus-modified CD19-specific human CD8+ central memory T cells manufactured at clinical scale. *J. Immunother.* 35, 689–701 (2012).
2. Poole, C. L. & James, S. H. Antiviral Therapies for Herpesviruses: Current Agents and New Directions. *Clin. Ther.* 40, 1282–1298 (2018).

3. Black, M. E., Kokoris, M. S. & Sabo, P. Herpes simplex virus-1 thymidine kinase mutants created by semi-random sequence mutagenesis improve prodrug-mediated tumor cell killing. *Cancer Res.* **61,** 3022–3026 (2001).
4. Caruso, M. *et al.* Regression of established macroscopic liver metastases after in situ transduction of a suicide gene. *Proc. Natl. Acad. Sci. U. S. A.* **90,** 7024–7028 (1993).
5. Jonnalagadda, M. *et al.* Efficient selection of genetically modified human T cells using methotrexate-resistant human dihydrofolate reductase. *Gene Ther.* **20,** 853–60 (2013).
6. Tolmachov, O., Tolmachova, T. & A., F. in *Viral Gene Therapy* **32,** 137–144 (InTech, 2011).
7. Figures created with BioRender.com

Chapter 5: Regulation of Hybrid Cytokine Receptor Expression by an Inducible Synthetic Promoter for Safe Implementation

ABSTRACT

We have developed two constitutive cytokine signaling platforms: chimeric cytokine receptors (CCRs, detailed in Chapter 1) and cytokine-independent receptors (CIndRs, detailed in Chapter 3). Both platforms feature signaling variants that lead to unrestricted and toxic T cell growth *in vivo*, heightening the need for a regulation system to ensure contraction of CAR T cell populations after tumor elimination. Chapter 4 examined drug-responsive molecular switches for control of cytokine-augmented CAR T cells. A less invasive approach would be to regulate cytokine signaling in a cell-autonomous manner, negating the need for elaborate regulation circuits and drug dosing. A talented colleague Jia Wei Ph.D. developed an inducible synthetic promoter (iSynPro) that drives expression of downstream genes in response to T cell activation. This chapter details our work to vet iSynPro as a regulation system for synthetic cytokine signaling technology, specifically CIndR7/21. We hypothesize that iSynPro regulation of CIndR7/21 will prevent unrestricted T cell growth while retaining the functional enhancements to CAR T cells offered by CIndR7/21.

MATERIALS AND METHODS

Construct Design. The constructs introduced in this chapter were assembled by inserting the genes encoding CIndR7, CIndR7/21, or a "Marker-Only" control in Her2tG (discussed in Chapters 2 and 3) downstream of an inducible synthetic promoter (iSynPro). These iSynPro-

regulated cistrons were introduced into piggyBac transposable constructs, as described in Chapter 3. Fully assembled, these constructs harbored two divergent coding sequences: 1) A polycistronic sequence driven by the human elongation factor 1 alpha (EF1α) promoter encoding the human G01S anti-CD19CAR, followed by a P2A ribosomal skip sequence, a double mutant of the dihydrofolate reductase (DHFRdm) for drug selection, a T2A ribosomal skip sequence, and finally a truncated epidermal growth factor receptor (EGFRt) to serve as cell surface marker; and 2) an upstream sequence encoding each CIndR variant and driven by iSynPro.

T Cell Production and Culture. Protocols to acquire human cells were approved by the institutional review board of Seattle Children's Hospital. $CD4^+$ and $CD8^+$ T cells were isolated from whole blood using a STEMCELL RoboSep-S automated cell separation instrument according to manufacturer's protocols. Flow-through from the T cell sorting was subjected to a LymphoPrep (STEMCELL, Cat. # 07811) overlay centrifuge-based protocol for the isolation of residual peripheral blood mononucleated cells (PBMCs). PiggyBac transposon constructs and RNA encoding transposase were introduced into T cells by electroporation using a Lonza 4D-Nucleovector instrument and the P3 Primary Cell Kit (Lonza, Cat. # V4XP-3032). Electroporated T cells were immediately seeded into 24-well G-Rex plates (Wilson Wolf, Cat. # 80240M) along with donor-matched PBMC feeder cells. Culture media consisted of X-Vivo 15 (Lonza, Cat. # BP04-744Q) supplemented with 2% KnockOut Serum Replacement (ThermoFisher, Cat. # 10828-028) by volume, 4.6ng/mL IL-2 (STEMCELL, Cat. # 78220.3), 20ng/mL IL-4 (Miltenyi, Cat. # 130-093-924), 10ng/mL IL-7 (Miltenyi, Cat. # 130-095-363) and 20ng/mL IL-21 (Miltenyi, Cat. #

130-095-784). Unmodified T cell control conditions were cultured in the absence PBMCs and treated with a TransAct (Miltenyi, Cat. # 130-111-116) CD3/CD28 stimulation. Three days later, drug selection of modified T cells was begun by adding 50nM methotrexate (Accord, Cat. # NDC 16729-277-30) to the culture medium. 21 days after culture initiation, T cells were collected and cryopreserved in CryoStor CS5 (STEMCELL, Cat. # 07933) for subsequent studies. All post-production assays were conducted in complete RPMI media (cRPMI), which consisted of RPMI 1640 (Gibco, Cat. # 22400-089) supplemented with 10% FBS (Hyclone, Cat. # SH30071.03) and 2mM L-glutamine (Gibco, 25030-081). Unless otherwise noted, all subsequent studies were conducted after mixing $CD4^+$ and $CD8^+$ T cell groups to achieve a 1:1 starting ratio.

Flow Cytometry. Flow cytometric analysis was performed to determine transduction marker expression and phenotypic surface marker expression using the following generalized protocol. Cells were removed from culture and placed into 96-well round-bottom plates, washed twice with PBS (Gibco, Cat. # 10010-023), stained with antibodies specific for cell surface markers, washed two more times with PBS and finally fixed with 0.5% paraformaldehyde (Electron Microscopy Sciences, Cat. # 15713) in PBS before analysis. Flow cytometric data was collected using a BD LSRFortessa flow cytometer and later analyzed using FlowJo software. Final flow plots were populated by cell populations remaining after the following gating strategy was performed. First, a “lymphocyte” gate was generated by drawing a polygon within the forward scatter vs side scatter scatterplot to isolate events with size and granularity characteristic of lymphocytes and remove debris and dead cell events. Within the lymphocyte gate, a second “single cell” gate was generated by gating on events that followed a linear relationship between forward scatter in the

height and area dimensions to remove cell doublets from downstream analysis. If applicable, a "live cells" gate was generated using the live dead stain to exclude cells with compromised membranes. A transgenic surface marker panel was employed during T cell production to track modified T cells: Erbitux APC (BD, Cat. # 624367), Herceptin PE (BD Cat. # 624255), Anti-CD3 BUV395 (BD, Cat. # 563546), Anti-CD4 BV785 (BioLegend, Cat. # 317442), Anti-CD8 Pacific Blue (BioLegend, Cat. # 344718) Live Dead Fixable Aqua viability dye (Thermo, Cat # L34957).

iSynPro Induction. Jurkat cells were treated overnight with eBioscience Cell Stimulation Cocktail (ThermoFisher, Cat. # 00-4970-93), containing PMA and ionomycin, to induce expression of iSynPro-regulated transgenes. Primary anti-CD19 CAR T cells were induced by co-culture with CD19+ Nalm-6 tumor cells at a 2 to 1 effector to target ratio.

Leukemia Xenograft Mouse Studies. T cells were cryopreserved for *in vivo* studies after being mixed to achieve a ~3:2 ratio of $CD4^+$ to $CD8^+$ T cells (Supp. Fig 1c). 11-13 week old NOD scid gamma (NSG) immunodeficient mice were injected via the tail vein with one million human leukemia Nalm-6 tumor cells, modified to express a fusion protein of mCherry and firefly luciferase. Six days after tumor injection, tumor engraftment in each mouse was quantified via bioluminescent imaging using an IVIS Spectrum In Vivo Imaging System (Perkin Elmer) and Living Image Software. Mice were then distributed into treatment groups to normalize average engraftment across groups as much as possible. Seven days after tumor injection, mice were injected via the tail vain with either two or four million T cells. Thereafter, mice were monitored for tumor growth by bioluminescent imaging. Health metrics and weight changes were also

recorded to capture effects of different T cell treatment groups. Mice were euthanized when they showed moderate to severe hind-limb paralysis, a result of unchecked tumor progression, or otherwise as recommended by veterinary staff. Beginning on day 17 and at weekly intervals thereafter, retro-orbital bleeds were performed to examine T cell engraftment in the peripheral blood.

T Cell Quantification in Retro-Orbital Bleed Samples. Peripheral blood samples were taken by retro-orbital bleeds of mice on a weekly basis, and the following flow cytometry protocol was performed to quantify T cells in the blood. 40uL of blood was moved into a 96 well plate. Remaining blood was pooled across samples and mixed with T cells from culture to serve as an FMO control staining mix. Other controls included T cell only samples and Nalm-6 only samples to allow for discrimination of these populations in the blood during analysis. Red blood cells were lysed using Pharm Lyse Buffer (BD, Cat. # 555899), and samples were treated with Fc blocking reagent (Miltenyi, Cat. # 130-059-901) to prevent indiscriminate antibody binding. Next, cells were stained with the following panel of reagents: anti-CD3 BUV737 (BD, Cat. # 612751), anti-human CD45 APC-Cy7 (BD, Cat. # 557833), anti-mouse CD45 PerCP/Cy5.5 (BioLegend, Cat. # 103132), and fixable viability stain 520 (BD, Cat. # 564407). Finally, samples were fixed in 0.5% paraformaldehyde (Electron Microscopy Sciences, Cat. # 15713) in PBS before analysis. CountBright absolute counting beads (Invitrogen, Cat. # 2207530) were added to each sample to allow for back-calculation of T cell counts per uL of blood analyzed. Flow cytometric data was collected using a BD LSRFortessa flow cytometer and analyzed using FlowJo software.

T Cell Characterization in Retro-Orbital Bleed Samples. To phenotypically characterize CIndR-expressing CAR T cells in mice, peripheral blood samples were taken by retro-orbital bleeds 35 days after tumor injection and analyzed following the protocol described above in the "T Cell Quantification in Retro-Orbital Bleed Samples" section using the staining reagents listed below. Finally, samples were examined using a Cytek Aurora spectral flow cytometer and analyzed using FlowJo software.

Target Antigen	**Fluorophore**	**Manufacturer**	**Catalog #**
CD25	BUV563	BD	741365
CD69	APC-eFluor 780	Invitrogen	47-0699-42
PD1	BUV615	BD	612991
TIGIT	RB780	BD	755561
CD57	BV510	BioLegend	393314
CD95	APC/Fire 810	BioLegend	305663
CD4	BV421	BD	562424
CD8	R718	BD	567345
CD19	BV711	BD	563036
CD45RA	BV786	BD	741010
CD62L	BV605	BD	562719
Human CD45	BUV395	BD	563792
Her2 (Herceptin)	PE	BD	624255
EGFR (Erbitux)	APC	BD	624367
CD3	BUV737	BD	612751
Mouse CD45	PerCP/Cy5.5	BioLegend	103132
Fixable Viability Stain 520	n/a	BD	564407

RESULTS

Regulation of Synthetic Cytokine Receptor Expression via a T Cell Activation-Dependent Promoter

Our lab has developed an inducible synthetic promoter (iSynPro) that activates transcription upon T cell activation by CAR signaling (**Fig. 3a**). This system offers a cell-autonomous approach to regulating synthetic cytokine receptor expression, avoiding the need for cell monitoring and drug administration, as in the SR39TK and TamR systems detailed in Chapter 4. To investigate the applicability of iSynPro to CIndR7 regulation, we designed a lentiviral construct featuring iSynPro upstream of CIndR7, followed by T2A and CD19t for cell surface detection (**Fig. 3b**). This construct was introduced into Jurkat cells alongside a control construct encoding iSynPro-CD19t. Both constructs showed minimal background expression in un-stimmed cells. Activation of the cells by phorbol myristate acetate and ionomycin (PMA/Iono) led to expression of CD19t in both constructs, increasing with lentivirus exposure. Transduction with the CIndR7-bearing construct also led to proportional expression of Her2 in PMA/Iono treated cells, showing that CIndR7 can be expressed to detectable levels by iSynPro and no additional surface tag is necessary for future studies.

Given that cytokine signaling provides a third signal for T cell activation, as discussed in Chapter 1, we investigated whether expression of CIndR7 could increase baseline activity of iSynPro through a positive feedback loop. The MFIs annotating the histograms in the top row in Figure 3b demonstrate that, while expression in un-stimmed cells does increase as more lentivirus is added, the introduction of CIndR7 under iSynPro regulation does not drastically

increase background signal and lead to run-away expression. iSynPro therefore offers an attractive option for cell-autonomous regulation of CIndR expression.

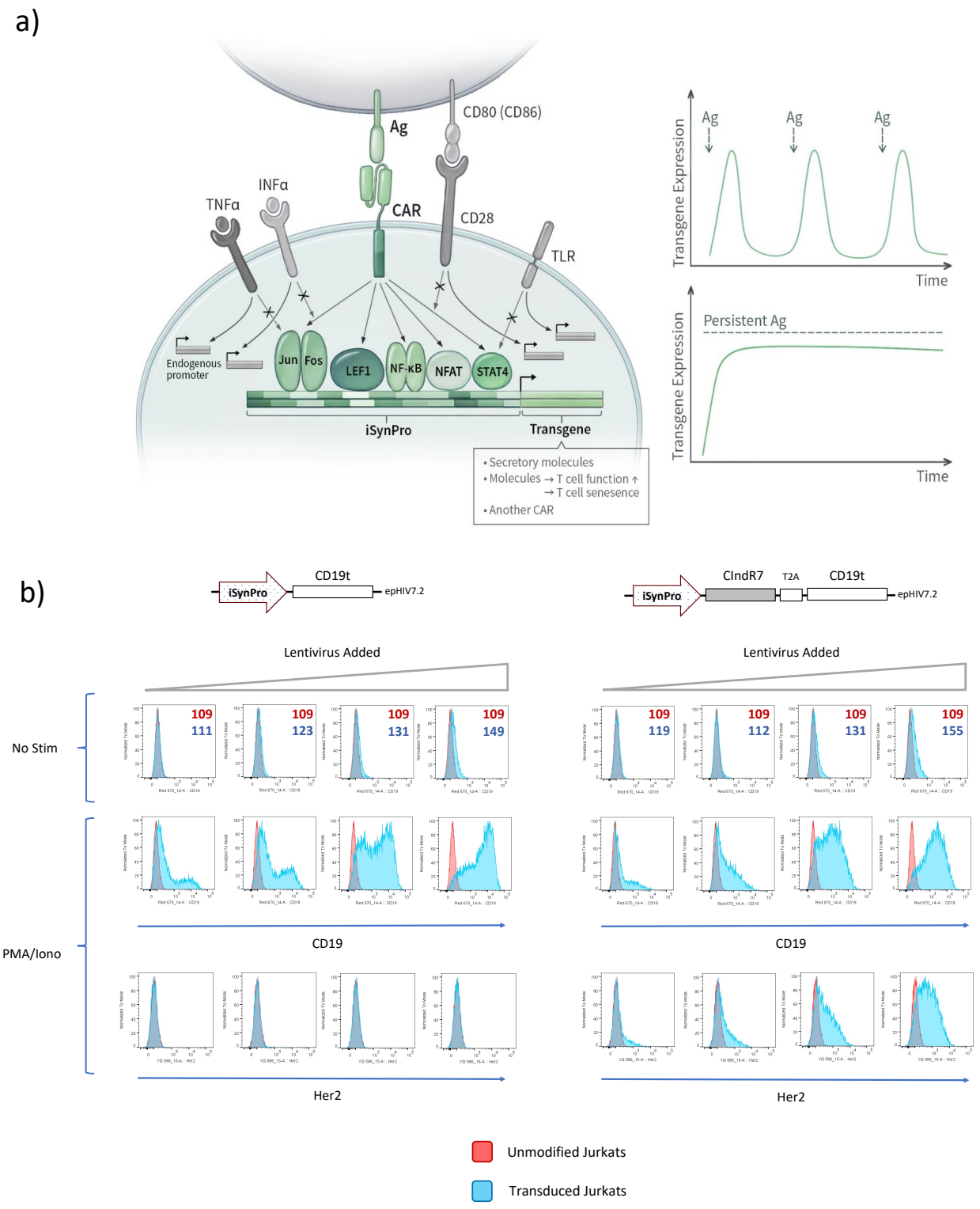

Figure 1: Regulation of Synthetic Cytokine Receptor Expression via a T Cell Activation-Dependent Promoter. a, Schematic detailing the design and functionality of the iSynPro system. **b**, Flow cytometric quantification PMA/Iono-triggered expression of CD19t and Her2tG in Jurkat cells modified with lentiviruses encoding iSynPro regulated transgenes. The annotations in the upper right corner of the first row of histograms reflect the median fluorescence intensity of each cell population.

Constitutive Expression of a Hybrid Cytokine Receptor Leads to Unrestricted T cell Growth *In Vivo*

The CIndR7/21 hybrid cytokine receptor provides constitutive STAT3 and STAT5 activation, as detailed in Chapter 3 (**Fig. 2a**). We found that introducing this transgene into human T cells under constitutive expression alongside an anti-CD19CAR (**Fig. 2b**) and administering to leukemia-bearing NSG mice (**Fig. 2c**) led to unrestricted T cell growth. CAR T cell supplementation with CIndR7/21 led to robust tumor clearance (**Fig. 2d**) and extension of survival (**Fig. 2e**). However, these mice also showed elevated concentrations of CAR T cells in the blood (**Fig. 2g**), and three of five total mice later became moribund and developed upper abdominal swelling, necessitating euthanasia. Necropsy revealed the origin of abdominal swelling to be enlargement of the spleen and liver (**Fig. 2g**). The elevated concentrations of CAR T cells in the blood paired with enlargement of spleen and liver indicate unrestricted T cell growth as a potential cause of moribundity. The enhancement of anti-tumor potency offered by CIndR7/21 make it an attractive candidate transgene to supplement CAR T cell products in the clinic, but the possibility of toxicity due to unchecked T cell growth necessitates a mechanism to regulate CIndR7/21 activity.

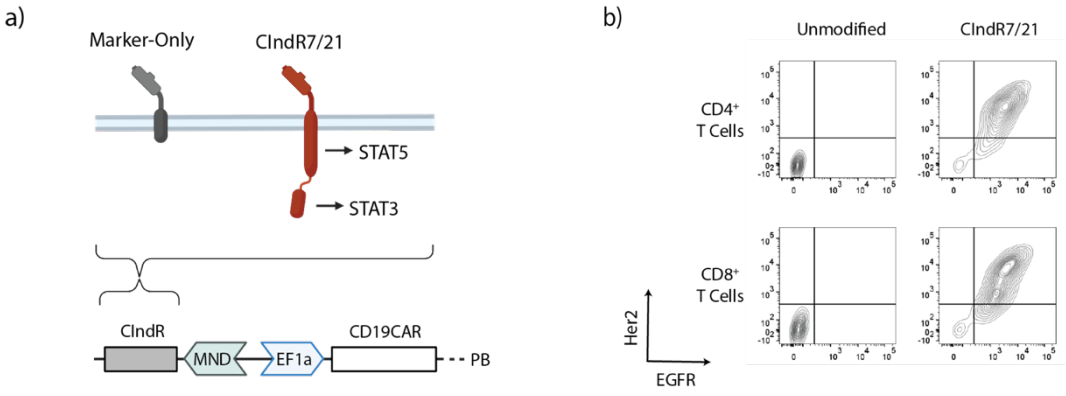
a)
Marker-Only
CIndR7/21
STAT5
STAT3
CIndR
MND
EF1a
CD19CAR
PB
b)
Unmodified
CIndR7/21
CD4+
T Cells
CD8+
T Cells
Her2
EGFR

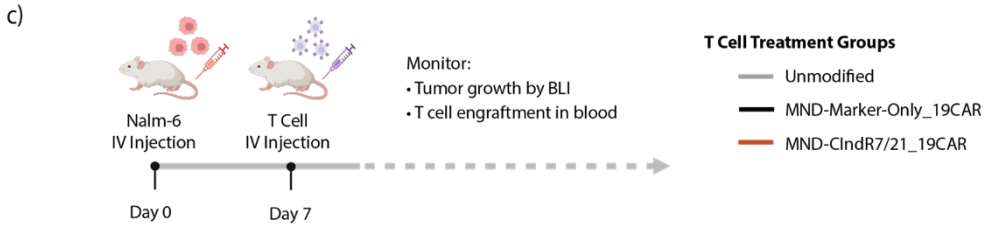
c)
Nalm-6
IV Injection
T Cell
IV Injection
Day 0
Day 7
Monitor:
• Tumor growth by BLI
• T cell engraftment in blood
T Cell Treatment Groups
Unmodified
MND-Marker-Only_19CAR
MND-CIndR7/21_19CAR

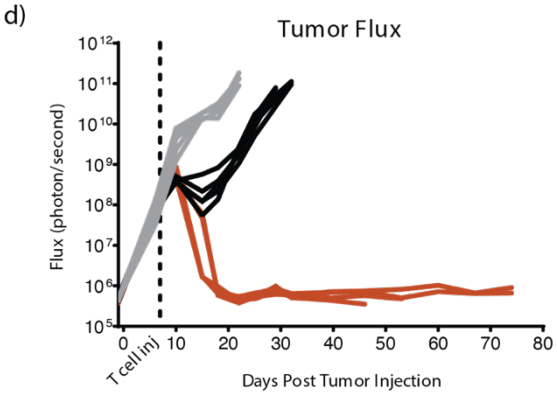
d)
Tumor Flux
Flux (photon/second)
T cell inj
Days Post Tumor Injection

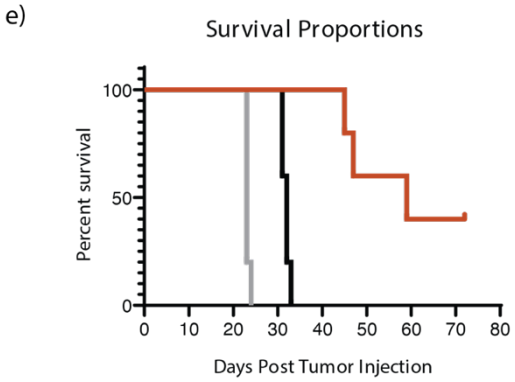
e)
Survival Proportions
Percent survival
Days Post Tumor Injection

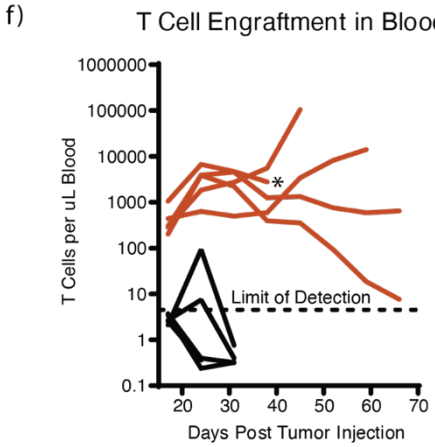
f)
T Cell Engraftment in Blood
T Cells per uL Blood
Limit of Detection
Days Post Tumor Injection

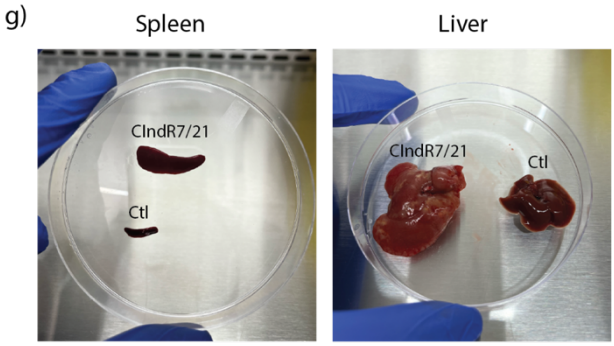
g)
Spleen
Liver
CIndR7/21
Ctl
CIndR7/21
Ctl

Figure 2: Constitutive Expression of a Hybrid Cytokine Receptor Leads to Unrestricted T cell Growth *In Vivo*. a, Schematic detailing the structure of CIndR variants and insertion into a divergent dual-promoter construct for constitutive expression of CIndR and anti-CD19CAR. **b**, Contour flow cytometry plots showing expression of CIndR7/21, marked by Her2tG, and anti-CD19CAR poly-cistron, marked by EGFRt. **c**, Experimental schema of human Nalm-6 leukemia xenograft *in vivo* model (n = 5 mice per group). **d**, Tumor tracking by bioluminescent imaging of mice. Each line represents an individual mouse. **e**, Kaplan Meier survival curve. **f**, Tracking of T cell concentration in peripheral blood. Each line represents an individual mouse. Asterisk indicates mouse featured in necropsy photos in subfigure g. **g**, Images of mouse organs taken during necropsy of a moribund mouse treated with CIndR7/21 CAR T cells and a healthy, untreated mouse ("Ctl").

Regulation of CIndR7/21 by an Inducible Synthetic Promoter Preserves Anti-Tumor Efficacy Enhancement and Protects Mice from Unrestricted T Cell Growth

We hypothesized that CIndR7/21 regulation by iSynPro would retain CAR T cell efficacy enhancement *in vivo* while curtailing T cell growth after tumor elimination. We inserted CIndR7/21 and a Marker-Only control transgene into a divergent dual-promoter construct under regulation by iSynPro (**Fig. 3a**). Introduction of these constructs into human T cells yielded robust expression of the anti-CD19CAR-containing polycistron (**Supp. Fig. 1b**) and antigen-inducible expression of CIndR7/21 in response to $CD19^{+}$ Nalm-6 cells (**Fig. 3b**). These cells were systemically administered to Nalm-6 leukemia-bearing NSG mice (**Fig. 3c**), and mice were monitored for tumor progression, T cell engraftment, health metrics, and weight changes. CIndR7/21 supplementation led to complete tumor elimination in four of five mice (**Fig. 3d**) and a significant improvement in mouse survival (**Fig. 3e**).

Concentrations of CIndR7/21-supplemented CAR T cells in the blood peaked between days 24 and 31 post-tumor injection and decreased thereafter (**Fig. 3f**), suggesting that iSynPro regulation of CIndR7/21 prevents unrestricted T cell growth. Furthermore, flow cytometric analysis of T cells in the blood of mice revealed that iSynPro regulation results in only 1.8% of

cells expressing CIndR7/21 at day 35 (**Fig. 3g**). This metric stands in contrast to MND-regulated CIndR7/21, which features 74.6% CIndR$^+$ cells at the same timepoint. Moreover, when we tracked mouse health metrics and weight changes, we found no evidence that treatment with CAR T cells supplemented with CIndR7/21 under iSynPro regulation led to toxicity (**Supp. Fig. 3b, c**). We conclude that iSynPro regulation allows the CAR T cell functional enhancements of CIndR7/21 to take effect and prevent unrestricted T cell growth after tumor has been eliminated.

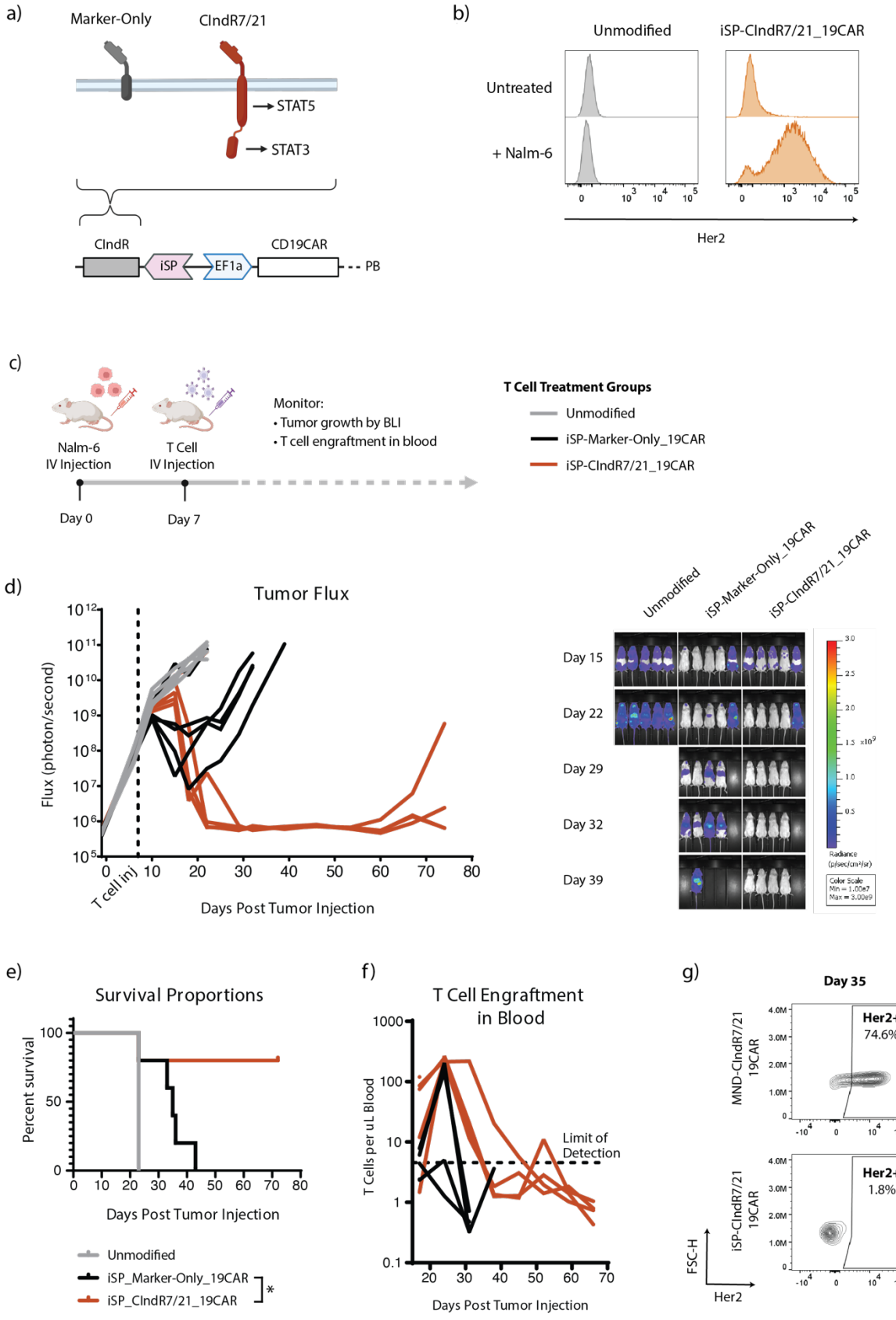
a)
Marker-Only
CIndR7/21
STAT5
STAT3
CIndR
iSP
EF1a
CD19CAR
PB
b)
Unmodified
iSP-CIndR7/21_19CAR
Untreated
+ Nalm-6
Her2
c)
Monitor:
• Tumor growth by BLI
• T cell engraftment in blood
Nalm-6
IV Injection
T Cell
IV Injection
Day 0
Day 7
T Cell Treatment Groups
Unmodified
iSP-Marker-Only_19CAR
iSP-CIndR7/21_19CAR
d)
Tumor Flux
Flux (photon/second)
T cell inj
Days Post Tumor Injection
Unmodified
iSP-Marker-Only_19CAR
iSP-CIndR7/21_19CAR
Day 15
Day 22
Day 29
Day 32
Day 39
Radiance (p/sec/cm²/sr)
e)
Survival Proportions
Percent survival
Days Post Tumor Injection
Unmodified
iSP_Marker-Only_19CAR
iSP_CIndR7/21_19CAR
*
f)
T Cell Engraftment in Blood
T Cells per uL Blood
Limit of Detection
Days Post Tumor Injection
g)
Day 35
MND-CIndR7/21 19CAR
Her2+ 74.6%
iSP-CIndR7/21 19CAR
Her2+ 1.8%
FSC-H
Her2

Figure 3: Regulation of CIndR7/21 by an Inducible Synthetic Promoter Preserves Anti-Tumor Efficacy Enhancement and Protects Mice from Unrestricted T Cell Growth. a, Schematic detailing insertion of CIndR transgenes into a divergent dual-promoter construct under regulation by iSynPro (iSP). **b**, Flow cytometry histograms showing T cell expression of CIndR7/21, marked by Her2tG, when untreated or co-cultured with $CD19^+$ Nalm-6 cells. **c**, Experimental schema of human Nalm-6 leukemia xenograft *in vivo* model (n = 5 mice per group). **d**, Tumor tracking by bioluminescent imaging of mice. Each line represents an individual mouse. **e**, Kaplan Meier survival curve with statistics comparing Marker-Only and CIndR7/21 groups (Mantel-Cox test: $p < 0.05$*). **f**, Tracking of T cell concentration in peripheral blood. Each line represents an individual mouse, and only mice surviving to day 24 were included in this chart. **g**, Contour flow cytometry plots displaying expression of CIndR7/21, marked by Her2tG, by human T cells in peripheral blood of mice 35 days after tumor injection. A sample from a parallel *in vivo* study featuring CIndR7/21 under constitutive expression by MND was included for comparison.

DISCUSSION

Constitutive expression of CIndR7/21 leads to unrestricted T cell growth and subsequent toxicity *in vivo*. Pathology appears to originate from organ failure due to accumulation of T cells rather than xenogeneic graft-versus-host disease, suggesting that curtailing T cell growth post-tumor elimination would prevent toxicity. The inducible synthetic promoter (iSynPro) was employed to link CIndR activity to CAR T cell activation with the goal of ceasing CIndR expression after antigen-bearing tumor cells have been eliminated. Initial studies indicate that CIndR regulation by iSynPro does not trigger a positive feedback loop, with CindR activity driving T cell activation and resulting in higher baseline CIndR expression.

iSynPro regulation of CIndR7/21 in anti-CD19CAR T cells prevented T cell overgrowth while retaining the desirable effects of cytokine signaling supplementation on CAR T cells. Unlike constitutively expressed CIndR7/21, iSynPro-regulated CIndR7/21 did not lead to significantly elevated T cell concentrations in the peripheral blood. Furthermore, CAR T cells showed minimal expression of CIndR7/21 approximately one week after tumor signal diminished, suggesting that iSynPro ceased CIndR expression in the absence of antigen.

ACKNOWLEDGEMENTS

Jia Wei Ph.D. developed the inducible synthetic promoter (iSynPro) detailed in Figure 1. James Rosser Ph.D. optimized the T cell production method used here to introduce dual-promoter constructs into human T cells. As my research advisor and mentor, Michael Jensen M.D. provided key insights and direction to the projects detailed in all chapters of this work. I would also like to thank my colleagues Michael Baldwin and Niels Rekers Ph.D. for assistance in planning and carrying out the *in vivo* studies described in this chapter. Rajesh Kumar Ph.D. was instrumental in assessing expression of phenotype, differentiation, and activation markers in *ex vivo* isolated T cells.

REFERENCES

1. Figures created with BioRender.com

SUPPLEMENTAL FIGURES

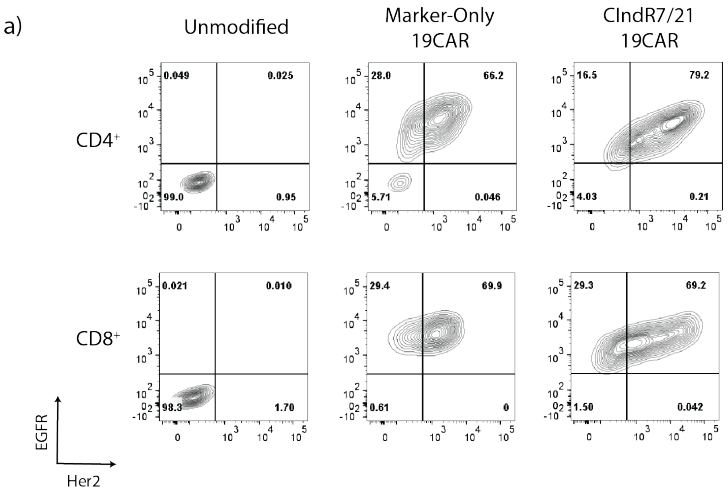

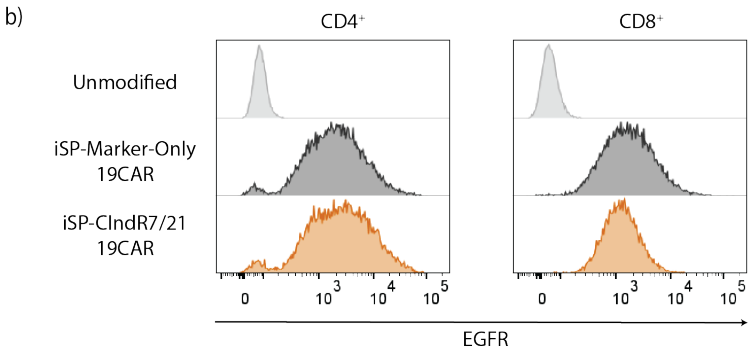

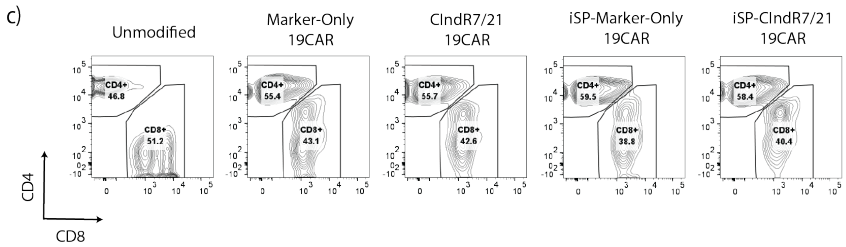

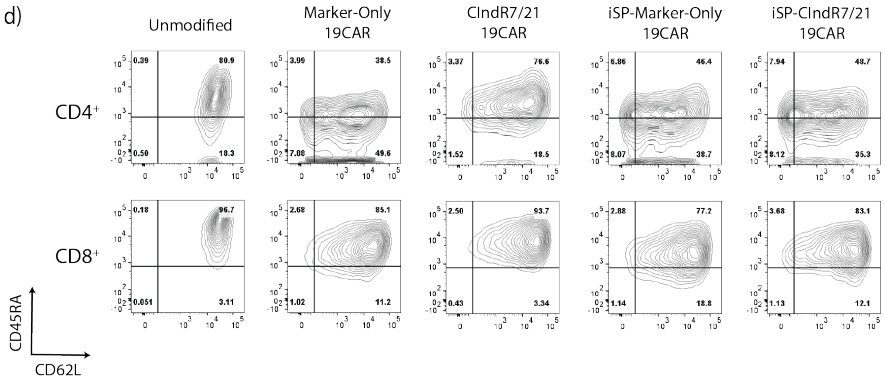

Supplemental Figure 1: Transgenic cell surface marker and phenotypic marker expression by T cells generated for *in vivo* studies. a, Flow cytometry contour plots showing constitutive cell surface expression of transgenic markers in $CD4^+$ and $CD8^+$ cells modified with divergent dual-promoter constructs for *in vivo* studies. EGFRt marks expression of the anti-CD19CAR-containing polycistron, and Her2tG marks expression of CIndR variants. **b**, EGFRt expression in $CD4^+$ and $CD8^+$ cells modified with iSynPro-bearing constructs for in *in vivo* studies. **c**, $CD4^+$ and $CD8^+$ T cell cultures were mixed to normalize the CD4:CD8 ratio across groups before cryopreservation in preparation for *in vivo* studies. Contour plots show CD4 and CD8 expression in each T cell group after thaw for *in vivo* studies. **c**, Expression of differentiation markers CD45RA and CD62L in $CD4^+$ and $CD8^+$ T cells produced for *in vivo* studies.

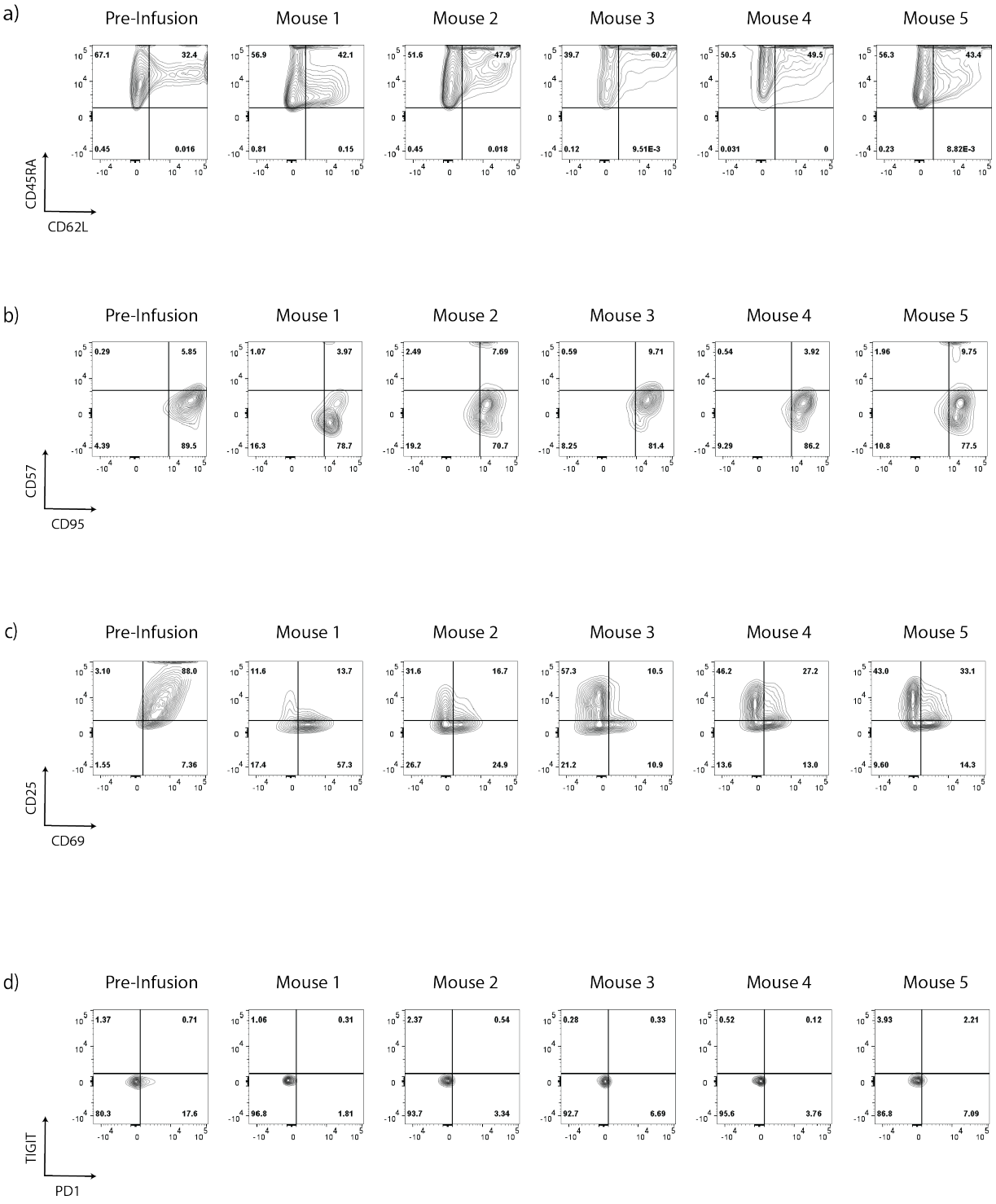

Supplemental Figure 2: Expression of phenotype, differentiation, and activation markers in CIndR7/21-expressing T cells after leukemia tumor clearance in mice. Flow cytometry contour plots comparing expression of cell surface proteins between pre-infusion CIndR7/21 CAR T cell products and T cells detected in the peripheral blood of CIndR7/21 CAR T Cell-treated mice 35 days after study initiation. Markers examined include: CD45RA and CD62L (**a**), CD57 and CD95 (**b**), CD25 and CD69 (**c**), and TIGIT and PD1 (**d**).

a)

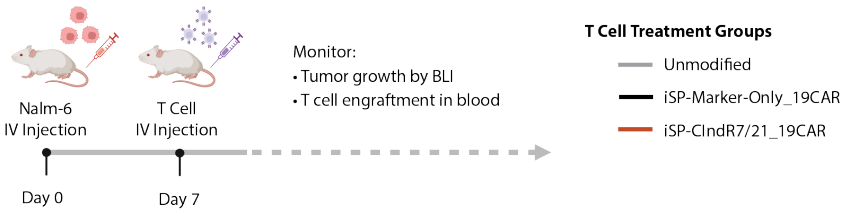

b)

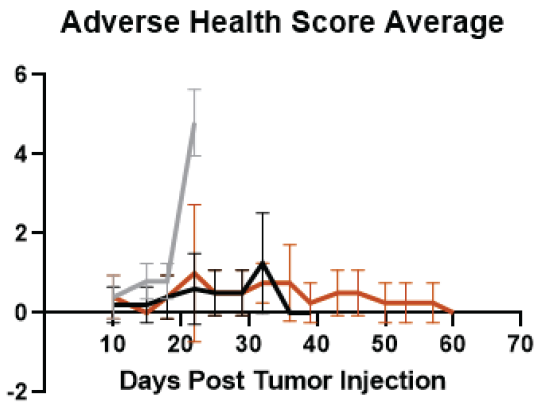

c)

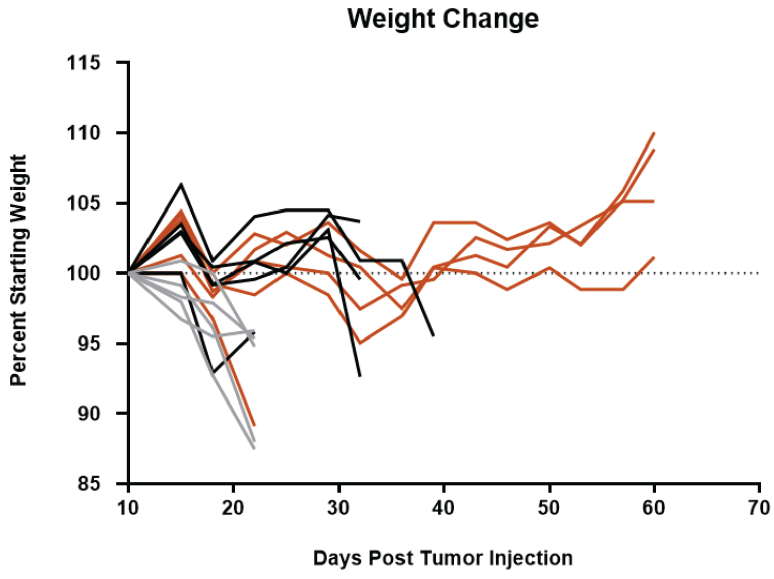

Supplemental Figure 3: Mouse health and weight tracking during treatment with CAR T cells bearing iSynPro-regulated CIndR7/21. a, Experimental schema of human Nalm-6 leukemia xenograft *in vivo* model (n = 5 mice per group). **b**, Average mouse adverse health score (mean +/- standard deviation) capturing changes in weight, posture, activity levels, fur texture, skin integrity and hindlimb paralysis. **c**, Mouse weight change over the course of study. Each line represents an individual mouse.